INFORMATION TO USERS

This manuscript has been reproduced from the microfilm master. UMI films the text directly from the original or copy submitted. Thus, some thesis and dissertation copies are in typewriter face, while others may be from any type of computer printer.

The quality of this reproduction is dependent upon the quality of the copy submitted. Broken or indistinct print, colored or poor quality illustrations and photographs, print bleedthrough, substandard margins, and improper alignment can adversely affect reproduction.

In the unlikely event that the author did not send UMI a complete manuscript and there are missing pages, these will be noted. Also, if unauthorized copyright material had to be removed, a note will indicate the deletion.

Oversize materials (e.g., maps, drawings, charts) are reproduced by sectioning the original, beginning at the upper left-hand corner and continuing from left to right in equal sections with small overlaps. Each original is also photographed in one exposure and is included in reduced form at the back of the book.

Photographs included in the original manuscript have been reproduced xerographically in this copy. Higher quality 6" x 9" black and white photographic prints are available for any photographs or illustrations appearing in this copy for an additional charge. Contact UMI directly to order.

UMI

A Bell & Howell Information Company
300 North Zeeb Road, Ann Arbor MI 48106-1346 USA
313/761-4700 800/521-0600

Modeling and Simulation of Custom Power Devices

by

Raxit A. Kagalwala

A dissertation submitted in partial fulfillment

of the requirements for the degree of

Doctor of Philosophy

University of Washington

1996

Approved by 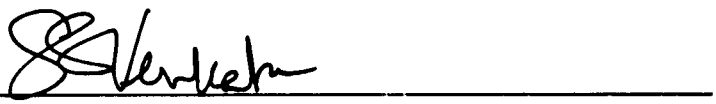

(Chairperson of Supervisory Committee)

Program Authorized to Offer Degree Electrical Engineering

Date May 30, 1996

In presenting this dissertation in partial fulfillment of the requirements for the Doctoral degree at the University of Washington, I agree that the Library shall make its copies freely available for inspection. I further agree that extensive copying of this dissertation is allowable only for scholarly purposes, consistent with "fair use" as prescribed in the U.S. Copyright Law. Requests for copying or reproduction of this dissertation may be referred to University Microfilms, 1490 Eisenhower Place, P. O. Box 975, Ann Arbor, MI 48106, to whom the author has granted "the right to reproduce and sell (a) copies of the manuscript in microfilm and/or (b) printed copies of the manuscript made from the microfilm."

Signature 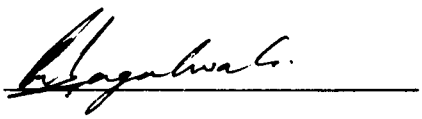

Date May 30, 1996

University of Washington

Abstract

Modeling and Simulation of Custom Power Devices

by Raxit A. Kagalwala

Chairperson of Supervisory Committee: Prof. S. S. Venkata

Department of Electrical Engineering

In the recent years, the utilities are becoming increasingly concerned over the issues of power quality and power flow control. At the same time, there has been a tremendous interest in the application of power electronic converters to solve problems such as those of power quality and power flow control. Due to the complexity of the system with embedded power controllers, computer aided simulations will play a crucial role in the evolution of this technology.

The goal of this dissertation is to develop simulation models for three power electronic converters - (i) a 12-pulse Static Compensator (STATCOM), (ii) a Pulse Width Modulated (PWM) STATCOM and (iii) a PWM Dynamic Voltage Restorer (DVR). These converters are also referred to as Custom Power Devices (CPD's). Their primary function is to improve the power quality of a distribution system. The models developed in this dissertation are important for utility engineers to explore possible solutions from both design, planning and operation point of view. The challenge involved in the development of the models is two fold.

Firstly, the voltage and current waveforms of power converters are discontinuous. The discontinuous waveforms, coupled with the large size of a typical power system, pose a challenge to develop computationally efficient simulation models. In this dissertation, a

new modeling technique is developed. The resulting power converter model, called the Transient Behavioral Model (TBM), will effectively replace the extensively used Ideal Switch Model (ISM) for the simulation of many power converters in power systems. The TBM is almost as accurate as the ISM and, at the same time, its continuous nature makes it compuationally more efficient than the discontinuous ISM.

Secondly, the design of these devices has to be system specific. Presently, these devices exist only in their prototype forms. In this dissertation, due to the lack of available information to develop the models, simulation studies are performed on a realistic distribution system in order to determine the various design parameters for the models. The TBM is shown to be extremely effective for these simulation studies.

Table of Contents

List of Figures

List of Tables

Acknowledgments

I am grateful to Professor S. S. Venkata who led me in this research and shared with me his wisdom and insights. I am also grateful to Professor Peter O. Laurtizen for his invaluable guidance throughout my Ph.D. program. I would like to thank Mr. Ashok Sundaram and Dr. Ram Adapa of the Electric Power Research Institute, Palo Alto, California for providing financial support for my research. I would like to thank Professor V. V. Sastry for his guidance. I would also like to thank my colleague Dr. N. Ravisekhar Raju for the valuable discussions regarding my research.

I would like to thank my wife Nandini, without whose constant support and encouragement, this work would not have been possible. I would also like to thank my parents, Avinash and Meera Kagalwala, and my brother Anuj Kagalwala for their many years of support and encouragement that prepared me for my doctoral degree.

1. Introduction

A survey of power systems literature reveals that the Ideal Switch Model (ISM) and the Variable Impedance Model (VIM) have been used extensively for transient simulation studies. However, these models are discontinuous in nature and in order to limit the numerical error during simulation, the simulation time step has to be kept small near the switching transitions. This reduction in time step results in computational inefficiency. The problem is worse in the case of simulators that use a fixed time step since the time step has to be kept small throughout the simulation. The discontinuous nature of these switch models also leads to problems of numerical oscillations. In this dissertation, a new modeling technique is developed. This new technique yields a continuous time domain model of a power converter. The resulting power converter model, called the Transient Behavioral Model (TBM), is almost as accurate as the ISM. Further, the continuous nature of the TBM makes it computationally more efficient than the discontinuous ISM. In contrast to the previously used continuous Average Switch Model (ASM), the TBM accurately simulates the switching frequency harmonics of the converter. In contrast to the previously used models for simulating switching frequency harmonics such as the Harmonic Balance Method (HBM) and the Generalized Average Switch Model (GASM), the TBM is well suited for implementation in a standard circuit simulator.

1.1 Background

The number of loads involving sensitive electronic circuits such as automated manufacturing plants and computers has increased tremendously in the recent years. These loads are extremely sensitive to the quality of electric power. Disturbances in the power

distribution system can result in expensive losses such as the interruption of an automated manufacturing plant [1]. With the increase in the number of sensitive loads, the development of Active Power Line Conditioners (APLC's) has become a very important area of research for electric power systems [2]. APLC's are also referred to as Active Power Quality Conditioners (APQC). They are power electronic converters that perform one or more of the following functions:

- voltage regulation,
- uninterrupted power supply,
- reactive power compensation,
- voltage and current harmonic compensation.

With the increase in the number of sensitive loads, there is also a demand that utilities provide high quality power. As a result of this demand, the utilities are also becoming increasingly concerned about power quality. A set of power electronic converters, referred to as *Custom Power Devices* (CPD's) are being developed under the sponsorship of the Electric Power Research Institute (EPRI) [3] to enable utilities to supply high quality power to their customers. Note that CPD's, APQC's and APLC's refer to a set of similar power electronic converters performing the function of power quality improvement.

The application of power electronics to power systems is not new. The first generation of power converters used in power systems are the High Voltage DC (HVDC) converters [4]. However, an HVDC system is relatively isolated from the rest of the power system. The interactions between the HVDC converters and the ac power system take place only at the boundary of the dc and the ac power system [5]. The second generation of power

converters include devices such as the Static Var Compensators (SVC's) [6] and the Advanced Series Compensators (ASC's) [7]. These devices are embedded within the ac power system and hence their interaction with the ac system is significantly greater than that of HVDC converters [8]. However, the number of these devices is few and hence their impact on the power system is not widespread. The third generation of power converters includes devices such as the CPD's and the APQC's. Unlike the first two generations, the third generation of power converters will be used extensively throughout the power system. A future power system may be envisioned with multiple power electronic converters on every transmission line as well as every distribution feeder. Due to such a widespread use, there will be many complex interactions between the converters and the power system.

In an industry where the cost of failures is extremely high, coupled with the availability of better computer resources, digital computer simulations will play a key role in the study of these complex interactions. It should be emphasized that simulation models developed for power converters in power systems are essential from two perspectives. Firstly, from the perspective of the designer of a power converter, these models are required for design purposes. Secondly, from the perspective of an electric utility, these models are required for system planning and operation studies. In fact, for devices as sophisticated as CPD's, it may not be possible to design a power converter without considering the planning and operation of the particular system in which the device is to be installed. Hence simulation models will play a critical role in designing *customized* power converters to solve power quality problems of a *specific* power system.

The discussions in this dissertation are mostly with reference to CPD's. However, the discussions are equally applicable to other power quality converters such as APQC's. In fact, the discussions are also applicable to power electronic converters used in Flexible AC Transmission Systems (FACTS) used at transmission level [9].

1.2 Research in Power Electronics Applied to Power Systems

Research in the area of power electronics applications to power systems is interdisciplinary in nature. It involves the areas of classical power systems, high power semiconductors, electronic circuits as well as control systems. Research in each of these disciplines has an impact on the future of power electronics integrated in power systems. From a power systems perspective, the on-going research can be broadly classified into four categories:

1.2.1 System Studies

System studies are the most basic requirement. These studies identify the problems and discuss solutions at a system level. For example in reference [10], the voltage flicker problem caused by an arc furnace is assessed and various solutions to mitigate the problem are discussed. In reference [11], the application of different reactive power compensation systems and their benefits in increasing steady-state loadability, security and transient stability of a power system are discussed.

1.2.2 Converter Design Studies

Based on the overall requirements determined by system level studies, numerous converter topologies are being proposed [12-14]. The focus of such research is to develop converters that can extract maximum benefits (in terms of switching speeds, power handling capability, etc.) from existing power semiconductor switches.

1.2.3 Control Strategy Studies

Power converters can be controlled in several ways to obtain the desired system level performance. Development of stable control strategies with a fast response time for harmonic compensation, reactive power compensation and voltage regulation are active

areas of research [15, 16]. Since the control system is the 'brain' of a power converter, the success of power electronics in power systems will largely depend on the intelligence of the control systems. In a system with multiple converters, the coordination of their control systems will be crucial. It has been shown that a radial feeder with multiple SVC's for voltage control can become unstable if the control gains of the various SVC's are not coordinated [17]. Similar instabilities can be expected in a feeder with multiple APQC's for voltage harmonic control.

1.2.4 Modeling and Simulation Studies

Due to the complex nature of the future power system, coupled with the high cost of prototype testing, digital simulators are becoming essential tools for the analysis and design of power systems, power converter topologies and control algorithms. Since the modeling and simulation of power converters in power systems is the focus of the dissertation, a detailed discussion of ongoing research in this area is given in Sections 1.3 and 1.4.

1.3 Survey of Power Electronics Literature

Power electronic switches are discrete (discontinuous) in nature. Their presence makes power converters different from other electronic circuits. Hence the primary issue in the modeling of power converters is the technique used to model the switching action. Several modeling and simulation techniques with different levels of accuracy, computational efficiency and ease of use, are found in the literature. Some techniques are significant milestones by themselves, whereas some techniques offer an improvement over existing techniques.

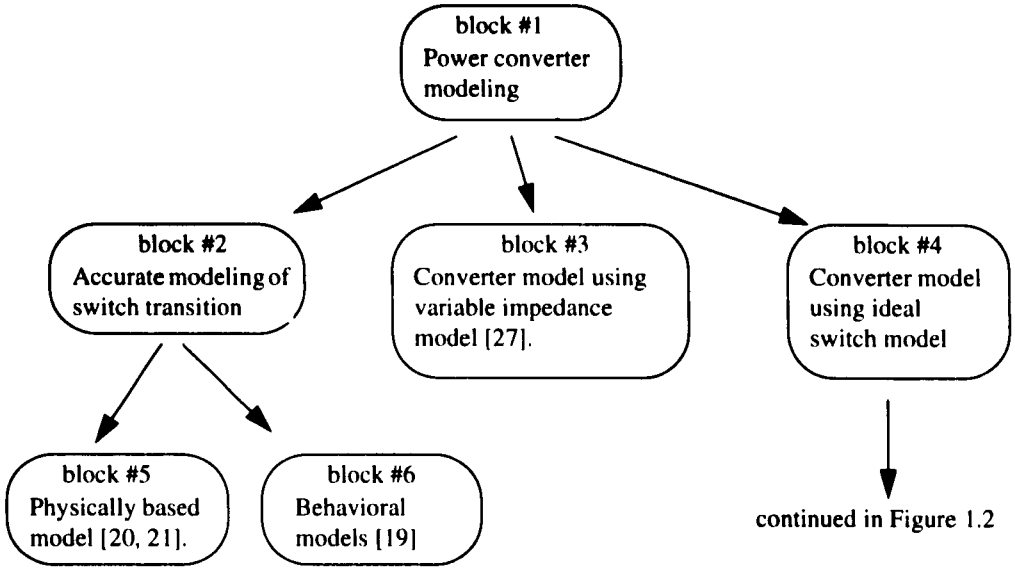

Figure 1.1 Overview of the significant developments in the modeling of power converters.

1.3.1 Power Converter Modeling

An overview of the significant developments in the modeling of power converters is given in Figure 1.1 and Figure 1.2. An explanation of each block shown in the figures, along with its merits and demerits, is given in this section. When applicable, the blocks are also classified as per the five level classification proposed by Budihardjo, Lauritzen et. al. [19].

For the most detailed models, the turn-on and turn-off characteristics of a switch are modeled accurately (see block #2 in Figure 1.1). Physically based models (block #5) are the most accurate. However, they are also computationally the most intensive [20, 21]. These models correspond to the level 2 models described in reference [19]. Certain behavioral models (block #6) are capable of accurately simulating the switch transition characteristics without involving the complexities of physically based models. These

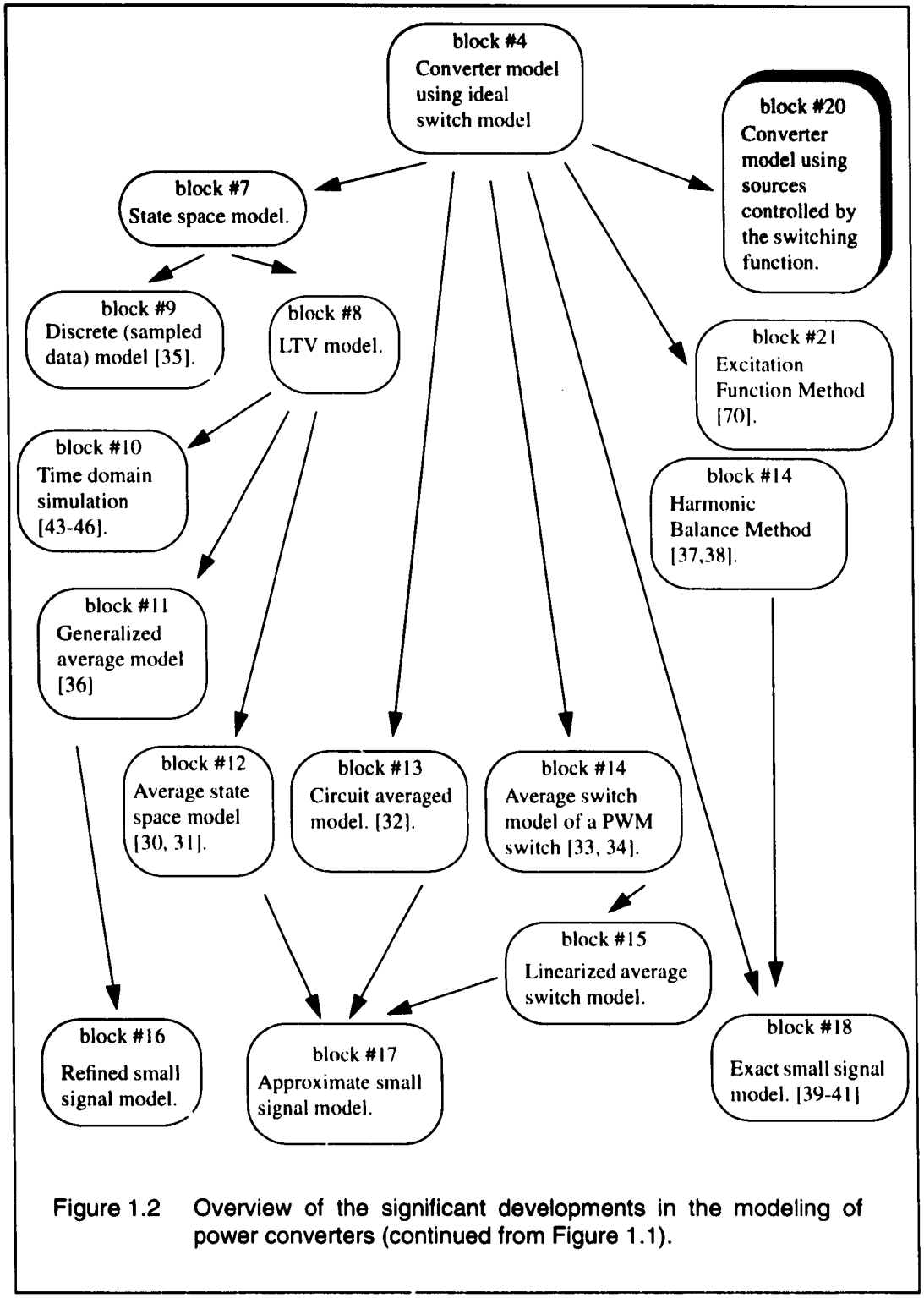

Figure 1.2 Overview of the significant developments in the modeling of power converters (continued from Figure 1.1).

models correspond to the level 1 models in reference [19]. Simulations using physically based models and behavioral models are performed with the aid of a circuit simulator such as SABER [22] or PSPICE [23].

The Ideal Switch Model (ISM) represents a switch by an open circuit during the off-state and a short circuit during the on-state (block #4). It corresponds to the level 0 models described [19]. It is simple and, hence useful for studying converter waveforms from the system point of view. However, the disadvantage of the ISM is that its use results in a network with variable topology. The techniques used to handle the numerical simulation of variable topology networks cost additional computational time. Most numerical simulators formulate a system admittance matrix from the individual circuit elements. The simulators then solve for the unknown node voltages by multiplying the system admittance matrix with the injected current matrix [24]. In the presence of an ideal switch, the simplest method to handle change in network topology is to reformulate the system admittance matrix. After reformulation, the matrix has to be inverted again in order to solve the system equations. Sudden changes in topology can also result in numerical convergence problems in digital simulators [25, 26].

The variable impedance model (VIM) of a switch (block #3) represents the switch by a high impedance during the off-state and by a low impedance during the on-state [27]. The main advantage of this model, over the ISM, is that the network topology is unchanged. Thus, when a switching action occurs, the entire system matrix need not be reformulated. However, due to the change in the impedance of the switch, some the elements of the matrix have to be modified and the inversion of the matrix has to be repeated. Further, the use of extreme values of resistance for the on- and off-states results in stiff equations (widely varying time constants of circuits) [28]. The transition between the off-state impedance and on-state impedance can be modeled as an instantaneous change, a linear change or an

exponential change. A linear or an exponential transition between the on- and off-states provides greater numerical stability than an instantaneous change.

Using the ISM, it is possible to develop a state space model for a power converter (see block #7 in Figure 1.2) [29]:

$$\frac{dx}{dt} = f(x, u, t) \tag{1.1}$$

In general, $f(.)$ is a non-linear, time variant (NLTV) function. An important special case, from power electronics point of view, is the linear time variant (LTV) state space model (block #8). The state space model is compact, and forms an excellent starting point for developing other models useful for analytical studies of a power converter. In 1976, Middlebrook and Cuk [30, 31] used the averaging technique to convert the LTV state space model into a non-linear, time invariant (NLTI) averaged state space model (block #12):

$$\frac{dx}{dt} = f(x, d, u) \tag{1.2}$$

where d is the duty ratio of a PWM switch. Middlebrook and Cuk obtained an approximate small signal model (block #17) by linearizing the state space average model around a fixed operating point:

$$\frac{d}{dt}\hat{x} = f(X, D, U, \hat{x}, \hat{d}, \hat{u}) \tag{1.3}$$

In equation (1.3), X, D and U are the steady state values of the states, duty cycle and the inputs respectively. $\hat{x}$, $\hat{d}$ and $\hat{u}$ are the corresponding small signal perturbations. The small signal model is linear time invariant (LTI), and is extremely useful for control design since the theories of linear control can be applied directly. The advantage of the state space averaging approach is that it is general and yet simple. However, the approach is not suitable for large systems with many switches.

A power converter model using the ISM can also be averaged using the direct circuit averaging technique (block #13) [32]. The average circuit obtained by this technique can be linearized around a fixed operating point to yield an approximate small signal model (block #17) of the converter. The circuit averaging method is more physically intuitive than the state space averaging method. However, direct circuit averaging involves manipulation of two or more switched circuit models into their topologically equivalent forms as shown in Figure 1.3. Such manipulations are difficult even for moderately complex circuits.

In 1990, Vorperian [33, 34] developed an Average Switch Model (ASM) by performing the process of circuit averaging on a Pulse Width Modulated (PWM) switch (block #14). The ASM is linearized around a fixed operating point to yield a small signal ASM (block #15). An approximate small signal model of a power converter (block #17) is obtained simply by replacing the PWM switch in a circuit by the small signal ASM. The advantage of this approach is its simplicity. The method is especially convenient for digital simulation studies since it is easy to replace the PWM switch in a circuit by the equivalent ASM and then perform simulations in the usual manner

The analysis of the state space model in discrete time domain yields the sampled data model of a power converter (block #9) [35]. Sampled data models simplify the analysis by describing the waveforms at only one point in each cycle rather than describing the waveforms through the entire switching period.

In 1991, Sanders et al. [36] developed the Generalized Averaging Switch Model (GASM) for power converters (block #11). This model is based on the assumption that a waveform $x(.)$ can be approximated on the interval $(t\text{-}T, t]$ by its Fourier series representation. The method is applied to state space models by replacing the state variables by their Fourier series representations. The result is an equivalent state space model in

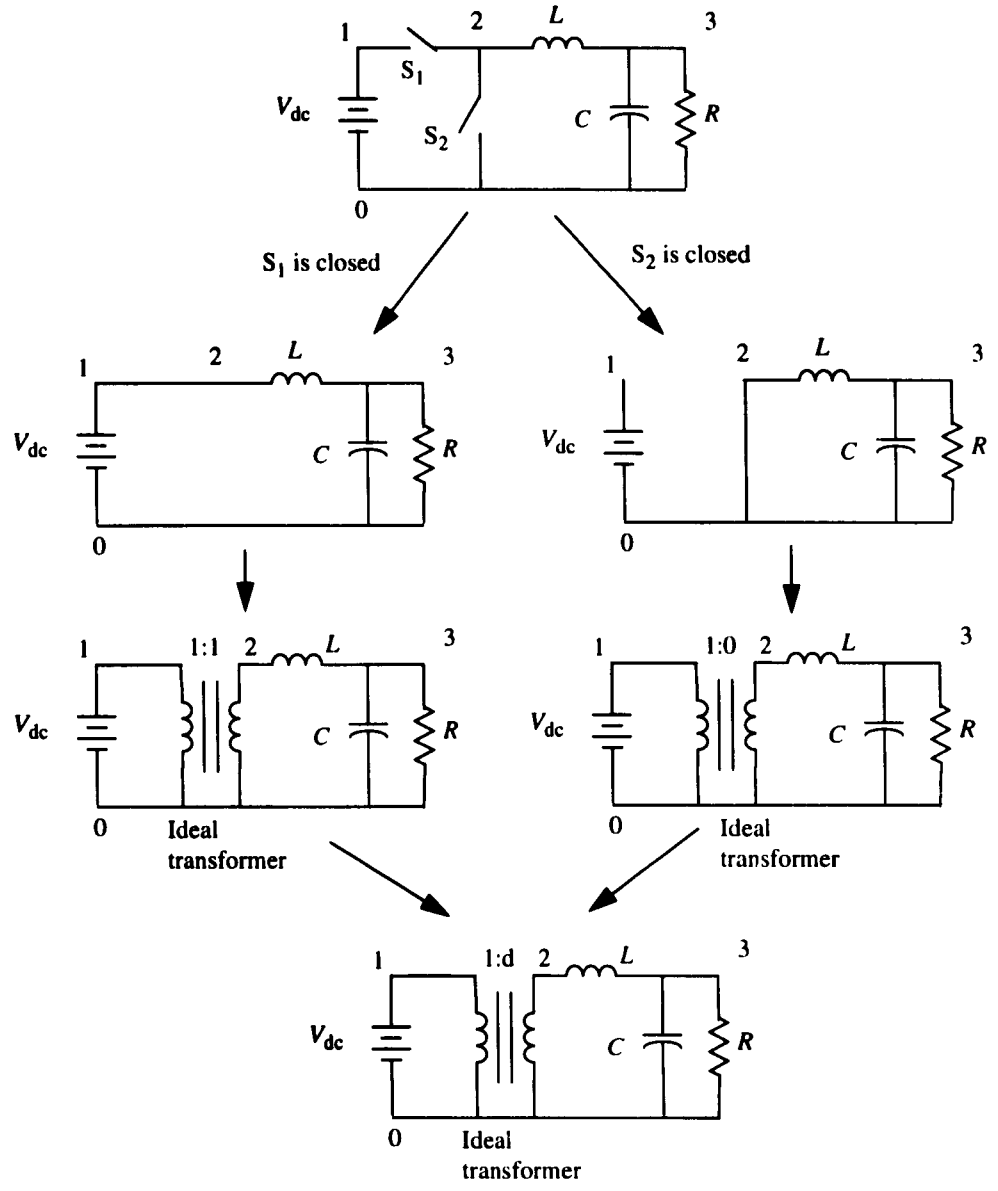

Figure 1.3 Direct circuit averaging of a buck converter.

which the Fourier coefficients are the states variables. This approach can be used to study the harmonics generated by a converter. However, it is more suited for analytical studies of small systems and is not convenient for large systems with many switches. Linearizing the

generalized average switch model and retaining only the zero frequency component yields a refined small signal average switch model (block #16).

In 1986, Kundert and Vincentelli [37] and Gilmore [38] applied the Harmonic Balance Method (HBM) to transform a set of piecewise, linear time domain equations into a set of non-linear frequency domain equations (block #19). In this way, a set of differential equations are transformed into corresponding algebraic equations. The HBM is powerful, however, it cannot be applied directly to perform time domain simulations using standard circuit simulators. The HBM has also been used to obtain exact small signal models for power converters (block #18) [39].

In 1991, Tymerski used a frequency domain approach to develop a time-varying transfer function for a power converter [40,41]. An exact small signal model is obtained by extracting the fundamental frequency behavior of this transfer function (block #18). In 1995, Wong and Groves used a combination of the Fourier series representation of waveforms and time domain simulations to obtain accurate small signal frequency responses of power converters [42].

Various algorithms have also been developed for computationally efficient time domain simulation of the LTV state space model (block #10) [43,44,45,46]. The main intent of these algorithms is to develop an efficient technique to handle the boundary conditions of a piecewise linear state space model. Using these algorithms, it is possible to perform fast simulations of hundreds of switching cycles of a power converter. However, state space formulation is difficult for large networks. Further, the implementation of these algorithms is difficult on standard circuit simulators that use nodal formulation.

The existence function method is a frequency domain approach used by Wood [70] to analyze the open loop steady state behavior of a power converter. The frequency domain

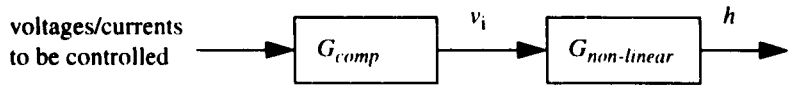

Figure 1.4 Typical control system of a power converter.

approach is difficult to use in comparison with the time domain approach. Hence Wood's approach has not been applied widely for studying the open loop steady state behavior of converter waveforms. However, Wood's concept of representing a power converter as a switching matrix controlled by an existence function is simple yet powerful. This concept is similar to the first step (Section 2.1) of the new modeling technique presented in this dissertation.

The modeling of a converter with voltage and current sources controlled by the switching function (block #20), shown in Figure 1.2, is a new approach developed in this dissertation. A detailed discussion of this approach is given in Chapter 2.

1.3.2 Control System Modeling

The control system is also an integral part of a power converter. Hence it is important to discuss the modeling of the control system. As shown in Figure 1.4, a typical control system senses the voltage or current that has to be controlled. The sensed signals are processed by a compensator (G_{comp}) to generate an input signal (v_i), which is processed by a non-linear switching function generator ($G_{non\text{-}linear}$) to generate the switching function (h). Usually, the compensator (G_{comp}) is first designed using linear control theory. This is used as the starting point for the design procedure. Accurate large signal simulations are then used to finalize the control system design. In order to apply the techniques of linear control theory, it is necessary to linearize the control system. For the average power converter models, the behavior of the switching function generator is averaged (block #B

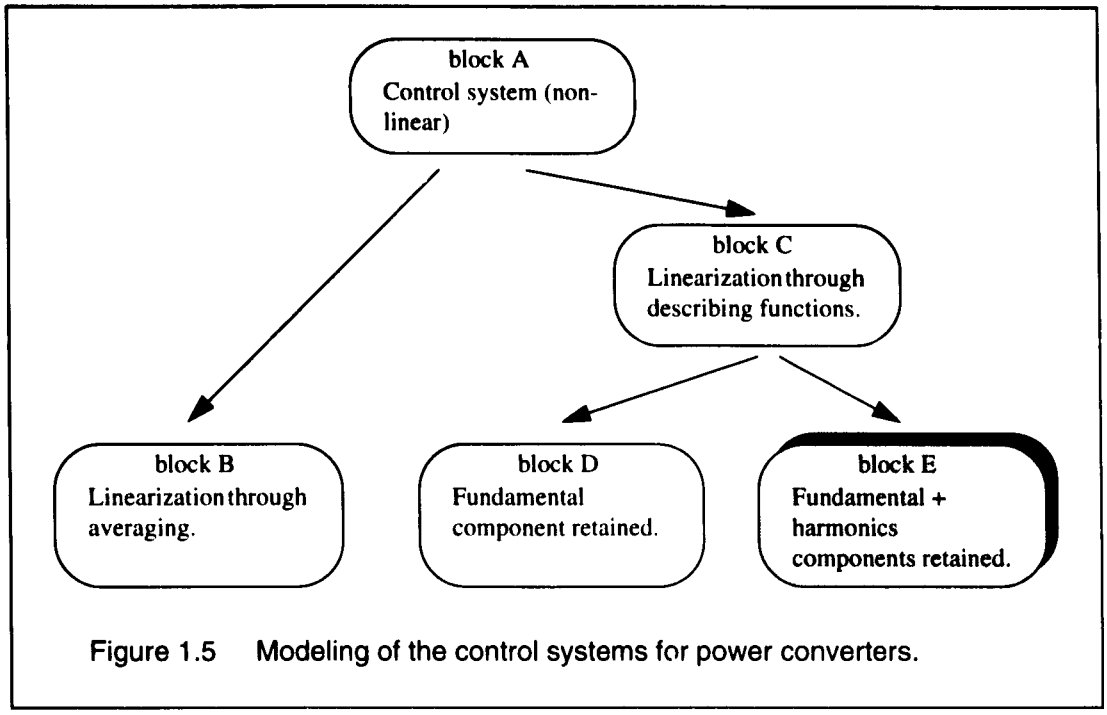

Figure 1.5 Modeling of the control systems for power converters.

of Figure 1.5). For example, the closed loop, small signal average state space model developed by Middlebrook and Cuk [30, 31] is a combination of block #8 in Figure 1.1 and block #B in Figure 1.5.

Another method to approximate nonlinear switching function generator is the describing function technique (block C) [48]. Using this technique, it is possible to approximate a non-linear transfer function by a complex function that includes only the amplification and phase shift of the fundamental component of the output relative to the input (block D). The describing function technique can be extended even for the harmonics of the fundamental frequency (block E). This extension is used by the new switch modeling technique developed in this dissertation. It should be noted that the process of averaging the non-linear function is, in fact, the same as retaining only the zero frequency behavior of the non-linear transfer function.

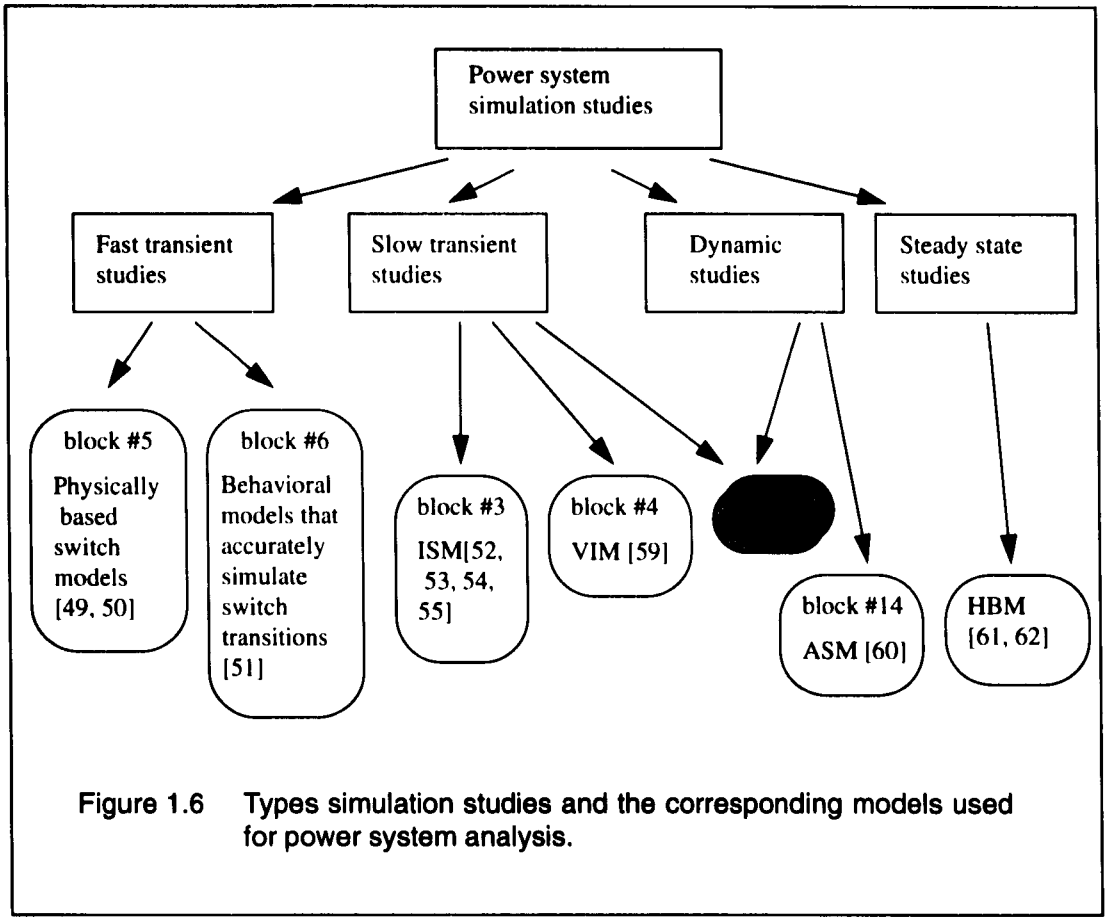

Figure 1.6 Types simulation studies and the corresponding models used for power system analysis.

1.4 Survey of Power Systems Literature

In this section, the various types of simulation studies found in the power systems literature are classified based on the time constants involved in the phenomena being simulated. The modeling techniques used for each of these simulation types are discussed.

1.4.1 Types of simulation studies

Figure 1.6 summarizes the types of simulation studies. The classification of the simulation studies is based on the time constants involved in the phenomena being studied:

1. *Fast transient studies*: The time constants are typically in the range of ten to hundreds of microseconds. The accurate modeling of switch transition is

necessary.

2. *Slow transient studies*: The time constants are typically in the range of few milliseconds. The harmonics in the switching waveforms are important, but the switch transition waveforms may be approximated.

3. *Dynamic studies*: The time constants are typically in the range of hundreds of milliseconds. The harmonics in the switching waveforms are not important and may be approximated by their average values.

4. *Steady state studies*: The final steady state reached by the system is of interest in such studies. The transient response before reaching steady state is not important.

1.4.2 Modeling techniques available in power systems literature

Due to the large size of a typical power system network, only a few of the modeling and simulation techniques available in the power electronics literature (shown in Figure 1.1 and Figure 1.2) can be directly applied to the study of power converters in power systems. Figure 1.6 shows models that have been used for each type of power system simulation study. The block numbers shown in Figure 1.6 correspond to those shown in Figure 1.1 and Figure 1.2.

Physically based models and behavioral models that accurately simulate switching transients have been used for fast transient studies. The noise interference caused by converter switching [49], the overvoltages caused by reverse recovery of diodes [50] and the switching of a solid state circuit breaker [51] are examples of such studies.

The ISM and the VIM have been extensively used for slow transient studies [52-55]. In general, simulations using these models are extremely useful when the focus of study is the overall behavior of the converter and not the detailed switching waveforms.

However, for a typical numerical integration method, the truncation error is dependent on the time step size used [56]. The truncation error is also dependent on the time derivative of the signal being simulated. In the case of a switched network, the time derivative at the instant of switching is very large. Hence, in order to limit the numerical truncation error, the simulation time step has to be kept very small during the switching instants. In the case of variable step simulators [22,23], smaller simulation steps are used during switch transitions. This reduction in time step results in computational inefficiency. The Electro Magnetic Transients Program (EMTP) is a simulator widely used in the electric power industry [57]. This simulator uses a fixed time step algorithm. The penalty of using small time steps is worse in the case of simulators such as the EMTP, since the time step has to be kept small throughout the simulation. The discontinuous nature of the ISM and the VIM also leads to problems of numerical oscillations [58]. The use of numerical snubbers is one method of avoiding the undesired oscillations [26]. However, besides being an unnecessary burden on the user, numerical snubbers also introduce inaccuracies [59]. The other methods, used to solve the oscillation problem, involve reduction of time step size, or the temporary use of different integration technique, or the use of smooth rather than instantaneous switching transitions [25,26,52, 59]. All these methods are at the expense of additional computational times.

The Average Switch Model (ASM) has been used for dynamic studies [60]. However, the ASM is accurate only if the time period of switching is significantly smaller than the time constants of the phenomena being studied.

The power flow solution of a network is an example of steady state studies. The Harmonic Balance Method (HBM) has been used to find the steady state harmonic power flow in a system [61]. The HBM has also been used to develop a steady state model for a Thyristor Switched Reactor (TSR) [62].

1.5 Basic Goals and Approach of Dissertation

The basic goal of this dissertation is to develop simulation models for three power electronic converters - (i) a 12-pulse Static Compensator, (ii) a Pulse Width Modulated (PWM) STATCOM and (iii) a PWM Dynamic Voltage Restorer (DVR). The challenge involved in the development of the model is two fold. Firstly, the current and voltage waveforms of power converters are discontinuous. The discontinuous waveforms, coupled with the large size of a typical power system, pose a challenge to develop computationally efficient simulation models. Secondly, the design of these converters has to be system specific. Presently, these devices exist only in their prototype forms. Hence the information regarding the design of the STATCOM and the DVR is not available prior to the development of the models. Hence the process of model development also involves the design of the power converters.

1.5.1 Disadvantages of previously used modeling techniques

As mentioned in section 1.4, the ISM and the VIM have been extensively used for slow transient studies. However these models are discontinuous in nature and the numerical problems associated with them are solved only at the cost of additional computation time. The ASM is continuous but it does not simulate the switching frequency harmonics of a converter and hence it can be used only for dynamic studies. The HBM is continuous in nature. It is also capable of simulating the switching frequency harmonics of a converter. However, it cannot be directly implemented on standard circuit simulators. The GASM, available in the power electronics literature [36], is continuous as well as capable of simulating the switching frequency harmonics of a converter. However, like the HBM, it cannot be directly implemented on standard circuit simulators. The other time domain simulation techniques available in the power electronics literature [43,44,45,46] are based

on state space formulation. Hence these techniques are incompatible with most standard circuit simulators [47].

1.5.2 Approach used in this dissertation

Based on the above observations, the specific goals of this dissertation may be stated as follows:

1. To develop and implement a new modeling technique that has accuracy comparable to that of the ISM, but does not have the numerical problems associated with the ISM.

2. To use the new modeling technique to develop simulation models for three CPD's - (i) 12-pulse Static Compensator (STATCOM), (ii) Pulse Width Modulated (PWM) STATCOM, (iii) PWM Dynamic Voltage Restorer (DVR).

In order to achieve the first goal, a new technique to model a power converter is developed. The resulting converter model is referred to as the *Transient Behavioral Model* (TBM) of a power converter. The starting point for developing the TBM is the ISM. In the TBM, the switches of the power converter are modeled as voltage and current sources controlled by the switching function (block #14 in Figure 1.1). Then the describing function method (block #E in Figure 1.5) is used to approximate the switching function generator. The resulting model is capable of performing slow transient simulations and dynamic simulations (Figure 1.6) with the accuracy provided by the ISM but without the numerical problems associated with it.

In order to achieve the second goal, it is necessary to have the information regarding the various components for the STATCOM and DVR. However, the design of these converters is system specific and hence the information regarding these models is not available prior to the development of the models. Hence the design of the converter and the

development of the model proceed simultaneously. The procedure essentially involves analytical calculations to determine the component parameters, followed by simulation studies to refine the analytically obtained parameter values. At the end of the process, a complete design of the power converter, along with its simulation model, is developed.

All simulations presented in this dissertation are performed using SABER due the ease of developing models with its Analogy Hardware Description Language (AHDL). Some of the simulation studies are also performed using EMTP.

1.6 Organization of Dissertation

The rest of the dissertation is organized as follows:

In Chapter 2, the development of a TBM of a converter is described in detail. The advantages as well as limitations of the TBM are identified. The use of the TBM is demonstrated with the help of three benchmark power converter configurations - (i) buck converter in voltage control mode, (ii) buck converter in current control mode and (iii) three phase dc/ac inverter in phase control mode. The TBM is validated by comparing its results with those of accurate physical models. The performance of the TBM is compared with that of the ISM.

In Chapter 3, the TBM technique is used to develop detailed models of two STATCOM's. A STATCOM is a shunt connected CPD, capable of injecting controlled amounts of current into the power system. Models are developed for two implementations of the STATCOM - the first using a 12-pulse dc/ac voltage source inverter, and the second using a high frequency PWM dc/ac voltage source inverter. A practical 15-kV distribution feeder with power quality problems [50] is simulated to study the performance of the STATCOM. For the sake of comparison and validation, the STATCOM models are also

developed using the ISM.

In Chapter 4, the TBM technique is used to develop a detailed model of a Dynamic Voltage Restorer (DVR). The DVR is a series connected CPD, capable of injecting controlled amounts of voltage into the power system. The DVR modeled here consists of three single phase PWM voltage source inverters. The 15-kV distribution feeder is simulated to study the performance of the DVR. For the sake of comparison and validation, the DVR model is also developed using the ISM.

In Chapter 5, the summary, contributions and recommendations for future work are presented.

For the reader's convenience, a list of abbreviation used in this dissertation is given in the Appendix A.

2. The Transient Behavioral Model

In this chapter, a new technique to model power electronic converters is described. The resulting power converter model is referred to as a Transient Behavioral Model (TBM). The TBM approximates an Ideal Switch Model (ISM) of a power converter by neglecting the higher order harmonics of the switching frequency. In Section 2.1, basic steps involved in the development of the TBM are described. In Section 2.2, the TBM is compared with the Harmonic Balance Method (HBM). The comparison shows that the TBM yields results as accurate as the HBM, without the cumbersome procedure involved in implementing the HBM in a time domain simulator. In Sections 2.4 through 2.6, the development of the TBM's for three benchmark power converter configurations is demonstrated. The three benchmark converters used for demonstration have been carefully selected so that the TBM for many other converters can be developed by following the example of one of the three benchmark converters. The performance of the TBM is compared with that of the Ideal Switch Model (ISM). For the sake of validation, the simulation results are also compared with those using accurate physically based switch models. The advantages as well as the limitations of the TBM are discussed.

2.1 Development of the Transient Behavioral Model

The development of the TBM is heuristic. It involves two simple steps -

1. representing the switching network of a power converter by a set of sources controlled by its switching function, and
2. approximating the nonlinear switching function generator in the control system by its describing function.

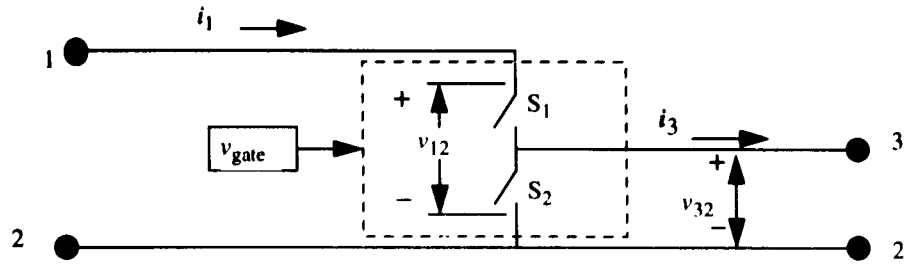

Figure 2.1 Typical switch configuration in a PWM power converter.

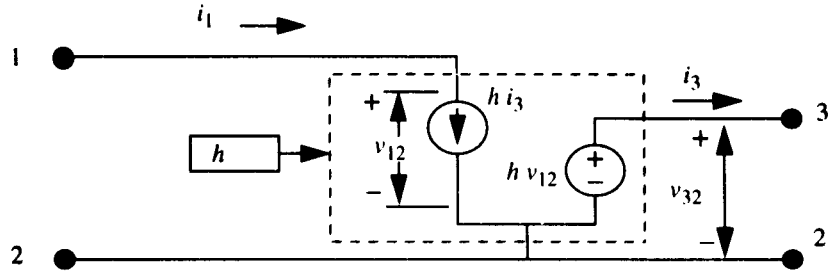

Figure 2.2 PWM switch modeled by a set of controlled sources.

Consider the typical Pulse Width Modulated (PWM) switch configuration shown in Figure 2.1. Let h be the switching function such that $h = 1$ when S_1 is closed, and $h = 0$ when S_2 is closed. If the PWM switch is modeled as an ideal switch, then the currents and voltages of the switch may be described by the following equation:

$$\begin{aligned} v_{32} &= (h)\ (v_{12}) \\ i_1 &= (h)\ (i_3) \end{aligned} \tag{2.1}$$

Based on equation (2.1), the PWM switch can be modeled by a set of controlled sources as shown in Figure 2.2. Now consider a power electronic converter operated in open loop. If each PWM switch of the converter is systematically replaced by the model shown in Figure 2.2, then the power converter can be modeled as shown in Figure 2.3.

Next, consider a power converter in closed loop (Figure 2.4). The output (y) is

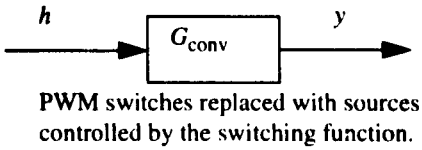

Figure 2.3 Model of a power converter in open loop.

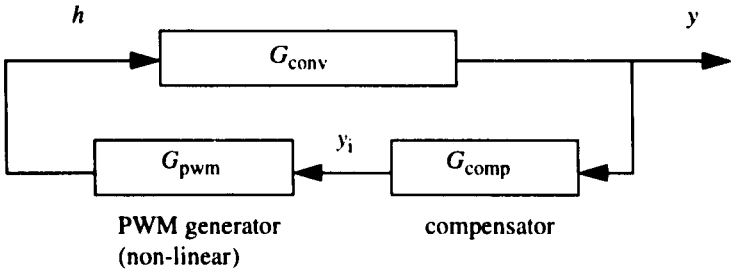

Figure 2.4 Power converter in closed loop.

processed through a compensator. The output of the compensator (y_i) is used as input to a nonlinear PWM generator that generates the switching function (h). A power converter model with the switches replaced by controlled sources is obtained by substituting the model of Figure 2.3 into Figure 2.4. This completes the first step in developing the TBM. Note that taking an average of the model in Figure 2.3 over the PWM period will yield the open loop ASM of a power converter.

The next step in deriving the TBM is to approximate the nonlinear PWM generator using the technique of describing functions [48]. Consider the Fourier approximation of the switching function (h):

$$h(t) = A_0 + \sum_{n=1}^{\infty} A_n \cos(\omega_s n t) + \sum_{n=1}^{\infty} B_n \sin(\omega_s n t) \qquad (2.2)$$

where ω_s is the switching frequency of the converter. For a typical power converter, G_{conv}

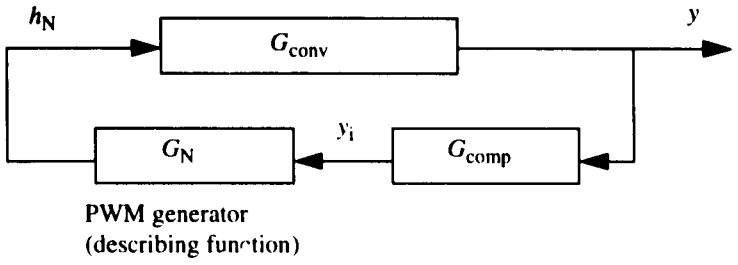

Figure 2.5 Transient behavioral model (TBM) of a power converter.

has low pass characteristics due to the presence of an output filter. Also, for a typical control system, G_{comp} has low pass characteristics. Under such conditions, it can be assumed that the higher order harmonics of h are filtered out such that the input (y_i) to the nonlinear block (G_{pwm}) contains only the lower order harmonics. Based on this consideration, a describing function G_N can be used to approximate the behavior of G_{PWM} as follows:

$$G_{pwm} \approx G_N = \frac{h_N}{y_i} = \frac{A_0 + \sum_{n=1}^{N} A_n \cos(\omega_s n t) + \sum_{n=1}^{N} B_n \sin(\omega_s n t)}{y_i} \qquad (2.3)$$

where N is the highest order harmonic desired. The resulting model (Figure 2.5) is the TBM of a power converter. Note that if only the zero frequency (dc) term of the Fourier series is included in the describing function (G_N), then h_N will reduce to the average value of h. Since the average value of h is nothing but the duty cycle (d) of the switching function, the TBM essentially reduces to the ASM. If all the Fourier terms are included in G_N, then the TBM yields results identical to the ISM. Thus, depending on the number of Fourier terms included in G_N, the accuracy of the TBM can be varied from that of the ASM to that of the ISM.

The number of Fourier terms in the TBM can be varied dynamically during a single

simulation run. For example, the initial portion of a simulation can be performed using a TBM with only the dc Fourier term. The TBM with only the dc term has the computational efficiency of an ASM. In this way, the simulation can rapidly reach a desired operating point. Once the desired operating point is reached, the higher order Fourier terms of the TBM are enabled, and the simulation proceeds with a higher level of accuracy.

2.2 Comparison with the Harmonic Balance Method

The HBM is a powerful method for performing the steady state analysis of a nonlinear system [61]. However, the procedure required to use the HBM for time domain simulations is cumbersome and inconvenient to implement on a standard circuit simulator [37]. In contrast to the HBM, the implementation of the TBM for time domain simulations is easy and convenient. Since both the TBM and the HBM approximate system equations by neglecting the higher order Fourier terms, a comparison of the two methods provides a better understanding of the approximation involved in the TBM.

A power converter can generally be expressed by a non-linear differential equation:

$$\boldsymbol{x} = G_{conv}(\boldsymbol{h},\boldsymbol{x}) \tag{2.4}$$

where $\boldsymbol{x}$ is a vector of system states and $\boldsymbol{h}$ is switching function. The HBM uses the Fourier representation of the system states so that equation (2.4) is converted into an equivalent set of simultaneous algebraic equations. The algebraic equations are then solved to obtain the steady state values of the system states. The HBM does not compute the exact solution of equation (2.4). In fact, it computes the exact solution of the following equation which is obtained by neglecting some terms on the right hand side of equation (2.4):

$$z = G_{conv}(\boldsymbol{h},z) - \varepsilon_{HBM}(\boldsymbol{h},z) \tag{2.5}$$

The solution z of equation (2.5) and is a good approximation of solution $\boldsymbol{x}$ of equation (2.4),

if ε_{HBM} is small.

In contrast to the HBM, the TBM uses a truncated Fourier series representation of $\boldsymbol{h}$. This is done in order to avoid numerical problems due to discontinuities during numerical simulation of equation (2.4). Hence even the TBM does not compute the exact solution of equation (2.4), but rather it computes the exact solution of:

$$z = G_{conv}(\boldsymbol{h}, z) - \varepsilon_{TBM}(\boldsymbol{h}, z) \tag{2.6}$$

The difference between the TBM and the HBM arises from the difference between ε_{HBM} and ε_{TBM} used in equations (2.5) and (2.6).

Consider a converter with S PWM switches operating in continuous conduction mode. Then, each PWM switch has two possible states and the power converter will have a total of 2^S switching states. If $h_i = 1$ when the converter is in the ith switching state and $h_i = 0$ otherwise, then the state space model of the converter is given by:

$$\frac{dx}{dt} = \left(\sum_{i=1}^{2^S} h_i A_i \right) x + \left(\sum_{i=1}^{2^S} h_i B_i \right) u \tag{2.7}$$

where A_i, B_i correspond to the converter topology when $h_i = 1$. For the sake of simplicity, it is assumed that there is only one state variable, hence x is a scalar in equation (2.7). Further, it is assumed that the forcing function u is constant since its time constants are large compared to the time constants of h_i and x. The Fourier representation of h_i and x are given by:

$$h_i = \sum_{m=0}^{\infty} h_{im} \sin(m\omega + \theta_{im}) \tag{2.8}$$

$$x = \sum_{n=0}^{\infty} x_n \sin(n\omega + \phi_n) \tag{2.9}$$

Substituting equations (2.8) and (2.9) in (2.7) gives:

$$\frac{d}{dt}\sum_{n=1}^{\infty} x_n \sin(n\omega + \phi_n) = \sum_{i=1}^{2^s}\sum_{m=0}^{\infty} h_{im}\sin(m\omega + \theta_{im})\, B_i u$$
$$+ \sum_{i=1}^{2^s}\sum_{m=0}^{\infty}\sum_{n=0}^{\infty} \frac{h_{im}A_i x_n}{2}\cos((m-n)\omega + \theta_{im} - \phi_n) \qquad (2.10)$$
$$- \sum_{i=1}^{2^s}\sum_{m=0}^{\infty}\sum_{n=0}^{\infty} \frac{h_{im}A_i x_n}{2}\cos((m+n)\omega + \theta_{im} + \phi_n)$$

In the HBM, the terms of the same frequency are equated. After some algebraic and trigonometric manipulations, the equation corresponding to the pth order harmonic is:

$$\frac{d}{dt}(x_p \sin(p\omega + \phi_p)) = \sum_{i=1}^{2^s} h_{ip}\sin(p\omega + \theta_{ip})\, B_i u \qquad (2.11)$$
$$+ \sum_{i=1}^{2^s}\sum_{n=0}^{\infty} \frac{h_{i(p+n)}A_i x_n}{2}\cos(p\omega + \theta_{i(p+n)} - \phi_n) \qquad p = 0 \text{ to } \infty$$
$$- \sum_{i=1}^{2^s}\sum_{n=0}^{\infty} \frac{h_{i(p-n)}A_i x_n}{2}\cos(p\omega + \theta_{i(p-n)} + \phi_n)$$

Equation (2.11) is a set of infinite simultaneous equations. Also note that each equation in (2.11) yields two equations, by equating the *cos* and *sin* terms. In some physical systems, such as a power converter, the magnitude of Fourier coefficients decreases as the order of the harmonic increases. Under such conditions, a reasonable approximation would be to neglect all x_n for ($n > N$). This leads to a system of infinite equations with $2N$ unknowns (N unknowns for magnitude x_n, and N unknowns for phase ϕ_n). In order to make the number of equations same as the number of unknowns, all equations for ($p > N$) are neglected. Note that neglecting the equations for ($p > N$) is consistent with the assumption that the

harmonics of order greater than N are negligible. The remaining equations are used to solve for the magnitude and phase of first N harmonics of x. The error in the solution results from the equations for ($p > N$) that are neglected. From equations (2.10) and (2.11) the following error term is obtained:

$$\begin{aligned}\varepsilon_{HBM} = & \sum_{i=1}^{2^S} \sum_{m=N+1}^{\infty} h_{im} \sin(m\omega + \theta_{im}) \\ & + \sum_{i=1}^{2^S} \sum_{n=0}^{N} \sum_{(m=N+1+n)}^{\infty} \frac{h_{im} A_i x_n}{2} \cos((m-n)\omega + \theta_{im} - \phi_n) \\ & - \sum_{i=1}^{2^S} \sum_{n=0}^{N} \sum_{(m=N+1-n)}^{\infty} \frac{h_{im} A_i x_n}{2} \cos((m+n)\omega + \theta_{im} + \phi_n)\end{aligned} \tag{2.12}$$

On the other hand, the error in the TBM is introduced by neglecting the higher order harmonics in h_i ($m > N$). Thus

$$\begin{aligned}\varepsilon_{TBM} = & \sum_{i=1}^{2^S} \sum_{m=N+1}^{\infty} h_{im} \sin(m\omega + \theta_{im}) \\ & + \sum_{i=1}^{2^S} \sum_{n=0}^{N} \sum_{m=N+1}^{\infty} \frac{h_{im} A_i x_n}{2} \cos((m-n)\omega + \theta_{im} - \phi_n) \\ & - \sum_{i=1}^{2^S} \sum_{n=0}^{N} \sum_{m=N+1}^{\infty} \frac{h_{im} A_i x_n}{2} \cos((m+n)\omega + \theta_{im} + \phi_n)\end{aligned} \tag{2.13}$$

It can be seen from equations (2.12) and (2.13) that if the Fourier coefficients of h are small for the higher order harmonics, then both of ε_{TBM} and ε_{HBM} are small. Hence, both the HBM and the TBM yield good approximations of the original system equations. However, the process of developing the HBM is cumbersome. Further, in order to use the HBM for time domain simulations, it is necessary to develop a special simulation algorithm. In contrast to this, the TBM is developed using a simple procedure. The resultant model is in a form that can be easily implemented in a standard circuit simulator. Thus, the

TBM is as accurate as the HBM and it also in a form that is easy to implement in a standard time domain simulator.

2.2.1 *Special Case of Linear Equations*

Consider a special case where $\boldsymbol{A}_i = \boldsymbol{A}$ for all i. For such cases, the state variable equation can be rewritten as:

$$\frac{d\boldsymbol{x}}{dt} = \left(\sum_{i=1}^{2^S} h_i \right) \boldsymbol{A}\boldsymbol{x} + \left(\sum_{i=1}^{2^S} h_i \boldsymbol{B}_i \right) \boldsymbol{u} \tag{2.14}$$

Now, at any given time, only one of the h_i's is 1 and the other h_i's are equal to 0. Hence equation (2.14) can be rewritten as:

$$\frac{d\boldsymbol{x}}{dt} = \boldsymbol{A}\boldsymbol{x} + \left(\sum_{i=1}^{2^S} h_i \boldsymbol{B}_i \right) \boldsymbol{u} \tag{2.15}$$

Equation (2.15) is a linear differential equation in $\boldsymbol{x}$ and h_i. Hence by principle of superposition, it is seen that if h_{iN} (the Nth order Fourier representation of h) is used in equation (2.15), then the solution $\boldsymbol{x}_N$ is indeed the Nth order Fourier representation of the solution $\boldsymbol{x}$. In other words, it can be said that if the matrix $\boldsymbol{A}$ does not change with each switching state, then using the TBM gives an accurate Nth order Fourier representation of the original system.

An important class of converters for which the matrix $\boldsymbol{A}$ does not change with different switch configurations are dc/ac inverters with an ideal dc voltage source. If the dc source has an internal resistance, then as long as the resistance is sufficiently low, the change in matrix $\boldsymbol{A}$ for different switch configurations is negligible. Hence the TBM gives accurate Nth order Fourier representation of the dc/ac inverter. Even for dc/ac inverters with a capacitor on the dc side, if the capacitor voltage is fairly constant during a single switching period, the resulting TBM is an accurate Nth order representation of the original system. As shown later in Chapters 3 and 4, STATCOM's and DVR's consist of dc/ac

inverters with a capacitor on the dc side. Hence, the TBM for these devices is an accurate *N*th order representation of the original system.

2.3 Selection of Benchmark Converters for Demonstration of TBM

In the rest of the chapter (Sections 2.4 through 2.6) the steps involved in the development of a TBM are demonstrated using the following benchmark power converter circuits [71]:

- buck converter in voltage control mode,
- buck converter in current control mode,
- dc/ac inverter in phase control mode.

As described in Section 2.1, the development of the TBM involves two basic steps. The first step can be easily performed for any converter that has the switch configuration shown in Figure 2.1. The second step is more involved and has to be performed differently for different converters. Specifically, each converter will require a different describing function (G_N) depending upon the switching technique used. In order to serve as examples for future use of the TBM, each converter configuration selected for demonstration purpose employs a different switching technique. The buck converter in voltage control mode, represent a case for which the duty cycle can be explicitly determined in terms of control signals. The buck converter in current control mode represent a case for which the duty cycle is implicitly determined in terms of the control signals. Finally, the dc/ac inverter in phase control mode represent a case for which the duty cycle is kept constant (at 50%) whereas the phase of the switching function is varied by the control circuit.

2.4 Buck Converter in Voltage Control Mode

Consider the buck converter shown in Figure 2.6. The converter is controlled such

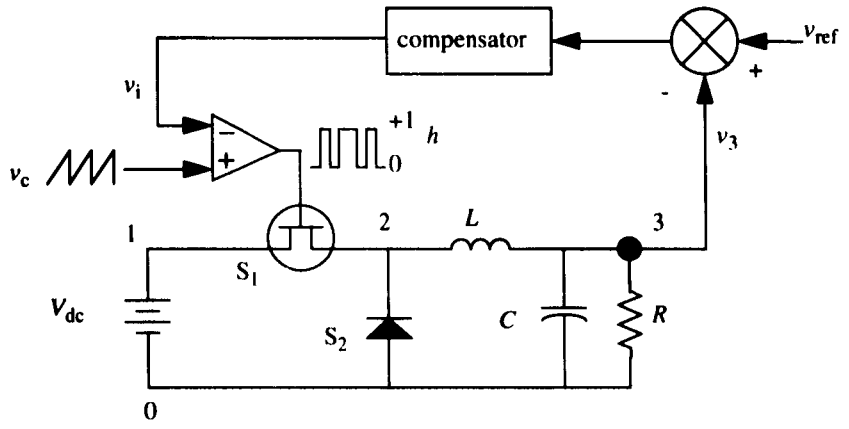

Figure 2.6 Buck converter in voltage control mode.

that its output voltage (v_3) is maintained at a desired reference value (v_{ref}). Since the configuration of the MOSFET (S_1) and the diode (S_2) is the same as that of the PWM switch configuration shown in Figure 2.1, it is possible to model them by the controlled sources shown in Figure 2.2. This completes the first step described in Section 2.1 for developing the TBM. The next step is to determine the describing function G_N.

2.4.1 Determination of the Describing Function

The switching function (h) is determined by the carrier signal (v_c) and the input signal (v_i). For a typical buck converter in voltage control mode, the change in v_i within a single switching period (T) is negligible. This assumption is consistent with the assumption made in Section 2.1 regarding the low pass characteristics of G_{comp}. Under this assumption, for a given carrier signal v_c, the switching function can be expressed explicitly in terms the input signal v_i. For a sawtooth carrier signal, with peak voltage of +1 and time period T (Figure 2.7), the switching function is:

$$h = 1 \text{ ..... for } 0 \le t \le v_i T \tag{2.16}$$

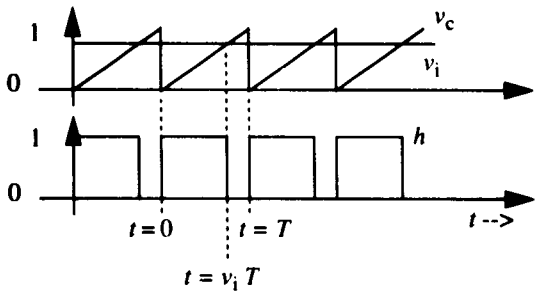

Figure 2.7 Top: saw tooth carrier signal (v_c) and input signal (v_i); bottom: switching function (h) for generating gate triggering signals.

$$h = 0 \text{ ..... for } \quad v_i T \le t \le T \tag{2.17}$$

Using equations (2.16) and (2.17), the following describing function is obtained:

$$G_N(v_i) = v_i + \sum_{n=1}^{N} \left(\frac{1}{\pi n} \sin(2\pi n v_i) \cos(\omega_s n t) \right) + \sum_{n=1}^{N} \left(\frac{1}{\pi n} [1 - \cos(2\pi n v_i)] \sin(\omega_s n t) \right) \tag{2.18}$$

The resulting model of the buck converter is shown in Figure 2.8.

2.4.2 *Validation and Performance Evaluation - Variable Time Step Simulator*

The purpose of the simulations described in this section is to study the performance of the TBM of the buck converter in a variable time step simulator such as SABER. The model described in Section 2.4.1 is developed on SABER. The switching frequency of the buck converter is 10 kHz. The response of the buck converter to a step in v_{ref} from 0 V to 8 V is simulated using the (a) ISM, (b) TBM with three Fourier terms, and (c) TBM with only the dc Fourier term. Note that the TBM with only the dc term reduces to the ASM. For the sake of validation, the simulation is also performed using physically based models of a

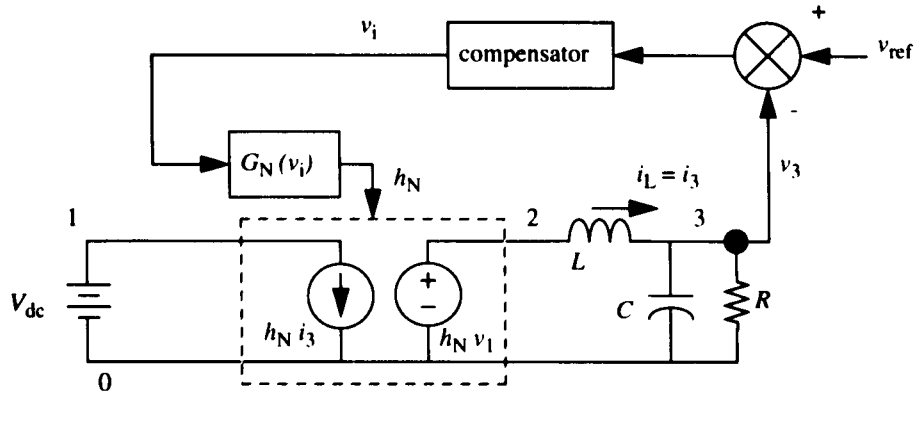

Figure 2.8 Model of the buck converter using the TBM.

MOSFET and a diode [63]. The accuracies of the physically based MOSFET and diode models have been established by comparison with experimental results in [63]. Figure 2.9 shows the voltage across switch S_2 and current through the inductor simulated using the physically based models. The results show:

- the turn-on and turn-off characteristics of the switches,
- the harmonics (ripples) in the voltage and current waveforms,
- the dynamics of the voltage and current (i.e. the rise from zero to their respective steady state values).

Figure 2.10 and Figure 2.11 show the results obtained using the different switch models. The voltage and current waveforms simulated by the three models differ in the amount of information that can be extracted from the waveforms. In general, the three models give results consistent with the physically based model. However, unlike the physically based model, the ISM approximates the switching waveforms by instantaneous transitions between the on and off states of the switch. The TBM with three Fourier terms

approximates the waveforms even more by neglecting the higher harmonic components in the voltage and current waveforms. The TBM with only the dc Fourier term simulates only the dynamics of the converter by neglecting all but the average component of the waveforms. The total CPU time required to simulate the buck converter over a period of 10 ms with the different switch models is shown in Table 2.1.

Table 2.1: Comparison of CPU time for different switch models - simulation of a buck converter in voltage control mode using SABER.

Switch model	CPU time (seconds)
Physically based model	475
ISM	15
TBM with three Fourier terms	7.85
TBM with only the dc Fourier term	1.45

The simulations are performed on an HP Series 700 workstation. The results show that the TBM with three Fourier terms is almost twice as computationally efficient as the ISM. The TBM with only dc term (which reduces to the ASM) is 10 times as efficient as the ISM.

2.4.3 Performance Evaluation - Fixed Time Step Simulator

The simulation of the buck converter in voltage control model is repeated on a fixed time step simulator. The EPRI-EMTP is used for this purpose. The Transient Analysis of Control Systems (TACS) feature of EMTP is used for the development of the TBM [64].

The usual procedure for determining the time step size in a fixed time step simulator is as follows:

1. Simulate the system with a large time step size.

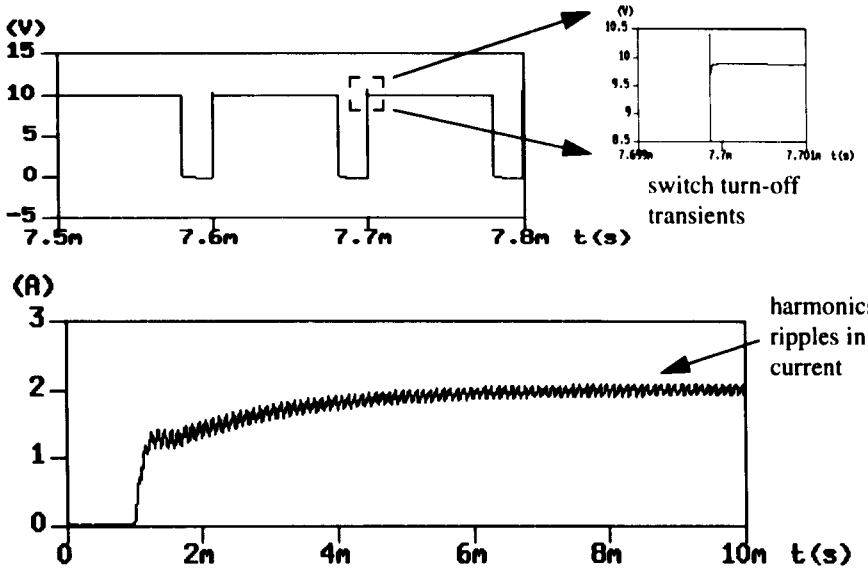

Figure 2.9 Simulation using physically based model - (a) voltage across switch S2, (b) inductor current.

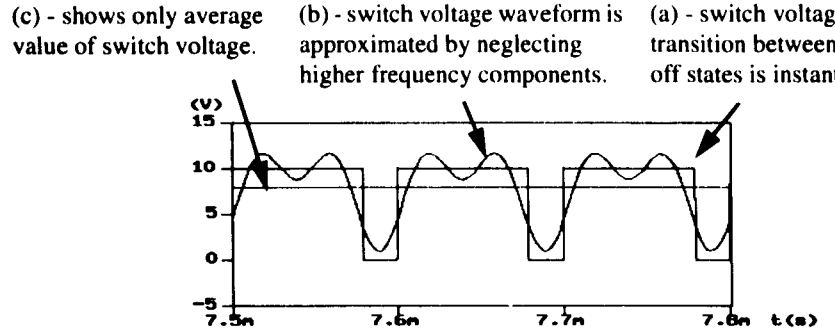

Figure 2.10 Voltage across switch S2 - (a) ISM, (b) TBM with three Fourier terms, (c) TBM with only the dc Fourier term.

2. Reduce time step size by half.

3. Repeat simulation with the reduced time step size.

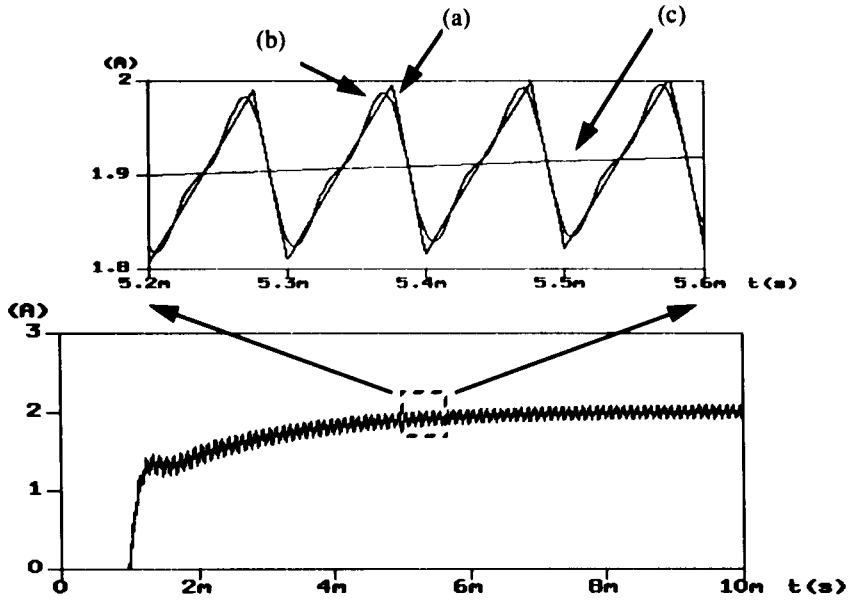

Figure 2.11 Inductor current - (a) ISM, (b) TBM with three Fourier terms, (c) TBM with only the dc Fourier term.

4. If results of simulation are significantly different from those using the previous (larger) time step size, then go to step 2.

5. If simulation results are not significantly different from those in with the previous (larger) time step size, then the previous time step size is the time step size to be used for the system being simulated.

The simulation of the buck converter shown in Figure 2.6 is performed using the (a) ISM, (b) TBM with three Fourier terms, and (c) TBM with only the dc Fourier term. The steps listed above are used to determine the appropriate time step size for each type of model. The results of the simulation are shown in Figure 2.12. The results from all the switch models are consistent. Also, the results obtained by EMTP are consistent with those obtained by SABER as observed by comparing Figure 2.11 and Figure 2.12. The only difference observed between the EMTP results and the SABER results is that with the

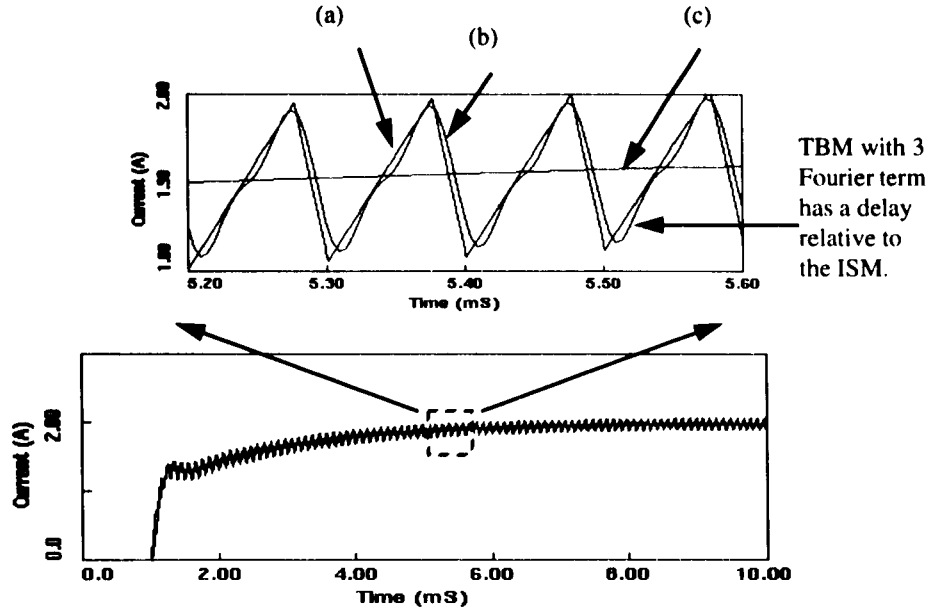

Figure 2.12 Simulation of buck converter in voltage control mode using the EMTP - (a) ISM, (b) TBM with three Fourier terms, (c) TBM with only the dc Fourier term.

EMTP, the inductor current simulated by TBM with three Fourier terms has a small delay relative to the inductor current simulated by the ISM as observed in Figure 2.12. This delay is due to the delay between the EMTP and the TACS network. The observations regarding the accuracy of the three models is similar to those made in Section 2.4.2.

The time step size used and the corresponding CPU time are summarized in Table 2.2. It is observed that the simulation with the ISM has to be performed using a time step size of 0.5 μs, whereas the simulation using the TBM can be performed with a time step size of 5 μs. As a result, the TBM is 3 times as computationally efficient as the ISM. The TBM with the only the dc Fourier term can be simulated with a time step of 20 μs, hence it is computationally most efficient amongst the three switch models.

In order to demonstrate the effect of time step size on the accuracy of the results,

Table 2.2: Comparison of CPU time for different switch models - simulation of a buck converter in voltage control mode using EMTP.

Switch model	Time step size (μs)	CPU time (seconds)
ISM	0.5	8.2
TBM with three Fourier terms	5	2.6
TBM with only the dc Fourier term	20	0.3

the simulation using the ISM is repeated with a larger time step size of 10 μs. The results are shown in Figure 2.13. The voltage across the capacitor and the current through the inductor show an irregular variation. This irregular behavior is the result of the inaccuracies caused by the large time step size. For a typical numerical integration method, such as the trapezoidal method used in the EMTP, the truncation error is dependent on the time step size used [56]. The truncation error is also dependent on the time derivative of the signal being simulated. In the case of a switched network, the time derivative at the instant of switching is very large. In order to limit the truncation error, the time step has to be reduced during the switching instants. The irregular behavior observed in Figure 2.13 is due to numerical problems and does not represent the true behavior of the circuit. This is confirmed by the simulation result shown in Figure 2.12, where a time step of 0.5 μs is used.

2.4.4 Variation of Accuracy of TBM During a Single Simulation Run

An interesting property of the TBM is that its accuracy can be easily varied by merely varying the number of Fourier terms used to approximate the switching function. Also, the lower the level of accuracy the higher is the computational efficiency of the TBM. This property is can be exploited in situations where the simulation has to be run for a long period of time for the system to reach a desired operating point. With a TBM, the initial part of the simulation can be performed with only the dc Fourier term so that the system rapidly reaches the desired operating point. Once the desired operating point is reached, the higher

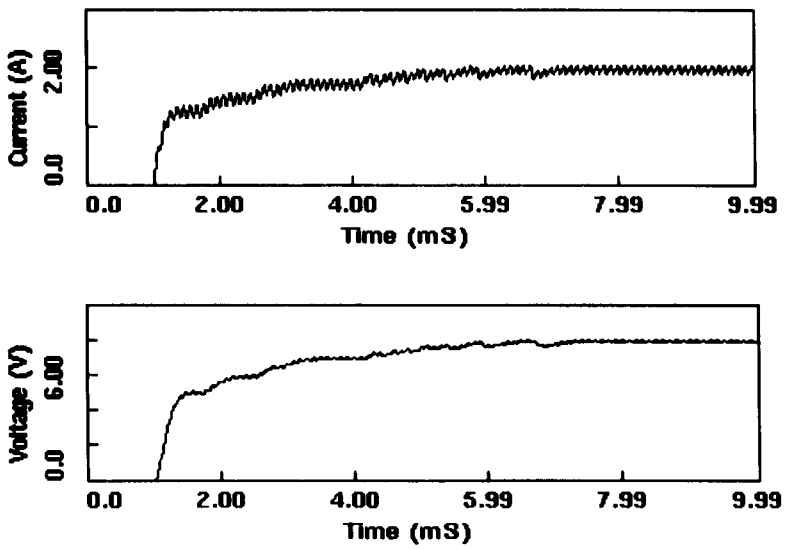

Figure 2.13 Simulation of the buck converter in voltage control mode using the EMTP - top: inductor current; bottom: capacitor voltage. The ISM with a time step of 10 μs is used.

order Fourier terms of the TBM are enabled and the simulation proceeds with a higher level of accuracy. This technique is especially useful since there are many cases where it is difficult, or even impossible, to manually set the desired initial conditions for the simulation. However, it should be noted that use of the dynamic variation of accuracy requires knowledge regarding the approximate time required to reach steady state.

Consider the simulation of the buck converter in voltage control mode. Consider a simulation to study the ripple in the inductor current during steady state. For such studies, the rise of the inductor current from 0 A to 2 A is not of interest. Hence, it is desirable that the simulation proceeds with the fastest possible computation speed from $t = 0$ to $t = 8$ ms. To achieve this, the TBM is modified such that only the dc Fourier term is used till $t = 8$ ms. After $t = 8$ ms, the higher order Fourier terms are activated. The simulation results are

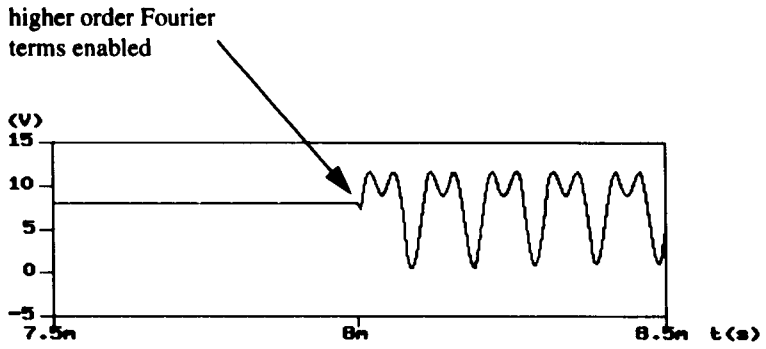

Figure 2.14 Voltage across switch S2 - simulation using TBM with only the dc Fourier term up to 8 ms, and three Fourier terms from 8 ms to 10 ms.

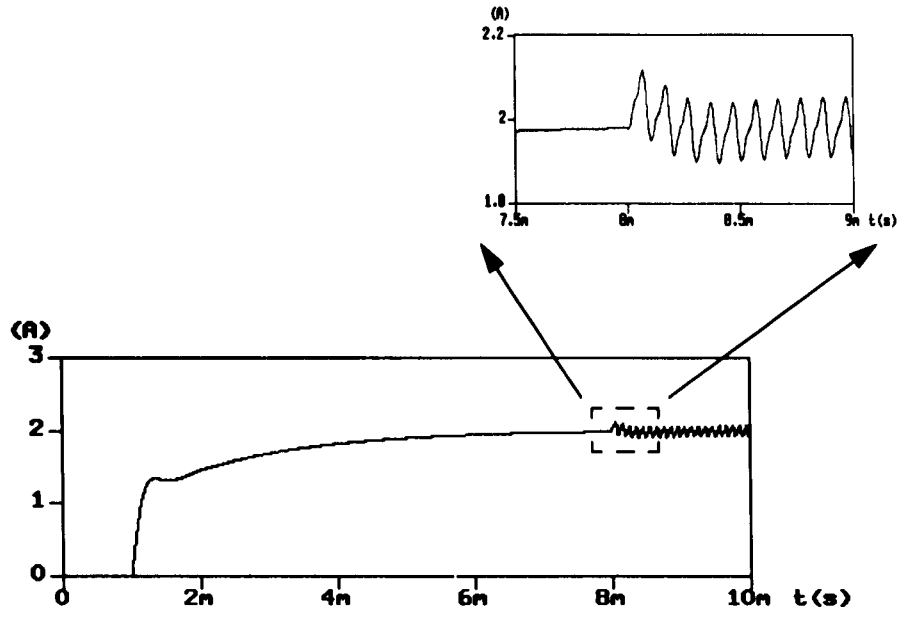

Figure 2.15 Inductor current - simulation using TBM with only the dc Fourier term up to 8 ms, and three Fourier terms from 8 ms to 10 ms.

shown in Figure 2.14 and Figure 2.15. The CPU time for this study, along with the CPU times summarized in Table 2.3. As expected, the TBM with dynamically varied accuracy

is faster than the TBM with three Fourier terms, but slower than the TBM with only the dc Fourier term.

Table 2.3: Comparison of CPU time for different switch models - simulation of a buck converter in voltage control mode using SABER.

Switch model	CPU time (seconds)
Physically based model	475
ISM	15
TBM with three Fourier terms	7.85
TBM with only the dc Fourier term up to 8 ms and three Fourier terms from 8 ms to 10 ms.	2.81
TBM with only the dc Fourier term	1.45

2.5 Buck Converter in Current Control Mode

Consider a buck converter operated in current control mode (Figure 2.16). The control system consists of two loops. The outer loop is the voltage control loop and the inner loop is the current control loop. The outer loop senses the error (v_e) in the load voltage and generates the necessary current reference (i^*). The inner loop controls the switching function (h) such that the inductor current (i_L) tracks the desired reference value (i^*). There are various methods available to implement a current control loop [65]. In this discussion, the constant frequency current control method is considered. In this method, switch S_1 is turned on at the positive edge of a constant frequency clock. This results in a positive voltage across the inductor and hence causes the current i_L to build. When the current reaches the desired reference value, S_1 is turned off and switch S_2 is turned on (Figure 2.17). At the next positive edge of the clock, switch S2 is turned off and the cycle is repeated. For stability reasons, a ramp signal (i_{ramp}) is subtracted from the actual current reference (i^*).

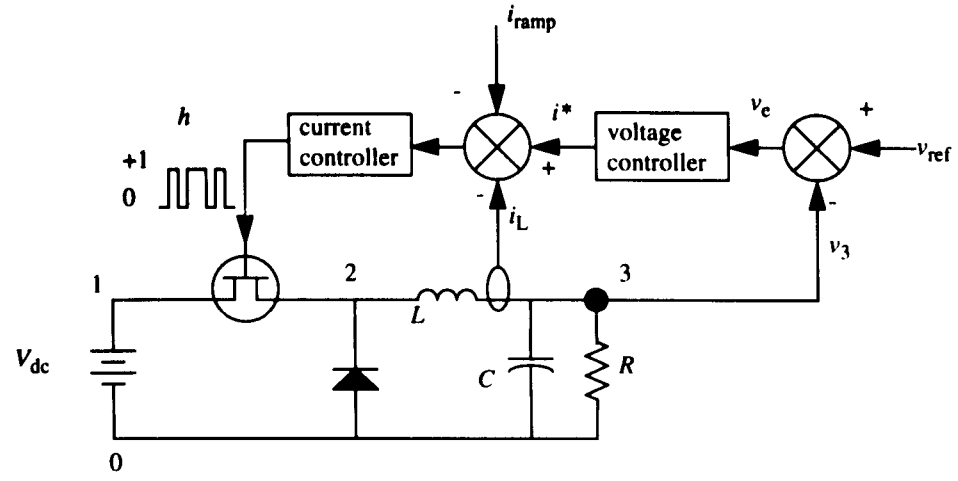

Figure 2.16 Buck converter in current control mode.

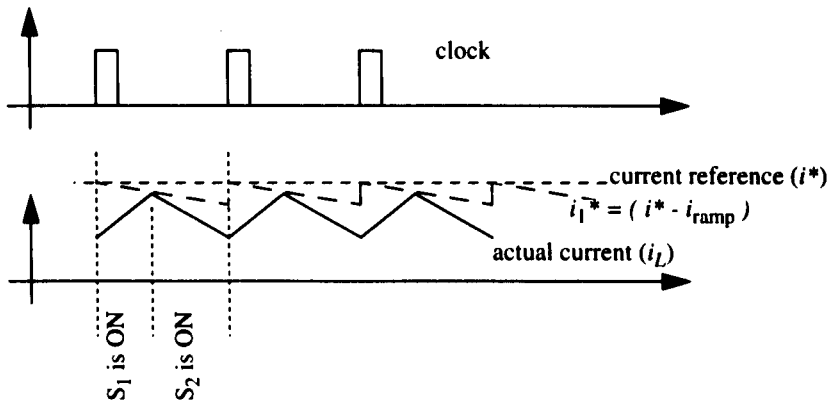

Figure 2.17 Constant frequency current control for buck converter.

2.5.1 Determination of the Describing Function

In the case of a current controlled converter, h is an implicit function of the current and the output filter inductance. Hence, in order to determine the describing function, it is necessary to consider the output filter inductor with the PWM switch (Figure 2.18).

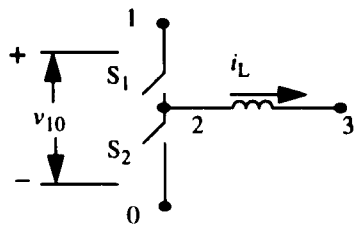

Figure 2.18 Typical configuration of switch and filter inductor in a current controlled PWM converter.

The current through the inductor (i_L) is controlled by the voltage across the inductor. If d is the duty cycle, and T is the time period, then the voltage across the inductor will be (v_1-v_3) during the period dT and (v_0-v_3) during the period $(1\text{-}d)T$. Due to the presence of the output filter capacitor (not shown in Figure 2.18), it can be assumed that the voltage at node 3 is almost constant within a single PWM cycle. The voltage between nodes 1 and 0 can also be assumed to be constant within a single PWM cycle due to the presence of a voltage source between nodes 1 and 0. Then, for known values of the stabilizing ramp magnitude (k), the filter inductor (L) and the voltages at nodes 1, 2 and 3, an implicit expression for the duty cycle can be obtained as below:

$$d^2T(v_1 - v_0) - d[kL - T(v_3 - v_0)] - L\Delta i_L = 0 \qquad (2.19)$$

The switching function for a duty cycle of d is given by:

$$h = 1 \text{ ..... for } \quad 0 \le t \le dT \qquad (2.20)$$

$$h = 0 \text{ ..... for } \quad dT \le t \le T \qquad (2.21)$$

Using equations (2.19) through (2.21), the Fourier coefficients of the describing function can be easily constructed. The resultant TBM is shown in Figure 2.19. Note that the dependence of the describing function on the output filter inductor, corresponds to the use of constraint equations that are incorporated in the ASM for converters in current control

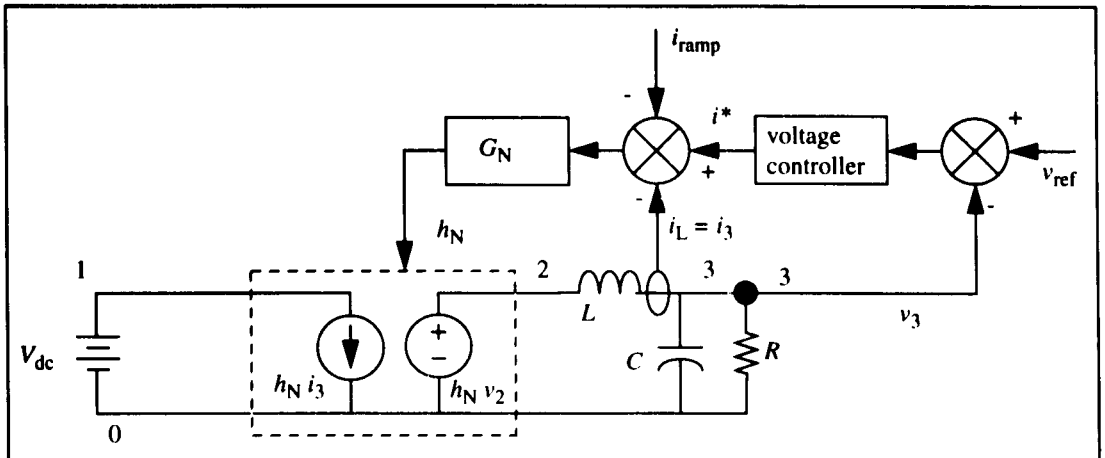

Figure 2.19 Transient behavioral model of a PWM converter in current control mode.

mode [66].

2.5.2 *Validation and Performance Evaluation*

The buck converter in current control mode is simulated first with the accurate physically based models. Then the simulations are performed using the (a) ISM, (b) TBM with only three Fourier terms and (c) TBM with only the dc Fourier term. The simulations are performed in SABER. The results are shown in Figure 2.20 and Figure 2.21. The simulation times required on a HP series 700 workstation are summarized in Table 2.4. The observations regarding the accuracy of the waveforms and the simulation speeds are similar to those for a buck converter in voltage control mode. It should be noted that in the case of the buck converter in voltage control mode, the TBM with three Fourier terms is twice as fast as the ISM. However, in the case of the buck converter in current control mode, the TBM with three Fourier terms is only 50% faster than the ISM due to the additional computation burden of the constraint equation.

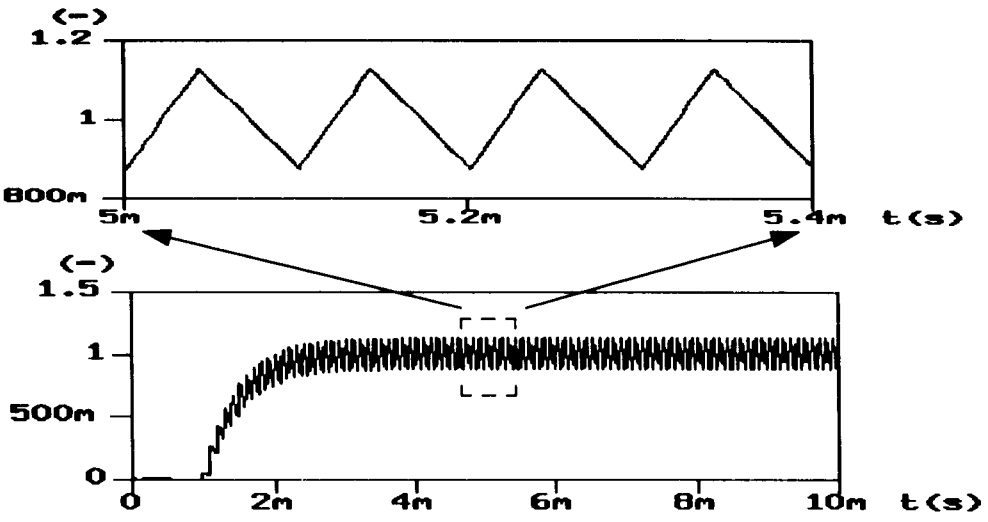

Figure 2.20 Inductor current - simulation of a buck converter in current control mode using physically based switch models.

Table 2.4. Comparison of CPU for different switch models - simulation of buck converter in current control model.

Switch model	CPU time (seconds)
Physical models	507
ISM	16.9
TBM with three Fourier terms	11.0
TBM with only dc term	1.22

2.6 DC/AC Inverter in Phase Control Mode

Consider a six-pulse, three phase dc/ac inverter in phase control mode (Figure 2.22). To make the example more interesting, the inverter control is configured similar to that of a Static Compensator (STATCOM) [15]. The output of the inverter is tied to a three phase voltage source through inductors. The three phase ac source corresponds to the power system and the inductors correspond to the impedance of the transformer that ties a

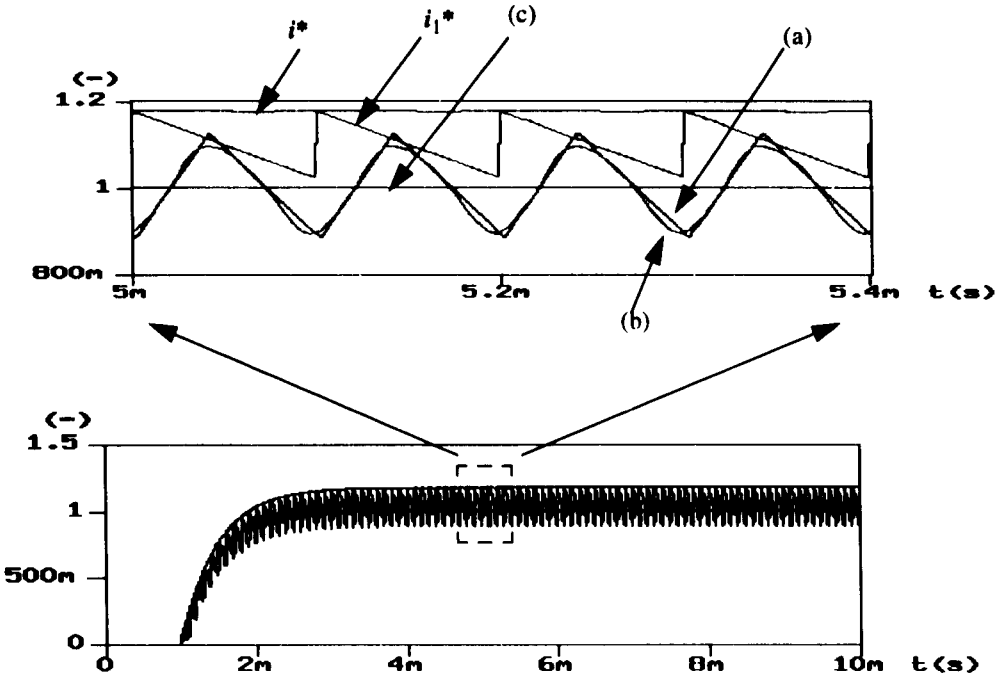

Figure 2.21 Inductor current - simulation of a buck converter in current control mode using (a) ISM, (b) TBM, (c) ASM.

STATCOM to the power system. The phase of the inverter output voltage is controlled such that the inverter output currents (i_a, i_b, i_c) are always 90^0 out of phase with the respective power system voltages (v_a, v_b, v_c). In order to achieve such a control, the inverter output currents are transformed from the *abc* coordinates to the rotating *dq* coordinates. The *dq* reference axes are selected such that the *q* component of the power system voltage is zero. With such a reference, the desired control is achieved simply by ensuring that the *d* component of the inverter current is zero. The error in the *d* component of the current is processed through a compensator. The output of the compensator is given as input to three voltage controlled oscillators (VCO's). The outputs of the oscillators provide the phase references for the gate trigger generators.

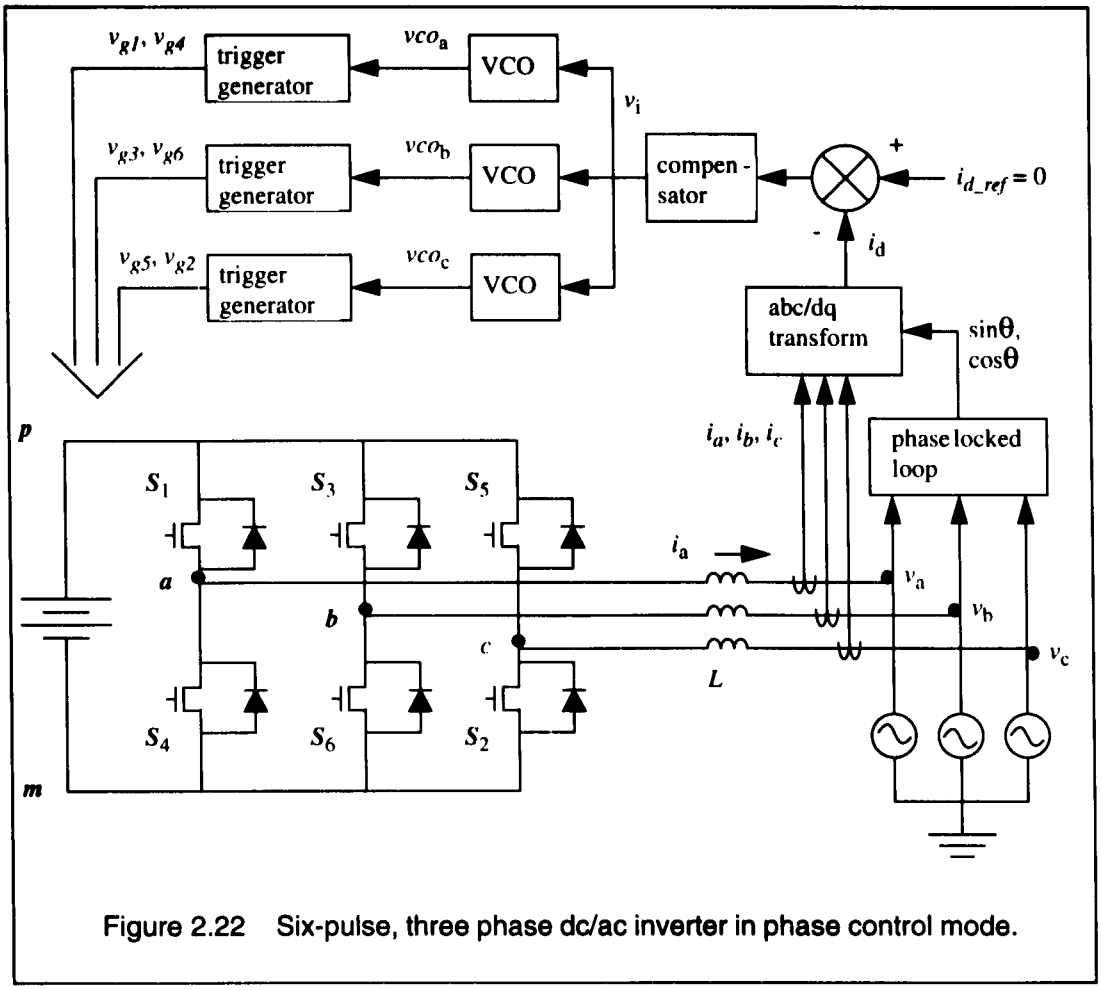

Figure 2.22 Six-pulse, three phase dc/ac inverter in phase control mode.

2.6.1 *Determination of the Describing Function*

In this case, there are three switching functions, one for each phase. The switching function for phase A is given by:

$$h_a = \text{sgn}\,(vco_a) \tag{2.22}$$

where *sgn(.)* is the sign function, and

$$vco_a(t) = \sin\left(\int_0^t (\omega_0 + v_i)\,d\tau + \phi_a\right) \tag{2.23}$$

where ω_0 is the base frequency and ϕ_a is the phase of the VCO. The describing function

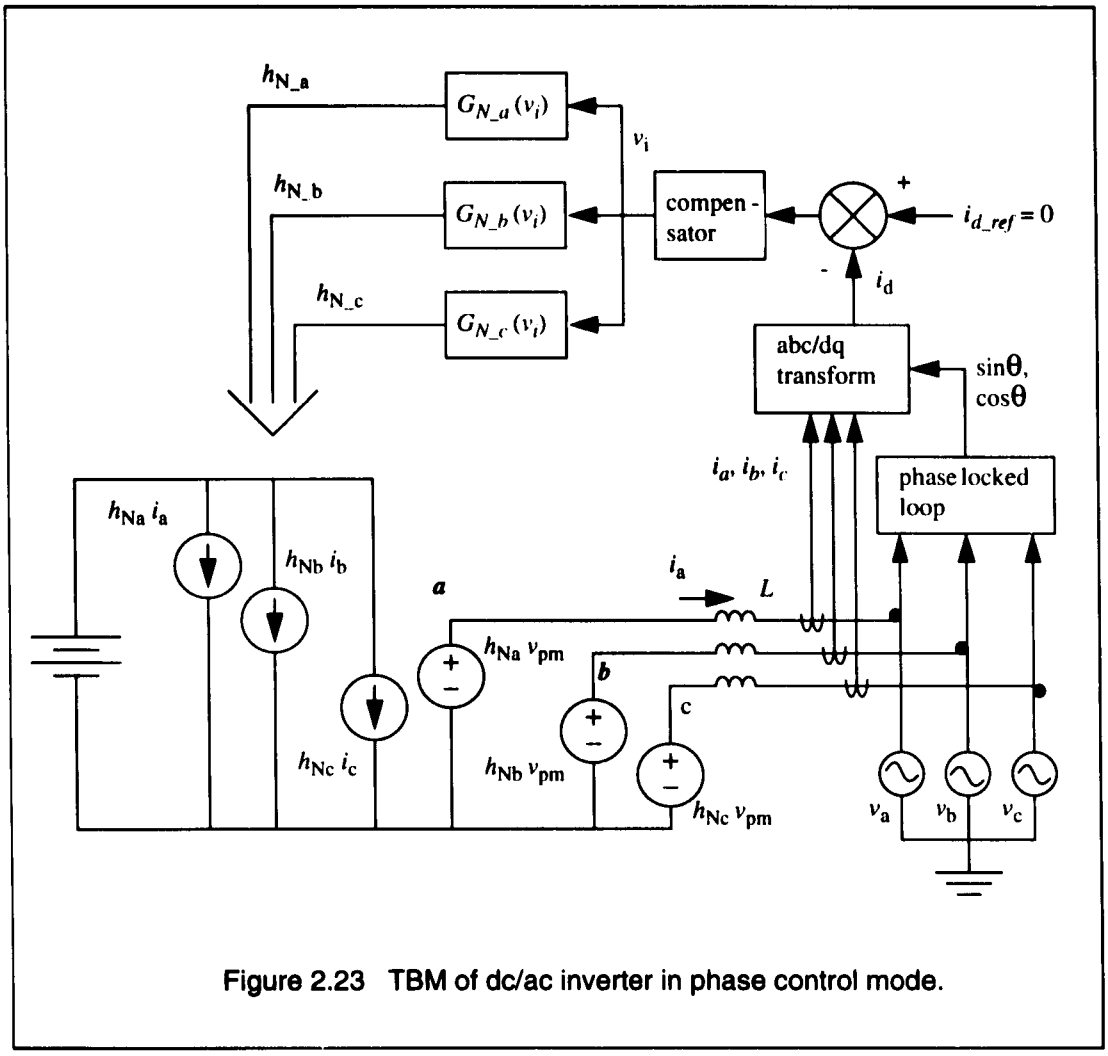

Figure 2.23 TBM of dc/ac inverter in phase control mode.

can be easily determined from equations (2.22) and (2.23). The resulting TBM is shown in Figure 2.23.

2.6.2 *Validation and Performance Evaluation*

The dc/ac inverter in phase control mode is simulated first with the accurate physically based models. Then the simulations are performed using the (a) ISM and the (b) TBM with up to 7th Fourier term. The simulations are performed in SABER. The SABER

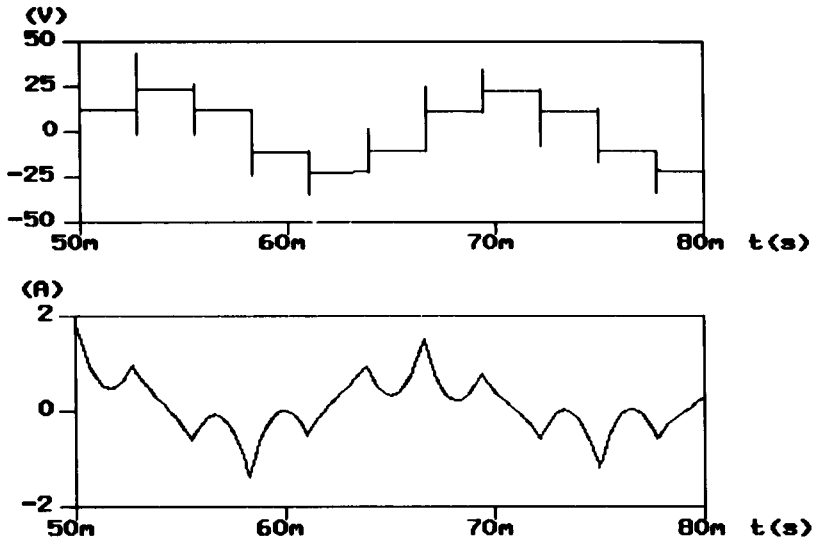

Figure 2.24 Phase A inverter voltage (top) current (bottom) - simulation using physically based models.

input files are given in D.3. The results are shown in Figure 2.24 and Figure 2.25. The simulation times required on a HP series 700 workstation are summarized in Table 2.5. The observations regarding the accuracy of the waveforms and simulation speeds of the ISM and the TBM are similar to those of the buck converter in voltage control mode. The efficiency of the TBM is 20% higher than the efficiency of the ISM. This is lower than in the case of the buck converter in voltage control mode because the number of switching transitions in the case of a dc/ac inverter are significantly lower than in the case of the buck converter. It should be noted that the TBM with only the dc Fourier term or the ASM cannot be used for this study since the dynamics of the converter depend on the frequency changes in the switching function while keeping the duty cycle ratio constant at 0.5.

2.7 Conclusions

A new modeling technique has been introduced. The resulting model is referred to

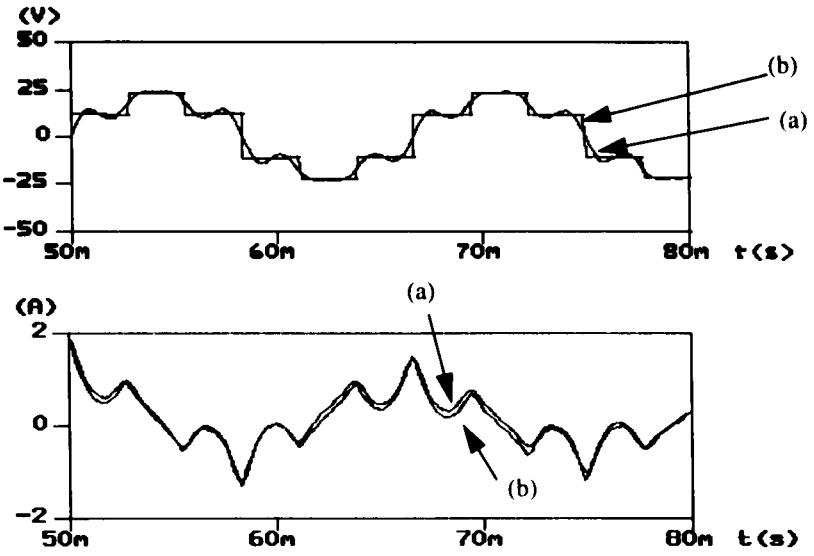

Figure 2.25 Phase A inverter voltage (top) and current (bottom) - simulation using (a) TBM, (b) ISM.

Table 2.5. Comparison of CPU for different switch models - simulation of dc/ac inverter in phase control mode.

Switch model	CPU time (seconds)
Physical models	692
ISM	31.8
TBM with up to 7th harmonic	26.0

as a Transient Behavioral Model (TBM). The TBM of a power converter is obtained by systematically replacing the switches by controlled sources and the non-linear switching function generator by its approximate describing function. The number of Fourier terms included in the describing function approximation determine the accuracy of the TBM. When only the dc Fourier term is included, the TBM reduces to the ASM. When all the Fourier terms are included, the TBM yields results identical to those of an ISM. Thus the

accuracy of the TBM can be varied easily from that of an ASM to that of an ISM. In fact, the change in the level of accuracy can be made dynamically during a single simulation run. As shown in the case of the buck converter in voltage control mode, a simulation can be started with a TBM using only the dc Fourier term so that the simulation proceeds with a high computational efficiency. When the circuit reaches the desired state, the number of Fourier terms in the TBM can be increased to give more accurate results. In the case of the buck converter, the transition of the model from a low accuracy level to high accuracy level did not cause any numerical stability problems. However, it should be noted that the step change in accuracy may lead to numerical instability.

The power of the TBM lies in its ease of use and implementation in standard circuit simulators such as SABER and EMTP. Thus the TBM is superior to other methods that use Fourier series representation (such as the HBM and the generalized average switch model). The TBM is also superior to the ISM. With the ISM, it is necessary to use small time steps near discontinuities. With the TBM, there are no discontinuities in the current and voltage waveforms. Hence the TBM uses larger time steps and is computationally more efficient than the ISM. The computational efficiency of the TBM is twice that of the ISM in the case of the buck converter in voltage control mode. In the case of the buck converter in current control mode, the efficiency of the TBM is 50% more than that of the ISM. Hence it can be concluded that constraint equations reduce the efficiency of the TBM. In the case of the dc/ ac inverter in phase control mode, the TBM is about 20% more efficient than the ISM. Hence it can be concluded that the TBM is more efficient when the number of switching transitions are large. The simulation of the buck converter in voltage control mode shows that the higher efficiency of the TBM is even more significant in the case of simulators that use a fixed time step algorithm.

Even though the TBM requires considerably less modeling effort than techniques

such as the HBM and the GASM, it should be noted that the TBM requires more modeling effort than the ISM. Further, since the TBM models only up to a limited number of harmonics, the use of the TBM requires the user to exercise judgement over the number of Fourier terms that need to be included in the model. Omission of essential Fourier terms can lead to erroneous results.

It should also be noted that the TBM is valid only for switch configurations shown in Figure 2.1. Further, it assumes that at any instant of time, exactly one of the two switches (S_1 or S_2), is closed. Thus the TBM assumes continuous operation of the converter and cannot be used for studies which involve discontinuous current conduction, or an abnormal switching condition.

3. Static Compensator (STATCOM) - Models and Simulation Studies

A Static Compensator (STATCOM) is a recently proposed shunt connected, solid state device that injects currents into the system in order to improve the power quality of the system. A brief description of its basic structure and functions is given in Section 3.1. Various circuit topologies and control schemes can be used to implement a STATCOM. In Sections 3.2 and 3.3, the proposed TBM is developed for two implementations of a STATCOM, namely, (i) 12-pulse and (ii) PWM. The 12-pulse implementation consists of a low switching frequency converter capable of compensating load reactive power. The PWM implementation consists of a high switching frequency converter capable of regulating the voltage at the tie point as well as compensating load harmonic currents. It is important to note that the design of these devices is specific to the system in which they are installed. In this chapter, it is shown that in order to design the various parameters such as the size of filter components, the voltage and current ratings, the impedance of the coupling transformer and the control system parameters it is necessary simulate the STATCOM along with the entire power system. The TBM's for the two STATCOM's are extremely effective for these simulation studies. The studies are performed on a practical 15 kV distribution feeder having serious power quality problems. A comparison is made between the use of the TBM's and the ISM's for such simulation studies.

3.1 Introduction

A Static Compensator (STATCOM) is a shunt connected, solid state device capable of providing variable var support without the use of large reactive components like capacitors and inductors. It is also known as an Advanced Static Var Compensator (ASVC) [67], an Advanced Static Var Generator (ASVG) [68], or a Static Condenser (STATCON)

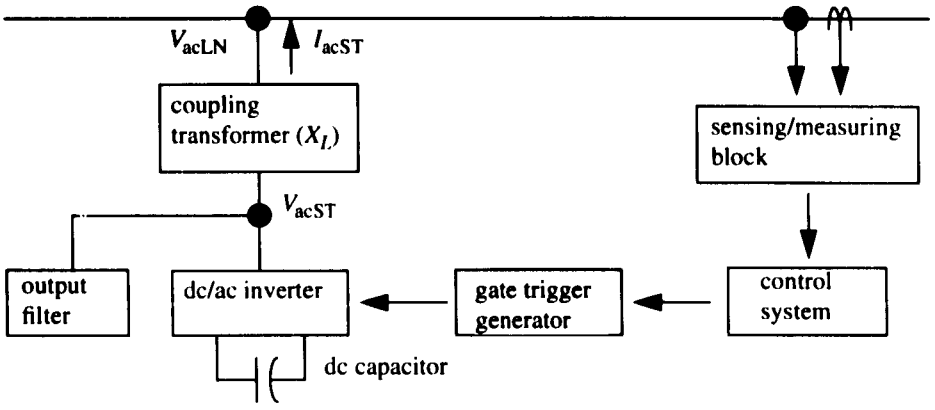

Figure 3.1 Basic functional modules of a STATCOM implemented as a solid state dc/ac voltage source inverter connected to the system through an inductive impedance.

[69]. Its primary functions include one or more of the following:

- reactive power compensation,
- voltage control (by reactive power management),
- harmonic voltage and current compensation.

A STATCOM can be implemented using a Current Source Inverter (CSI), or a Voltage Source Inverter (VSI) in current control mode. Due to the difficulties involved in implementing a high power rating CSI, practical implementations of a STATCOM have been developed using a VSI connected to the power system through the inductive impedance of a coupling transformer as shown in Figure 3.1. For the configuration shown in Figure 3.1, the current injected into the system depends on the voltage across the coupling inductance (X_L). By controlling the output voltage of the inverter (V_{acST}), the current injected into the system can be controlled as:

$$I_{acST} = \frac{(V_{acST}) - (V_{acLN})}{jX_L} \tag{3.1}$$

Figure 3.2 Phasor diagram showing var generation and absorption by a STATCON.

If the output voltage (V_{acST}) is synchronized with ac system voltage (V_{acLN}), then the current injected into the system (I_{acST}) is purely reactive. Further, by varying the magnitude of V_{acST}, the reactive power supplied/absorbed is controlled. The phasor diagram showing the reactive power generation and absorption is given in Figure 3.2 [69].

In this chapter, the TBM's are developed for two types of STATCOM's:

(i) 12-pulse (non-PWM): for reactive power compensation,

(ii) PWM: for voltage regulation and current harmonic compensation.

The development of the TBM's for the 12-pulse and the PWM STATCOM is described in sections 3.2 and 3.3 respectively. The effectiveness of the TBM in simulation studies for the design of these converters is demonstrated. It should be emphasized that the design of a STATCOM is not independent of the specifics of the system in which the STATCOM is to be installed. Hence a practical 15-kV distribution feeder with serious power quality problems is considered for the simulation studies presented in this chapter.

3.2 12-Pulse STATCOM

The main feature of a 12-pulse STATCOM is that the VSI consists of two 6-pulse inverters connected by a combination of delta-wye and wye-wye transformers to give a 12-

pulse output as shown in Figure 3.3 [68]. The VSI is operated in phase control mode such that the STATCOM output current leads the system voltage by 90^{o}. The magnitude of the output current is controlled by controlling the STATCOM output voltage, which in turn is controlled by the dc capacitor voltage [15]. Under steady state conditions, the only real power absorbed by the STATCOM is to supply its losses. In steady state, the dc capacitor voltage is constant and hence the output current injected into the system is constant. The STATCOM senses the reactive current demand of the load and adjusts its dc capacitor voltage by exchanging real power with the system. This type of a STATCOM is capable of providing reactive power compensation or voltage compensation. Due to its low switching frequency, it is not capable of providing harmonic compensation.

3.2.1 Configuration of the Power Converter

The 12-pulse VSI consists of two 6-pulse VSI's connected to a common dc capacitor as shown in Figure 3.3. The first 6-pulse VSI leads the second 6-pulse VSI by 30^{o}. The outputs of the two VSI's are added by a combination of a wye-wye and a delta-wye transformer. Note that the mid-point of the dc capacitor is connected to the ground, whereas the neutral on the ac side is floating. The resultant inverter output voltage consists of a 12-pulse waveform with associated $(12n\pm1)$ harmonics. The output filter consists of two series LC circuits tuned to the 11th and the 13th harmonic. The coupling transformer is a wye-delta transformer with a turns ratio of $1:\sqrt{3}$. The turns ratio is selected such that the magnitude of the line to line voltages on the primary side is same as that on the secondary side.

3.2.2 Configuration of the Control System

When the STATCOM output voltage is kept in phase with the system voltage, then the STATCOM output current is purely reactive. Under such conditions, there is no real

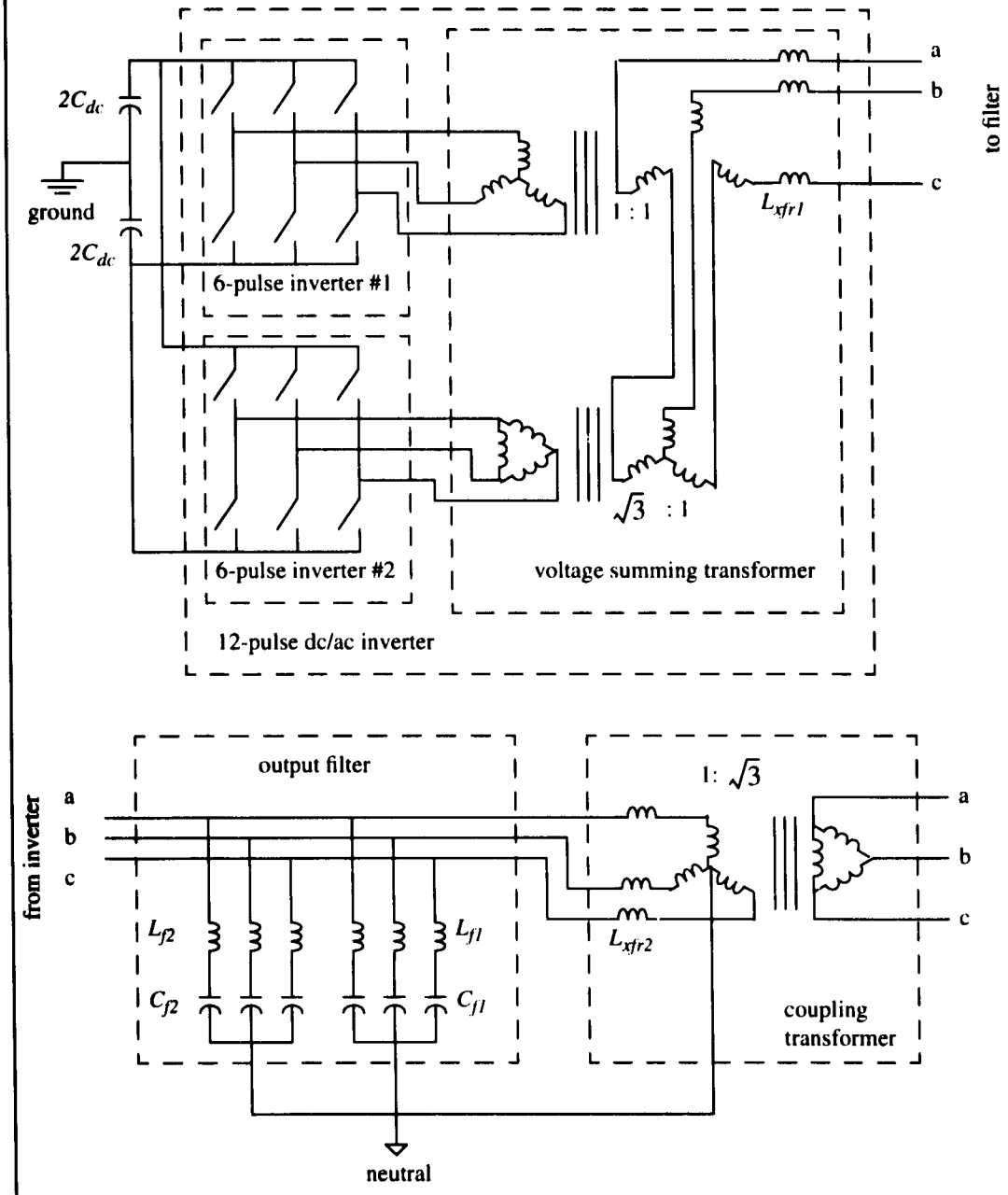

Figure 3.3 Topology of Power Converter for the 12-Pulse STATCOM.

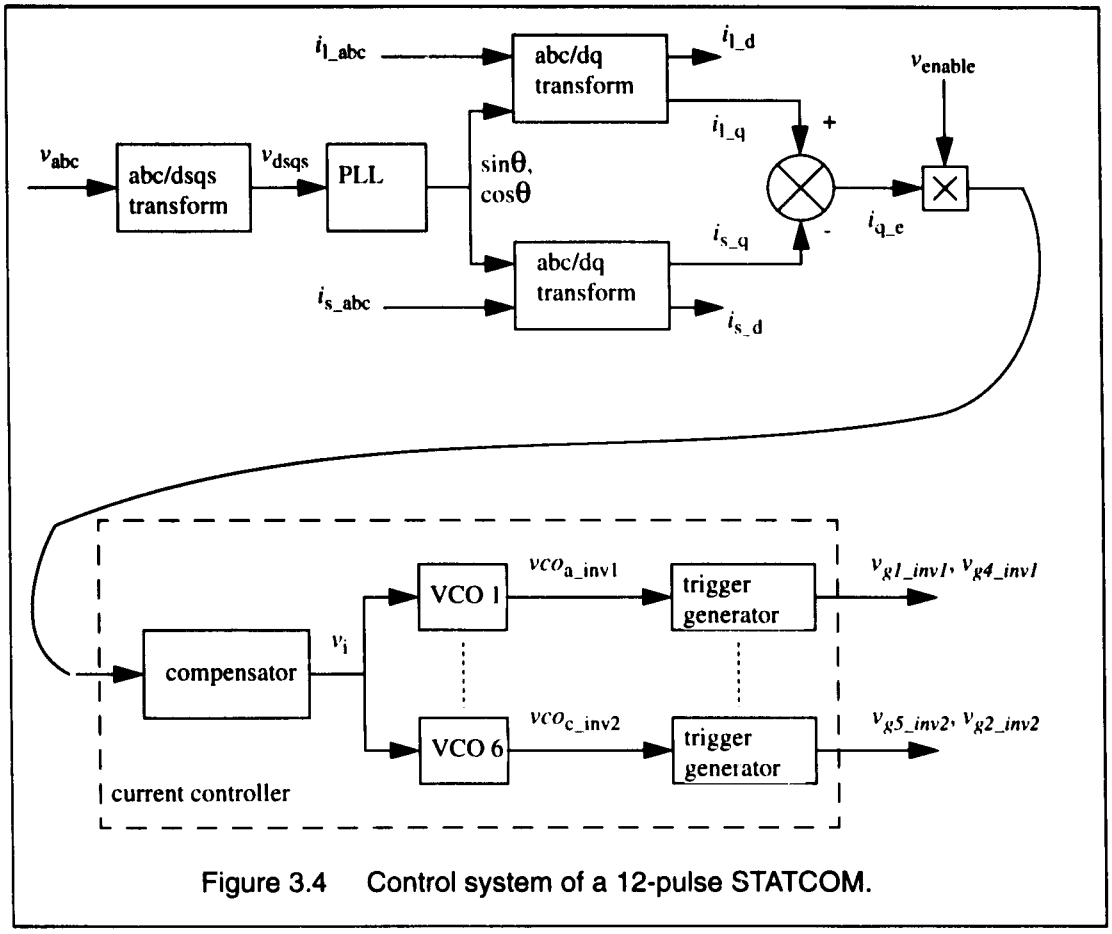

Figure 3.4 Control system of a 12-pulse STATCOM.

power exchange and hence the dc capacitor voltage is held constant. If the STATCOM output voltage is made to lag the system voltage, then the STATCOM will absorb real power and hence the dc capacitor voltage will increase. Thus the dc capacitor voltage can be controlled by the phase angle of the output voltage. The dc capacitor voltage will in turn control the reactive current injected into the system. This is the basic control strategy of the 12-pulse STATCOM as shown in Figure 3.4. The q-axis component of the load current (i_{l_q}) and the STATCOM current (i_{s_q}) are used as a measure of the instantaneous reactive power absorbed by the load and the STATCOM respectively. The error in the reactive current (i_{q_e}) is computed and processed through a compensator. The output of the

compensator (v_i) controls the phase of six voltage controlled oscillators (VCO's). Under steady state conditions, i_{q_e} and v_i are zero, and the output of the VCO is at constant frequency, locked in phase with the system voltage. Upon an increase in i_{q_l}, v_i becomes positive and the output of the VCO lags the system voltage. As a result of this lag, the dc capacitor charges up, which in turn causes an increase in i_{q_s}. The STATCOM reaches a new steady state when i_{q_s} becomes equal to the new i_{q_l}. The outputs of the VCO's are converted into gate triggering signals by gate trigger generator modules.

3.2.3 Design of the STATCOM Components

For the development of a model, it is necessary to know the various design parameters of the STATCOM such as the filter size, the coupling transformer impedance and the control system parameters. However, in the case of the 12-pulse STATCOM described here, the information regarding the parameters is not available prior to the model development. Hence, a systematic step by step procedure is followed in order to develop the model. The procedure essentially involves analytical calculations to determine the STATCOM parameters, followed by simulation studies to refine the calculated parameter values. The various steps in the design procedure are:

1. Analytically calculate the following parameters - the voltage and current ratings of the dc/ac inverter, the dc voltage level, the size of the filter components, leakage impedance of the coupling transformer and the gains of the PI block for inverter current control.

2. Develop the TBM for the STATCOM using the parameters determined in step 1.

3. Perform simulation studies with STATCOM in open loop and refine the parameters determined in step 1, namely, the dc voltage level, size of filter components and leakage impedance of transformer.

4. Perform simulation studies with STATCOM in closed loop and refine the control system parameters for load reactive power compensation.

Note that in the above listed steps, the design of the snubber circuits is omitted. The selection of the snubber circuits involves simulations using switch models that accurately simulate the switch turn-on and turn-off characteristics. Such simulations are beyond the scope of this dissertation and hence the issue of snubber design is not addressed here.

The TBM developed for the 12-pulse STATCOM is described in Section 3.2.4. The various analytical calculations involved in step 1 are shown in Appendix B.1. The simulation studies involved in steps 3 and 4 are described in Section 3.2.6 and 3.2.7 respectively. The TBM is used for these simulation studies. Comparisons are made with the corresponding use of the ISM for such simulation studies. The simulations are performed with the STATCOM installed at node 3 of the 15-kV distribution feeder shown in Figure 3.5. The detailed description of the system is given in Section 3.2.5.

3.2.4 Model Description

The basic functional blocks of the 12-pulse STATCOM are the same as shown in Figure 3.1. A modular approach to modeling is used, i.e. each functional block is modeled as a separate module. The complete model is obtained by appropriately connecting the individual modules. It should be noted that the TBM of the 12-pulse STATCOM differs from the ISM of the 12-pulse STATCOM only in the VSI module and the control system module. The other modules are common to the TBM and the ISM of the STATCOM.

The SABER simulator [22] is used for developing the various modules. The TBM for each 6-pulse inverter is similar to that of the phase controlled dc/ac inverter described in Section 2.6. The coupling transformer module is modeled by standard SABER library models. The output filter module consists of series LC elements tuned to the 11th and 13th

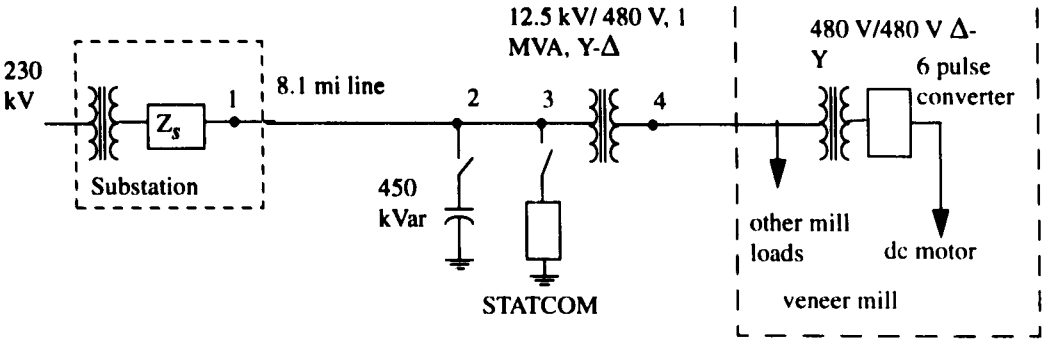

Figure 3.5 One line diagram of 15 kV distribution feeder.

harmonics. The sensing module consists of ideal current and voltage sensors with low-pass noise filters. The describing function approximation of the switching function generator is similar to that given in section 2.6.

3.2.5 Description of the 15 kV Distribution Feeder

The model of a 15-kV distribution feeder is used to demonstrate the STATCOM models (Figure 3.5). This distribution feeder is located in Oregon and supplies a veneer mill [50]. The veneer mill includes linear loads such as synchronous motors. The load varies rapidly and hence causes voltage flicker problems. The veneer mill also includes a nonlinear load in the form of a rectifier-fed dc motor. This nonlinear load is a source of current harmonics and causes severe harmonic distortion in the system. The 8.1 mile long line feeding the load has a relatively high impedance and worsens the power quality problems.

3.2.6 Simulation Study - Output Filter Design

This study is performed to refine the filter component sizes determined analytically in Appendix B.1. For this study, the STATCOM is operated in open loop. The control

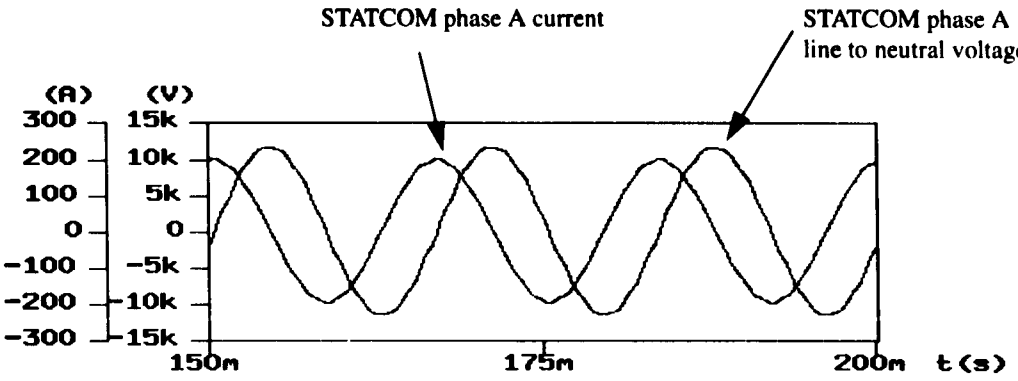

Figure 3.6 Simulation of 12-pulse STATCOM in open loop using the TBM.

system is given a command to inject a fixed amount of reactive current starting at 30 ms. The system load is turned off. The simulations are performed using the TBM. The describing function used to approximate the switching function, as described in Section 2.6, includes the fundamental, 11th and 13th Fourier terms.

The first simulation is performed using the parameters determined in Appendix B.1. The simulation results are shown in Figure 3.6. A Fast Fourier Transform (FFT) of the voltage and current waveforms shows that the waveforms have 11th and 13th harmonic distortion of 1.78% and 1.01% respectively, as shown in Table 3.1. It should be noted that the level of harmonic distortion is significantly high for the system under consideration due to the fact that the system voltage is not stiff. Based upon the planning and operation requirements of the power system in which the STATCOM is installed, such levels of harmonic distortion may or may not be acceptable. If such levels of harmonics are not acceptable, then the simulation study reveals that the parameters determined in Appendix B.1 are not satisfactory. This situation reflects the need for the STATCOM design to be customized for the particular system in which it is installed.

In order to decrease the harmonic distortion due to the current injected by the

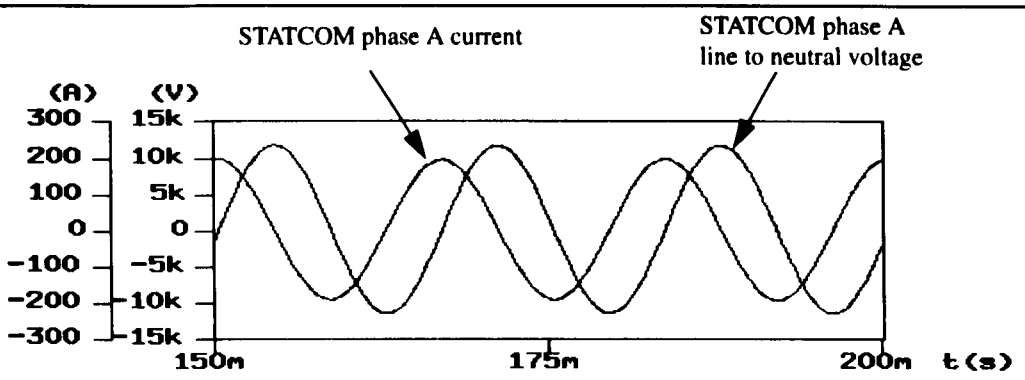

Figure 3.7 Simulation of 12-pulse STATCOM in open loop using the TBM - L_{xfr1} is increased to 30 mH.

Table 3.1: Harmonics in STATCOM voltage and current: simulation using TBM with the parameters determined in Appendix B.1.

Harmonic	Voltage (magnitude)		Current (magnitude)	
	Volts	%	Amps	%
Fundamental	11530	100	195.9	100
11th	205.5	1.78	2.32	1.18
13th	116.9	1.01	1.11	0.57

STATCOM, one method is to modify the design of the output filter. However, the impedance of the 8.1-mile line from the substation to node 3, in Figure 3.5, is approximately 15 mH (inductive) and 9 Ω (resistive). This impedance is of the same order as the combined impedance of the STATCOM voltage summing transformer (L_{xfr1} = 10.6 mH) and coupling transformer (L_{xfr2} = 10.6 mH). This makes the voltage at node 3 very sensitive to the distortion in the STATCOM current. Hence, rather than re-designing the output filter, the inductor L_{xfr1} is increased to 30 mH. An important consequence of this modification is that for the same amount of injected current, the dc voltage rating of the STATCOM has to be increased.

The open loop simulation is repeated with the modified values of the inductors. The results are shown in Figure 3.7. Table 3.2 summarizes the results of an FFT analysis of the current and voltage waveforms. A comparison of Figure 3.6 and Figure 3.7 as well as Table 3.1 and Table 3.2 shows that the harmonic distortion in the voltage and current waveforms is significantly reduced after the modifying the STATCOM design.

Table 3.2: Harmonics in STATCOM voltage and current: simulation with L_{xfrl} increased to 30 mH.

Harmonic	Voltage (magnitude)		Current (magnitude)	
	Volts	%	Amps	%
Fundamental	11510	100	194.2	100
11th	81.33	0.71	0.90	.46
13th	42.61	0.37	0.40	.21

Table 3.3: Harmonics in STATCOM voltage and current: comparison of simulation using TBM with simulation using ISM.

Harmonic	Voltage (magnitude in V)		Current (magnitude in A)	
	TBM	ISM	TBM	ISM
Fundamental	11510	11510	194.2	194.1
11th	81.33	79.68	0.90	0.94
13th	42.61	35.44	0.40	0.40
23rd	0.10	98.48	0.01	0.55
25th	0.32	91.3	0.01	0.46

Table 3.4: Comparison of simulation times using TBM with simulation using ISM.

Model	CPU time (s)
TBM	268
ISM	333

For the sake of comparison, the simulation with the modified inductor values is

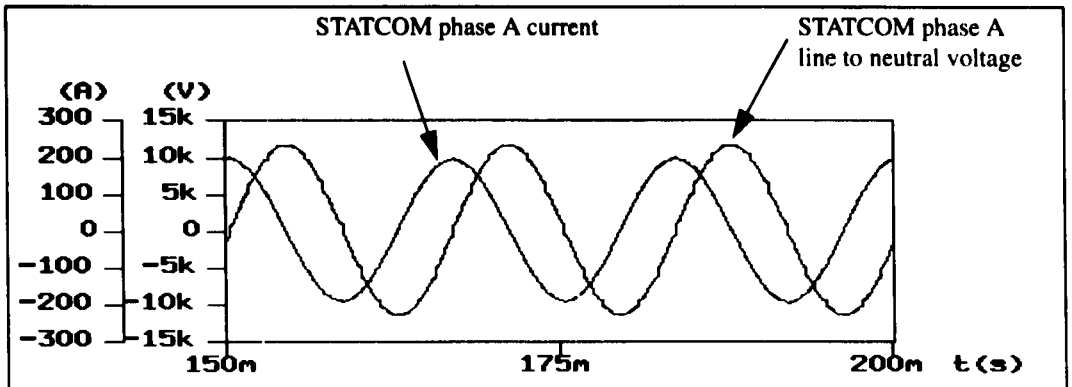

Figure 3.8 Simulation of 12-pulse STATCOM in open loop using the ISM - L_{xfr1} is increased to 30 mH.

repeated using the ISM. The corresponding results are shown in Figure 3.8. A comparison of Figure 3.7 and Figure 3.8 shows that the results of the TBM are consistent with those of the ISM. Table 3.3 shows that the TBM accurately simulates up to the 13th harmonic component. This is due to the fact that the describing function approximation used for the TBM includes Fourier terms up to the 13th harmonic frequency. This example illustrates a potential source of error in the use of the TBM. Since the TBM requires the user to predetermine the number of harmonics to be included in the model, it is necessary for the user to exercise judgement over the number of Fourier terms to be included in the model. Table 3.4 shows that the TBM is computationally 20% more efficient than the ISM

3.2.7 Simulation Study - Reactive Power Compensation

The response of the STATCOM to a step increase in the load reactive current is studied in this simulation. The linear load is switched on at 70ms. Simulations are performed using the TBM with the switching function approximated by the fundamental, 11th and 13th fourier terms. Figure 3.9 shows the system phase A line to neutral voltage, the phase A source current and the phase A load current. The load current lags the voltage

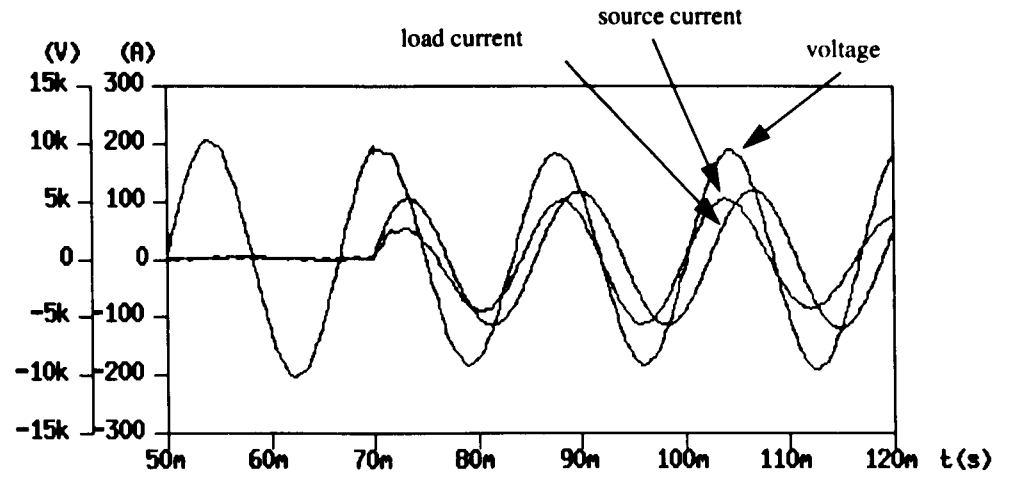

Figure 3.9 Phase A system line to neutral voltage, load current and source current - simulation using TBM.

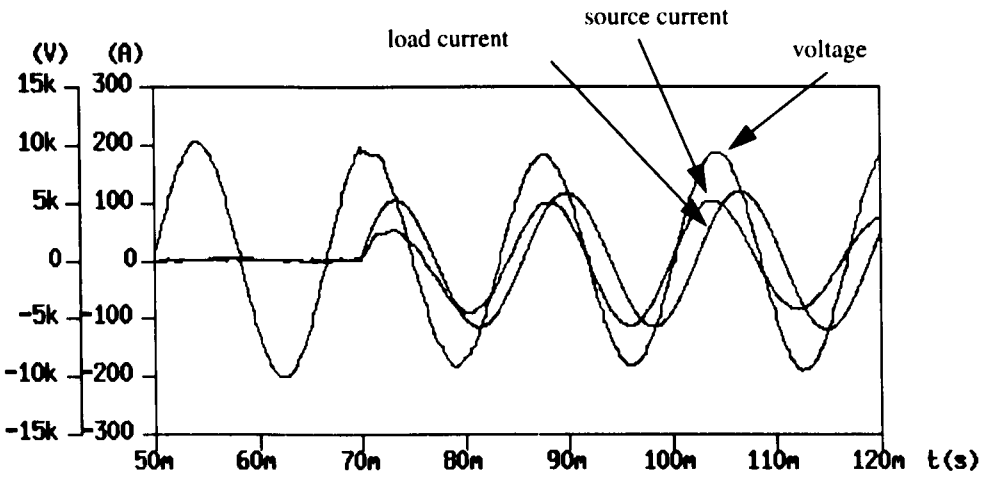

Figure 3.10 Phase A system line to neutral voltage, load current and source current - simulation using ISM.

whereas the source current is in phase with the system voltage, thus showing that power drawn from the source is at unity power factor. The response of the STATCOM is within two 60 Hz cycle. For the sake of comparison, the simulations are repeated using the ISM. The results are shown Figure 3.10. Comparing Figure 3.9 and Figure 3.10, it can be seen

that the results of the TBM are consistent with those of the ISM. However, the CPU times required by the two models on a HP 700 series workstation shows that the TBM is 20% more efficient than the ISM as indicated in Table 3.5.

Table 3.5: CPU times with different switch models for a simulation period of 150 ms.

Model	CPU time (s)
ISM	349
TBM (up to 13th Fourier term)	280

3.3 Pulse Width Modulated STATCOM

The main feature of a PWM STATCOM is that the VSI consists of a 6-switch, high frequency, H-bridge inverter. The primary control functions of the STATCOM modeled here are -- (i) to regulate the fundamental voltage at the coupling point by injecting appropriate amounts of fundamental reactive current and (ii) to inject harmonic currents to compensate the load harmonic currents. The reactive current injected into the system is controlled by varying the modulation index while keeping the dc capacitor voltage constant [15]. The load current harmonics are compensated by injecting equal and opposite amounts of harmonics into the system.

3.3.1 Configuration of the Power Converter

Figure 3.11 shows the topology of the power converter part of PWM STATCOM under consideration. The dc/ac inverter consists of 6 switches in an H-bridge configuration. On the dc side of the inverter, the mid-point of the capacitor is connected to the ground. On the ac side of the inverter, the neutral is floating. The output filter consists of a two inductors and one capacitor in each phase. Inductor L_{f1} and capacitor C_f are selected so as to give a cut off frequency sufficiently lower than the switching frequency. The inductor L_{f2} and capacitor C_f are tuned to the switching frequency in order to provide a low impedance path

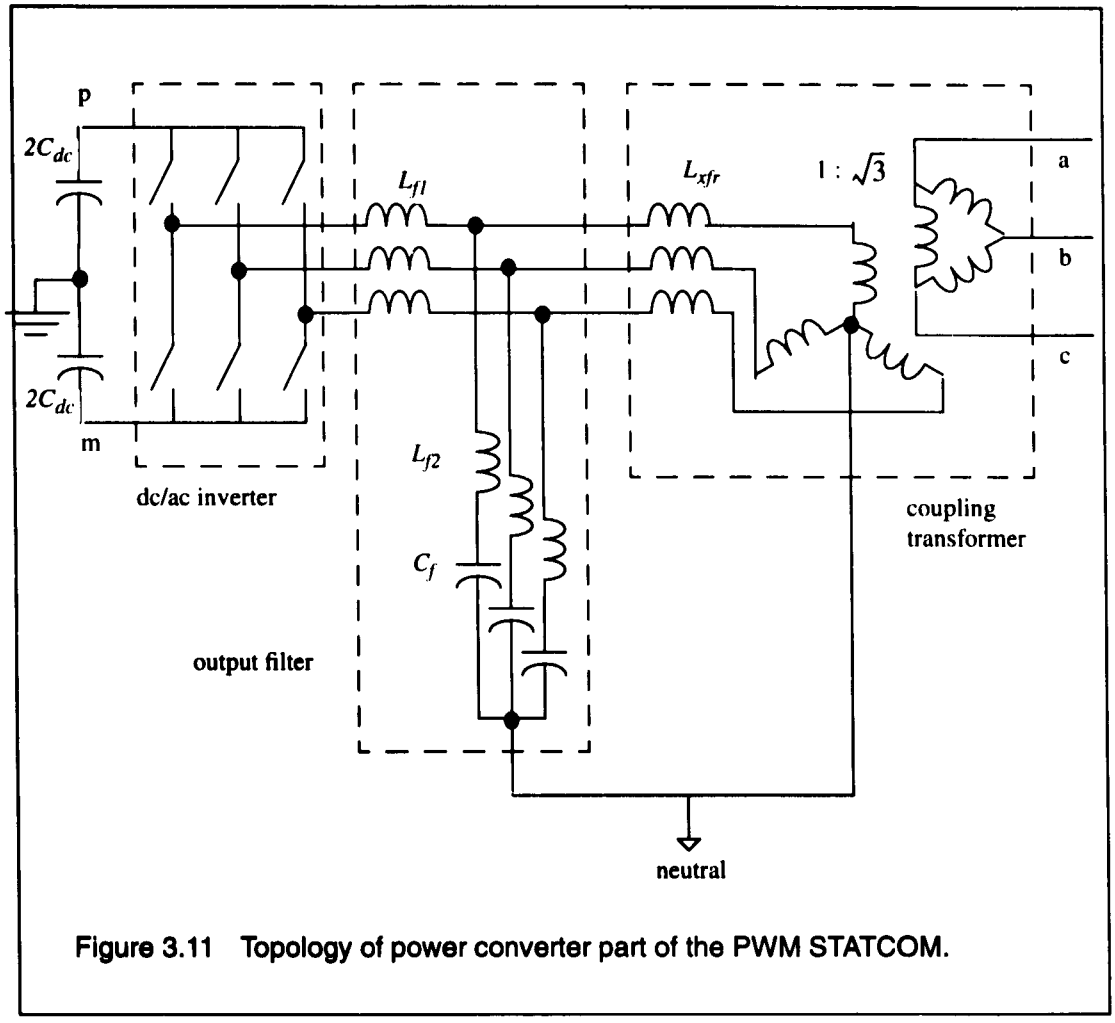

Figure 3.11 Topology of power converter part of the PWM STATCOM.

for the switching frequency component of the inverter output current. The coupling transformer is a wye-delta transformer with a turns ratio of $1:\sqrt{3}$ so that the line-to-line voltages on the primary and secondary of the transformer are of the same magnitude.

3.3.2 Configuration of the Control System

Figure 3.12 shows the control system of the STATCOM. The control is implemented using two loops - the outer loop determines the amount of current to be injected into the system. The inner loop controls the inverter so as to inject the currents

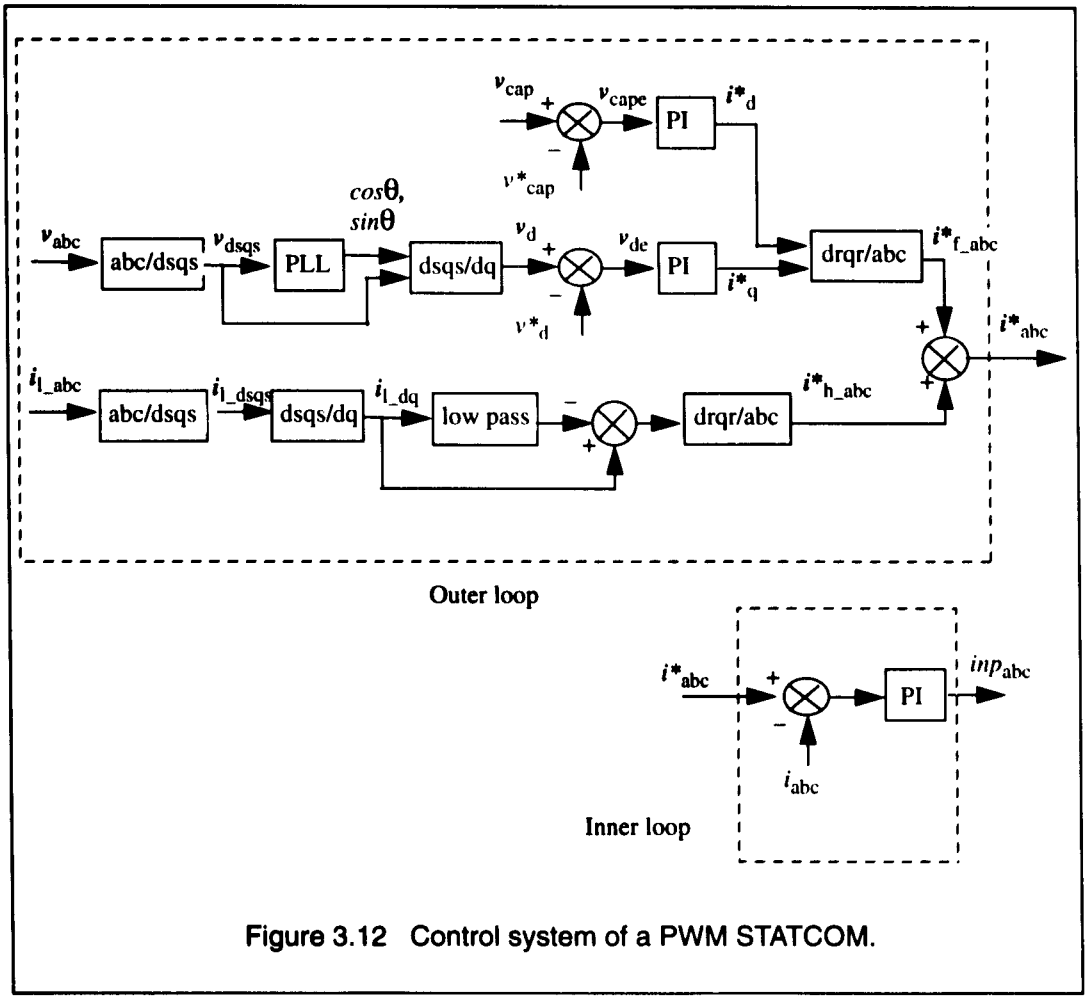

Figure 3.12 Control system of a PWM STATCOM.

determined by the outer loop [65]. The outer loop converts the sensed voltages (v_{abc}) from *abc* to *dq0* coordinates [15]. The error in the *d* component is processed through a PI block to generate the amount of instantaneous reactive current i_q* required. The error in the capacitor voltage (v_{cape}) is processed through a PI block to determine the amount of instantaneous real current i_d* required. The i_d* and i_q* are transformed into the *abc* coordinates to determine the amount of fundamental current ($i^*_{f\_abc}$) to be injected. The outer loop also computes the amount of harmonic current in the load ($i^*_{h\_abc}$). The total current to be injected by the STATCOM (i^*_{abc}) is supplied as input to the inner control loop.

Based on the current demand, the inner control loop generates the input signals inp_{abc} for the gate trigger generator. In the gate trigger generator module, these signals are compared to a triangular carrier wave to generate the PWM gate triggers.

3.3.3 Design of the STATCOM Components

As in the case of the 12-pulse STATCOM, the information regarding the parameters of the PWM STATCOM is not available prior to model development. Hence, the procedure to develop the PWM STATCOM model is similar to that of the 12-pulse STATCOM model. The various steps in the design procedure are:

1. Analytically calculate the following parameters - voltage, current and frequency rating of the dc/ac inverter, size of the filter components, leakage impedance of the coupling transformer, gains of the PI block in the inner current control loop.

2. Develop the TBM for the STATCOM using the parameters determined in step 1. Note that only the inner loop of the control system is modeled at this stage, the outer loop is yet to be modeled. Also note that the dc capacitor size has not been determined as yet, hence a dc voltage source of appropriate magnitude is connected to the dc side of the dc/ac inverter.

3. Perform simulation studies to refine the parameters determined in step 1.

4. Analytically calculate the following parameters - size of dc capacitor required, gains of the PI block for dc voltage control. Modify the model to include the dc capacitor and the dc voltage control loop.

5. Perform simulation studies to refine the parameters determined in step 4.

6. Analytically calculate the gains of the PI block for system voltage regulation and harmonic current compensation. Modify the model to include the system voltage control loop and the harmonic current compensation loop.

7. Perform simulation studies to refine the parameters determined in step 6.

The TBM developed for the STATCOM is described in Section 3.3.4. The various analytical calculations involved in steps 1, 4 and 6 are shown in Appendix B.2. The simulation studies involved in steps 3, 5 and 7 are described in Section 3.3.5, 3.3.6 and 3.3.7 respectively. The TBM is used for these simulation studies. Comparisons are made with the corresponding use of the ISM for such simulation studies. It should be noted the TBM of the PWM STATCOM differs from the ISM of the PWM STATCOM only in the VSI module and the control system module. The other modules are unchanged.

The simulations are performed with the STATCOM installed at node 3 of the 15-kV distribution feeder shown in Figure 3.5. The detailed description of the system is given in Section 3.2.5.

3.3.4 Model Description

As in the case of the 12-pulse STATCOM, a modular approach is used for model development. The models have been developed using the SABER simulator. The TBM of the inverter is developed by replacing the PWM switches by a set of controlled sources (section 2.6). The coupling transformer is developed using a wye-delta transformer from the standard model library. No saturation effects have been included in the transformer model. The output filter module is also developed using standard components from the model library. The sensing module is developed using ideal transformers and low-pass noise filters. The approximate switching function necessary for the TBM is similar to that described for the buck converter in voltage control mode (section 2.4).

3.3.5 Simulation Study - Output Filter Design

The purpose of this simulation is to study the current control loop and the inverter

current ripple. The response of the current control loop depends upon the magnitude of the dc side voltage. Proper selection of dc voltage level is necessary in order to obtain the desired response in the current control loop. The magnitude of the ripple depends upon the switching frequency and the size of the filter inductor L_{fl}. Proper selection of switching frequency and filter inductor is necessary in order to keep the ripple within tolerable limits.

The STATCOM is operated in open loop so that it injects a predetermined amount of current into the system. The system load is kept off for this study. Starting at 20 ms, the STATCOM current controller is given a command to inject fundamental (60 Hz) reactive current of magnitude 100 A. An 11th harmonic (660 Hz) current of magnitude 10 A is added to the reference current at 40 ms. The simulation is performed using the TBM with the switching function approximated by 3 Fourier terms. The system reaches the desired initial steady state condition at about 18 ms. Hence the time period from 0 to 18 ms is not of any interest in this simulation study. In order to reach the desired initial steady state condition with least possible CPU time, only the dc Fourier term is used from 0 to 18 ms. At 18 ms, the 1st and 2nd Fourier terms of the TBM are enabled.

The first simulation is performed using filter components and dc voltage level determined analytically as shown in Appendix B.2. The phase A inverter current and current reference are shown in Figure 3.13. The maximum ripple observed in the inverter current is very high (40%). Figure 3.13 also shows that the inverter current does not respond fast enough for the 11th harmonic component in the reference current. Hence the simulation results show that the filter size and the dc voltage level determined analytically are not satisfactory. The next simulation is performed with the dc voltage level increased to 28.2 kV in order to improve the current controller response for the 11th harmonic component. Increasing the dc voltage level would result in an increase in the ripple. Hence L_{xfr} and L_{fl} are increased to 10.6 mH in order to reduce the current ripple. The filter

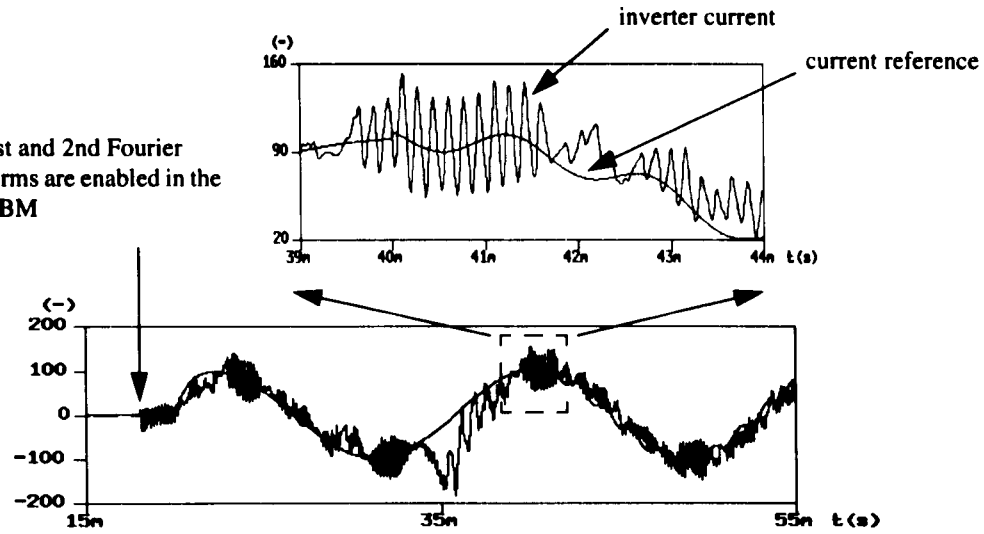

Figure 3.13 Phase A inverter current and inverter current reference - simulation using TBM with $L_{f1} = L_{xfr} = 5.3$ mH, $C_f = 0.51$ µF, $L_{f1} = 1.4$ mH, $V_{dc} = 94.4$ kV; current controller response is not satisfactory.

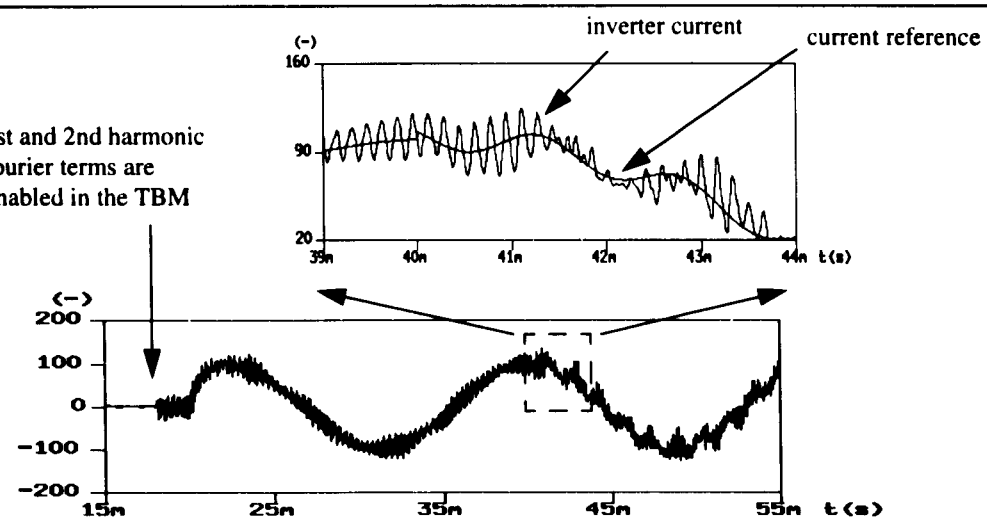

Figure 3.14 Phase A inverter current and inverter current reference - simulation using TBM with $L_f = L_{xfr} = 10.6$ mH, $C_f = 0.255$ µF, $L_{f1} = 2.8$ mH, $V_{dc} = 28.2$ kV.

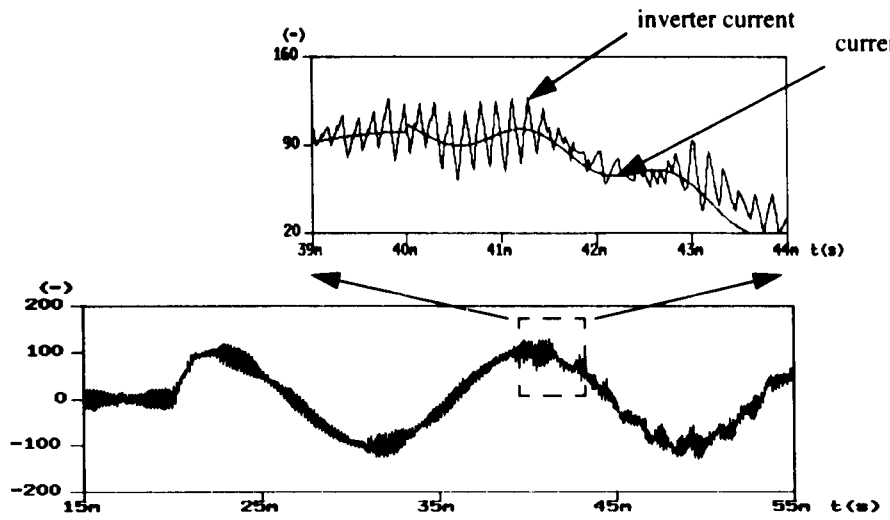

Figure 3.15 Phase A inverter current and inverter current reference - simulation using ISM with $L_f = L_{xfr} = 10.6$ mH, $C_f = 0.255$ µF, $L_{f1} = 2.8$ mH, $V_{dc} = 28.2$ kV

capacitor (C_f) size is reduced to 0.255 µF so as to maintain the cut-off frequency of the filter at 3060 Hz. L_{f2} is increased to 2.8 mH in order to maintain the resonance frequency of C_f and L_{f2} at 6060 Hz. As shown in Figure 3.14, the ripple content is reduced to 20% and the response of the current controller to the 11th harmonic component is also satisfactory. For the sake of comparison, the simulation is repeated with a STATCOM model using an ISM. The results are shown in Figure 3.15. A comparison of Figure 3.14 and Figure 3.15 shows that the TBM and the ISM give consistent results, thus validating the results of the TBM. Table 3.6 shows the CPU time required for the two models on an HP series 700 workstation. The TBM yields significantly a faster simulation speed than the ISM.

Table 3.6. CPU time for simulation of STATCOM in open loop.

Switch model	CPU time (s)
TBM	434
ISM	1530

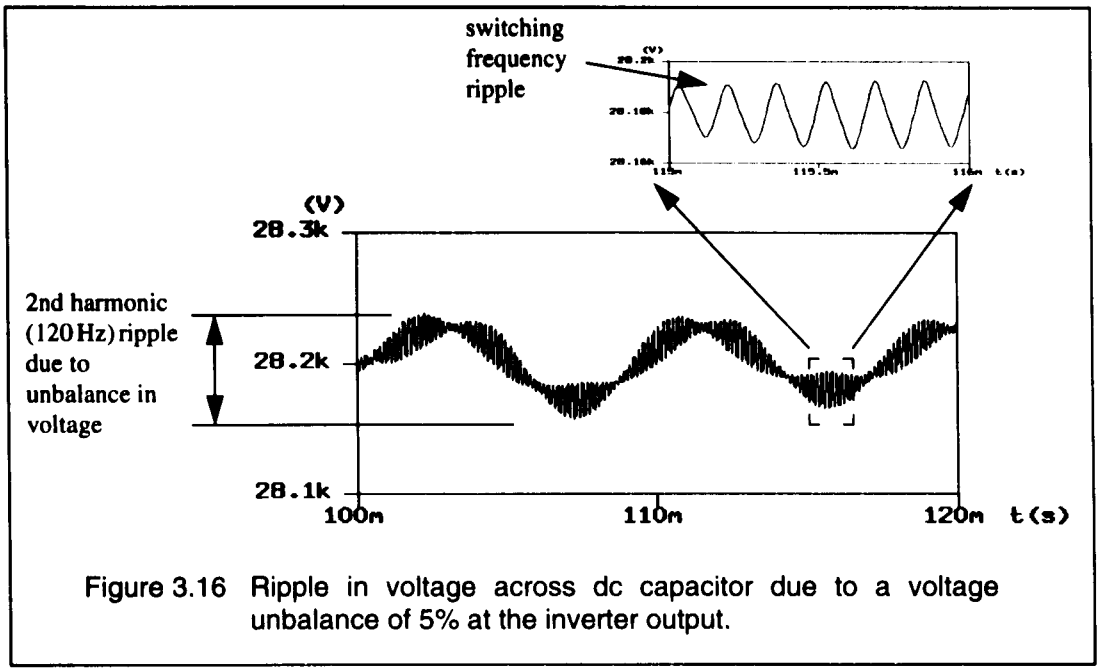

Figure 3.16 Ripple in voltage across dc capacitor due to a voltage unbalance of 5% at the inverter output.

3.3.6 Simulation Study - DC Capacitor Design

In Appendix B.2, a dc capacitor of 110 μF is selected based on a 0.1% ripple tolerance for an unbalance of 5% in the phase A voltage. The purpose of this simulation study is to verify the design of the dc capacitor. The TBM with 3 Fourier terms is used in this study. The STATCOM is operated in open loop so that it injects a reactive current of magnitude 130 A (rated current). For the sake of simplicity, the system load is kept off. Phase A source voltage at the substation is reduced to 0.93 p.u. This unbalance results in a phase A voltage of 0.95 p.u. at the inverter. Figure 3.16 shows the voltage across the dc capacitor. A ripple of 48 V (0.1%) is observed. This result is in agreement with the analytical calculations shown in Appendix B.2 and hence confirms the design of the dc capacitor. Note that there are two types of ripples in the capacitor voltage - the switching frequency ripple (6 kHz) and the 2nd harmonic ripple (120 Hz). The simulation shown in Figure 3.16 is performed with a TBM that includes 3 Fourier terms. Hence the simulation

results show both the ripple contents. If the TBM with only dc fourier term is used, then the simulated capacitor voltage will show only the 120 Hz ripple. Since the dc capacitor design is based on the 120 Hz ripple, a TBM with only the dc term is sufficient for this simulation study. However, a TBM with 3 Fourier terms is used to show the switching frequency ripple in the capacitor voltage.

3.3.7 Simulation Study - Voltage Regulation and Current Harmonic Compensation

In this study, the voltage regulation and current harmonic compensation capabilities of the STATCOM are simulated. Both the linear and nonlinear components of the load are used. The linear load is switched on at 100 ms. The nonlinear load is switched on at 200 ms and switched off at 250 ms.

In this case study, the phenomena of interest are the voltage sag caused by the loads and the harmonic currents injected by the non-linear load. The time constants involved in both these phenomena are sufficiently smaller than the switching period of the STATCOM (0.1667 ms). Hence it is sufficient to use the TBM with only the dc term approximation of switching function.

Simulations are performed first with the control loop disabled and then with the control loop enabled. Figure 3.17 shows the direct axis component (v_d) of the phase voltages (Figure 3.12). With the control disabled, v_d dips when the linear load is switched on. v_d also shows the harmonics in the voltage when the non-linear load is switched on. With the control enabled, the STATCOM regulates the voltage at the tie point. It responds to the voltage dip by boosting the voltage within 10ms. The voltage harmonics are also reduced. Figure 3.18 shows the load current and the source current for the case with the STATCOM control enabled. A Fast Fourier Transform (FFT) analysis of the current waveforms during the period of the 130 ms to 136.667 ms is performed. The results of the

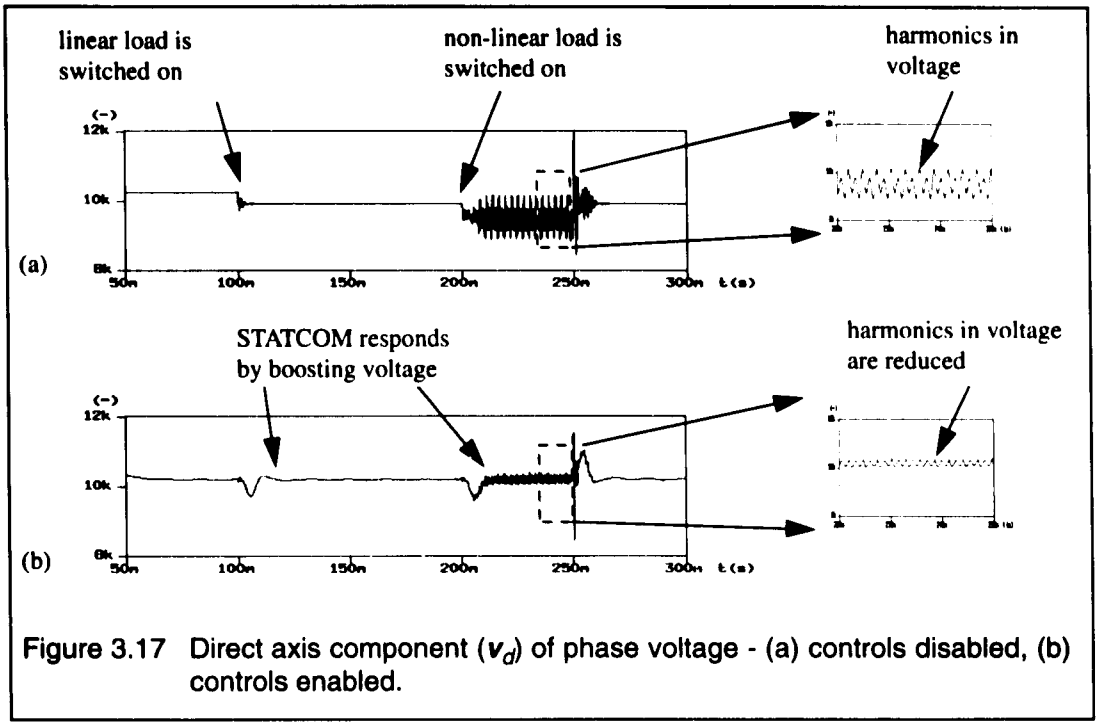

Figure 3.17 Direct axis component (v_d) of phase voltage - (a) controls disabled, (b) controls enabled.

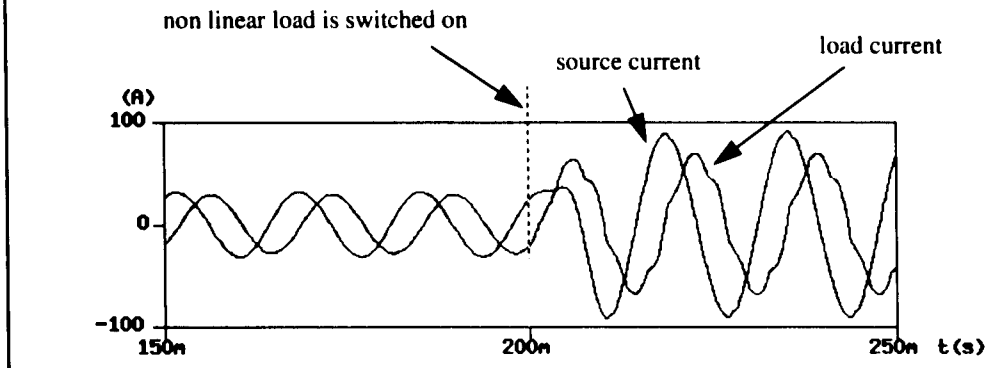

Figure 3.18 Phase A load current and source current, case with STATCOM control enabled - source current is free of harmonics.

FFT analysis are shown in Table 3.7

It is observed that the 5th and 7th harmonic components in the source current are significantly lower than those in the load current. Thus the STATCOM successfully

Table 3.7. Magnitudes of harmonics in phase A load current and phase A source current.

Harmonic	Load current		Source current	
	Amperes	% of fund.	Amperes	% of fund.
Fundamental	66.31	100	90.26	100
5th	5.305	8.0	0.141	0.2
7th	2.482	3.7	0.343	0.4
11th	0.705	1.0	0.897	1.0
13th	0.530	0.8	0.358	0.4

compensates the 5th and 7th harmonic components of the load current. However, the percentage of the 11th and 13th harmonic components of the source current are same as that in the load current. The reason for this is that the design of the STATCOM filter is such that the response for the 11th and 13th harmonic component is not satisfactory. One possible method to correct this problem is by modifying the filter design. Another method is to modify the control circuit to account for the influence of the filter for 11th and 13th harmonic compensation. These modifications are mentioned for the sake of completeness, they have not been implemented in the STATCOM model.

3.4 Conclusions

Models have been developed for two types of STATCOM's - the first using a 12-pulse dc/ac inverter and the second using a PWM dc/ac inverter. The designs of each STATCOM has to be system specific. Hence the STATCOM's along with the entire power systems is simulated in order to design the various parameters such as the filter component size and the control system gains which are not known prior to model development. Hence a systematic procedure is followed in order to design both the STATCOM's discussed in this chapter.

The TBM is used for the modeling and simulation studies. The number of Fourier

terms used in the TBM is varied depending upon the level of accuracy desired for a particular simulation study. Higher order Fourier terms are included in the TBM for the study of the switching frequency ripple and harmonics generated by the 12-pulse and the PWM STATCOM. The TBM is especially useful in the case of the 12-pulse STATCOM, where the switching frequency is as low as the 12th harmonic frequency (720 Hz). The TBM is also useful for the study of ripples in the voltages and currents of the PWM STATCOM. For the study of voltage regulation by the PWM STATCOM, where the phenomena of interest involves time constants larger than the switching time period, only the dc Fourier term is included in the TBM. The results of the TBM are consistent with those of the ISM. The TBM is 20% faster than the ISM in the case of the 12-pulse STATCOM and almost 3 times faster than the ISM in the case of the PWM STATCOM.

The number of Fourier terms in the TBM are also varied dynamically during a single simulation run. For the study of ripples in the voltages and currents of the PWM STATCOM, the initial portion of the simulation is performed using TBM with only the dc Fourier term. In this way, the simulation reaches the desired operating point with the least amount of computational time. Once the desired operating point is reached, the higher order Fourier terms of the TBM are enabled.

From Table 3.3, it is observed that the ISM predicts significant amount of 17th and 19th harmonic components in voltage and current. However, the TBM does not predict these harmonics since the TBM included only up to the 13th harmonic. This result indicates that the TBM requires the user to exercise judgement regarding the number of Fourier terms that should be included in the model. This requirement on the part of the user can be viewed as a limitation of the TBM since omission of essential Fourier terms can yield erroneous results.

The simulation of the 12-pulse STATCOM shows that it is capable of compensating the load reactive power demand. The response time is less than one 60 Hz cycle. The 12-pulse STATCOM inverter current has a significant content of $(12n\pm1)$ harmonics. Hence tuned filters are required to reduce the harmonic content in the STATCOM current that is injected into the system.

Simulations of the PWM STATCOM show that it capable of regulating the voltage at the tie point. Simulation results show also that the 5th and 7th harmonic components in the load current are compensated effectively. However, the compensation of the 11th and 13th harmonic components is not as effective. This is because the output filters affect the response of the STATCOM near higher harmonic frequencies. The response can be improved either by redesigning the filter, or by improving the control system.

4. Dynamic Voltage Restorer (DVR) - Model and Simulation Studies

A Dynamic Voltage Restorer (DVR) is a recently proposed series connected solid state device that injects voltage into the system in order to regulate the load side voltage. A brief description of its basic structure and functions is given in Section 4.1. As in the case of a STATCOM, there are various circuit topologies and control schemes that can be used to implement a DVR. In Section 4.2, the proposed TBM is developed for a DVR implemented by three independent single phase PWM VSI's. The primary function of this DVR is to regulate the load side voltage. As in the case of the STATCOM, it is shown that in order to design the various parameters such as the size of filter components, the voltage and current ratings, the impedance of the coupling transformer and the control system parameters, it is necessary simulate the DVR along with the entire power system. The TBM is found to be extremely effective for such simulation studies. The studies are performed on a practical 15 kV distribution feeder with serious power quality problems. A comparison is made between the use of the TBM and the ISM for such simulation studies.

4.1 Introduction

A Dynamic Voltage Restorer (DVR) is a series connected device that injects a voltage into the system. It is the series dual of a STATCOM. It consists of a solid state ac voltage source connected in series with the power system as shown in Figure 4.1. The real and reactive powers injected into the system are controlled by the phase displacement of the injected voltage (v_{acDVR}) and the load current (i_{load}). Depending upon the ratio of v_{acDVR} to i_{load}, the DVR can behave as a series capacitance, a series inductance, a series positive resistance or a series negative resistance. Figure 4.2 shows the phasor diagram for a DVR [69]. The primary functions of a DVR include one or more of the following:

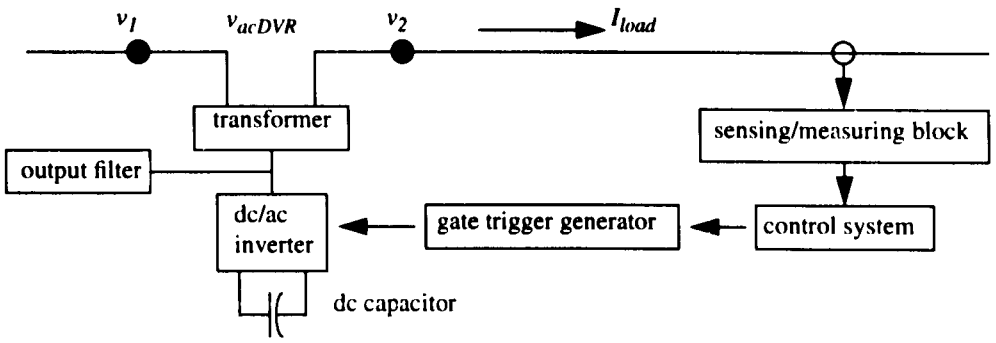

Figure 4.1 Implementation of a DVR as a solid state ac voltage source connected in series with the system.

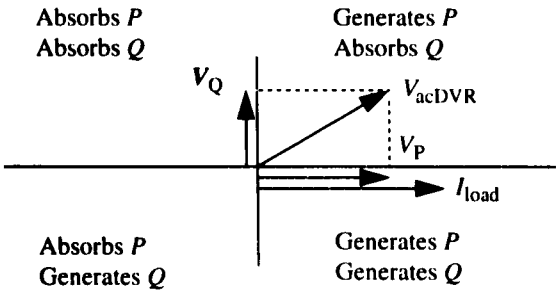

Figure 4.2 Phasor diagram showing supply generation and absorption of real power (P) and reactive power (Q) by the DVR.

- voltage regulation (by series compensation),
- line voltage harmonics compensation,
- reduction of sags, swells and transients in voltage,
- fault current limitations.

Figure 4.1 shows the basic functional blocks of a DVR. Each block can be implemented in a number of ways. The model of one such implementation, using three independent single phase PWM VSI's is described in this chapter. A modular approach to

modeling is used, i.e. independent modules are developed for each functional block. The complete model is obtained by appropriately connecting the individual modules.

4.2 Pulse Width Modulated DVR

The main feature of the DVR modeled here is that the VSI consists of three independent single phase PWM inverters. Each single phase inverter consists of four switches in the H-configuration as shown in Figure 4.3. The control function of the DVR modeled here is to regulate the load side voltage by injecting voltages in quadrature with the line currents. The injected voltage is controlled by the modulation index of the PWM inverter, while keeping the dc capacitor voltage constant. Since the voltages are in quadrature with the line current, the DVR behaves like a series capacitor and exchanges only reactive power with the system. A small amount of real power is drawn by the DVR to maintain the voltage of the dc capacitor. Independent single phase inverters are used for the DVR so that it can compensate unbalanced voltages. This type of a DVR is capable of compensating source side voltage transients and thus regulating the load side voltage

4.2.1 Configuration of the Power Converter

The VSI consists of three independent single phase VSI's as shown in Figure 4.3. The dc side to each inverter is connected to a common dc capacitor with the mid-point grounded. Each single phase inverter consists of four switches connected in an H-bridge type configuration. The output filter for each inverter consists of an LC combination. The output of the DVR is tied to the system through three single phase transformers.

4.2.2 Configuration of the Control System

The control scheme is implemented as shown in Figure 4.4. The line currents (i_{l_abc}) sensed by the sensing module are used to generate the reference *sin* and *cos* waves

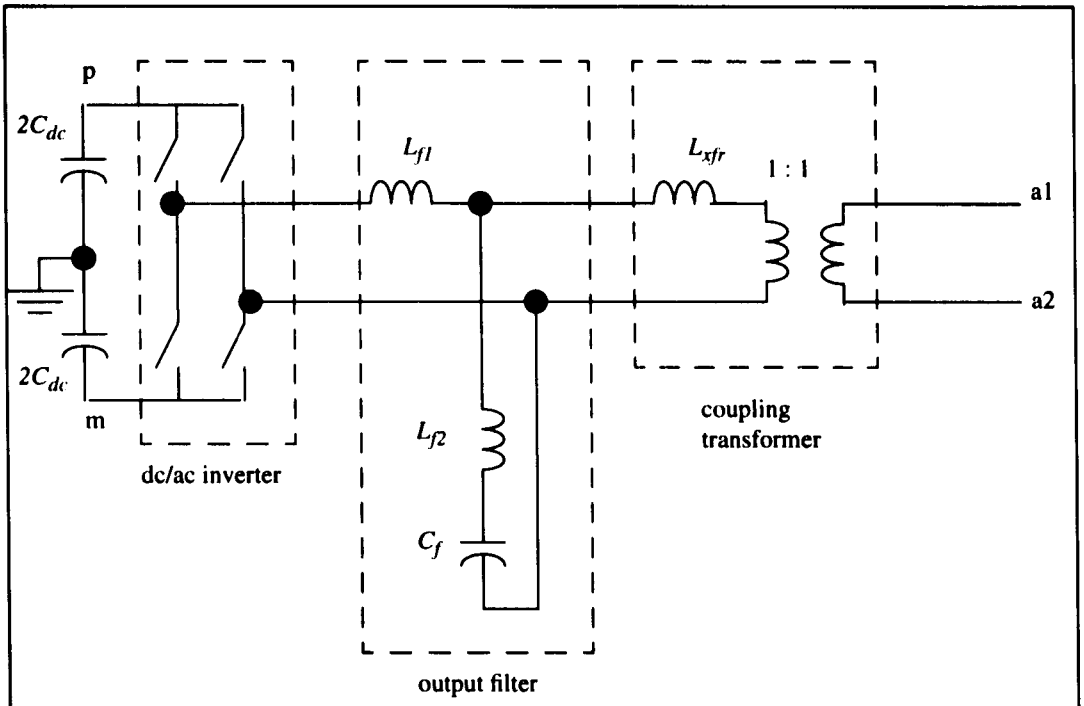

Figure 4.3 Topology of the Power Converter for the PWM DVR (only one phase shown - other phases are identical).

using a phase locked loop (PLL). The *cos* wave is locked in phase with the phase A line current. The load side voltage (v_{2_abc}) is transformed into the dq coordinates (v_{2_dqo}). The magnitude of the load side voltage (v_{2_mag}) is computed from v_{2_d} and v_{2_q}. The error in v_{2_mag} is generated by comparing it with a reference voltage (v_{2_ref}). The error is processed through a PI block to compute the amount of reactive voltage (inp_q), in quadrature with line current, required to be injected into the system. The dc capacitor voltage (v_c) is compared to the desired reference value (v_{c_ref}). The error in the capacitor voltage is used to determine the amount of real voltage (inp_d), in phase with the line current, to be injected into the system. In order to avoid excessive voltage drop across the DVR during the charging of the dc capacitor, inp_d is limited to 0.1. These input signals (inp_{dq}) are transformed into the *abc*

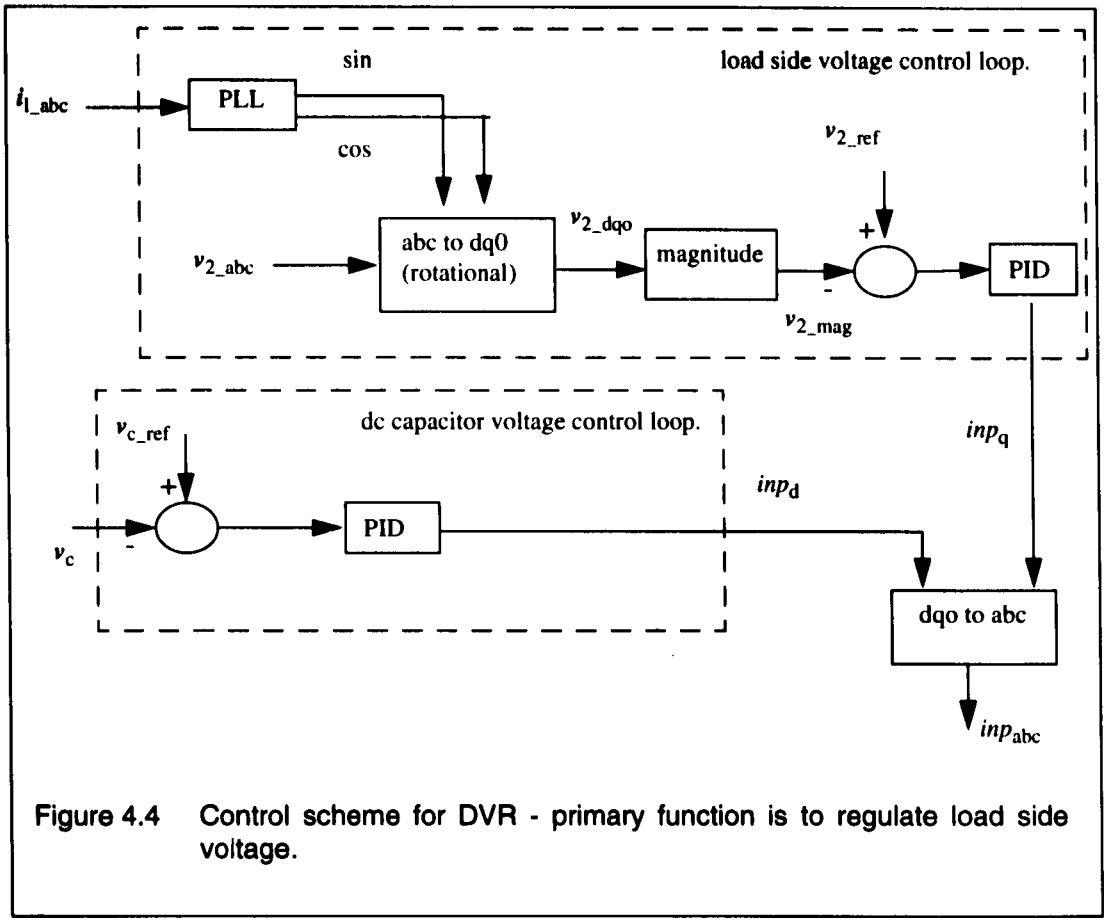

Figure 4.4 Control scheme for DVR - primary function is to regulate load side voltage.

coordinates, and are used by the triggering module to generate the necessary triggering signals. The gate signals are generated by comparing the input signals (inp_{abc}) to a triangular carrier wave.

4.2.3 Design of the DVR Components

As in the case of the 12-pulse STATCOM and the PWM STATCOM, the information regarding the parameters of the PWM DVR is not available prior to model development. Hence, the procedure followed to develop the model is similar to that of the 12-pulse STATCOM. The various steps in the design procedure are:

1. Analytically calculate the following parameters - voltage, current and

frequency rating of the dc/ac inverter, filter component sizes, coupling transformer impedance.

2. Perform open loop simulations, with a battery on the dc side of the inverter, to determine if the parameters selected in step 1 are satisfactory.

3. Analytically estimate the gains required for the dc voltage control loop and the load voltage control loop. Perform closed loop simulations to refine these parameters.

As in the case of the 12-pulse STATCOM and the PWM STATCOM, the design of snubber circuits involves accurate simulation of the switching waveforms. Such studies are beyond the scope of this dissertation and hence not addressed here.

The TBM developed for the PWM DVR is described in Section 4.2.4. The various analytical calculations involved in the design are described in Appendix C.1. The simulation studies involved in step 2 are described in Sections 4.2.5. In Section 4.2.1, a simulation is described to study the response of the DVR to a three phase to ground fault on the source side. The TBM is used for these simulation studies. Comparisons are made with the corresponding use of the ISM for such simulation studies. The simulations are performed with the DVR installed in the 15 kV distribution feeder described in Section 3.2.5. The model of the DVR is inserted between nodes 2 and 3 in the 15-kV distribution feeder (Figure 4.5).

4.2.4 Model Description

As in the case of the STATCOM models, a modular approach is used to develop the PWM DVR model. Each functional block of the DVR is modelled as a separate module. The complete model is obtained by appropriately connecting the individual modules. Also, the DVR models developed using the TBM and the ISM differ only in the VSI module and

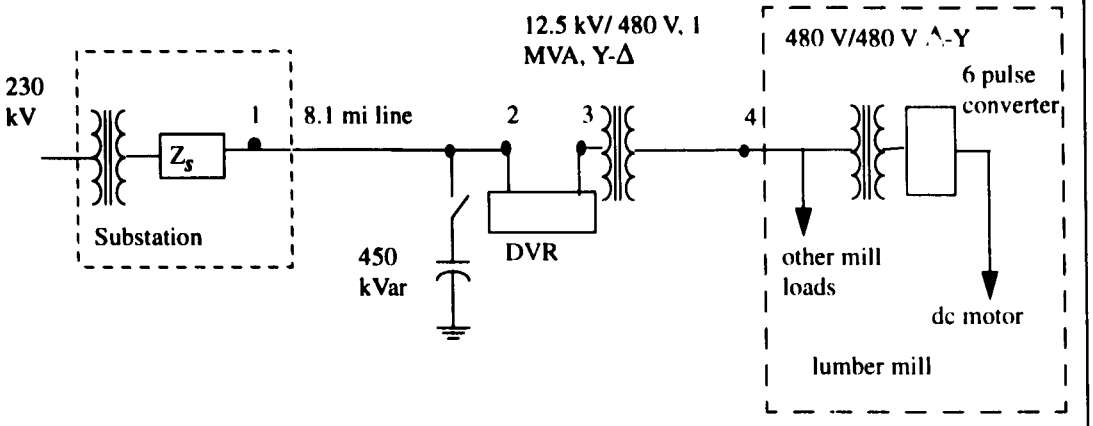

Figure 4.5 One-line Diagram of 15 kV Distribution Feeder.

the control system module. The rest of the modules are unchanged. The SABER simulator is used to develop the models. The TBM for each single phase inverter is developed by replacing the PWM switches by controlled voltage and current sources as described in section 2.6. The inverters are tied in series with the system, using three single phase coupling transformers. These transformers are modeled with standard EMTP library models. Saturation effects are not considered. The output filter module is implemented using series LC elements. The sensing module consists of ideal transformers and low-pass noise filters. The describing function approximation of the switching function generator is similar to that of a buck converter in voltage control mode as described in section 2.4.

4.2.5 Simulation Study - Output Filter Design

The purpose of this simulation study is to verify the design of the DVR output filter. The DVR is operated in open loop for this study. The dc capacitor is replaced by a battery. The dc voltage control loop is kept open. Starting at 20 ms, the load voltage control loop is given a command to inject a voltage of magnitude $0.2V_{dc}$ in quadrature with the line current. The simulation is performed using the TBM with the filter parameters determined

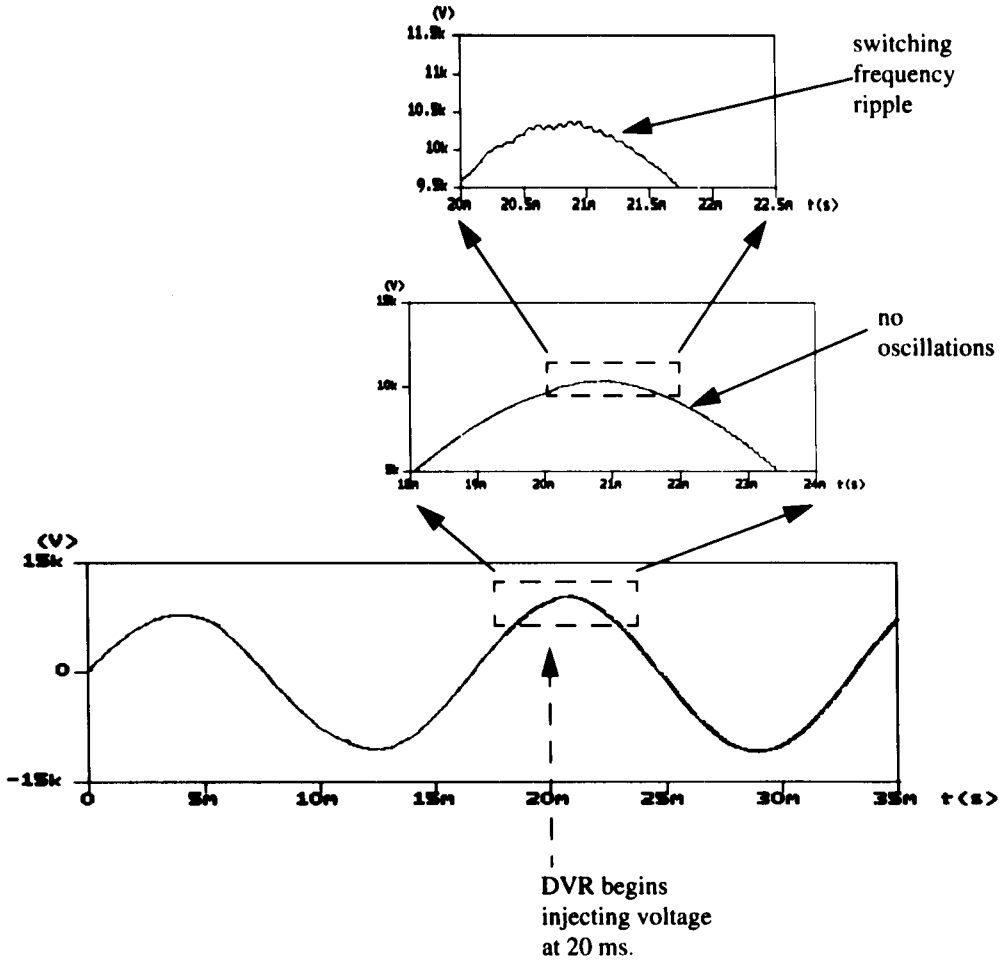

Figure 4.6 **Phase A Line to Neutral Voltage on load side (node 3) of DVR - simulation using TBM.**

in Appendix C.1. Figure 4.6 shows the phase A line to neutral voltage on the load side (node 3) of the DVR. The voltage waveform shows very small switching frequency ripple, hence it can be concluded that the DVR filters are sufficient to mitigate switching frequency harmonics in the DVR output voltage. For the sake of comparison, the simulations are also performed using the ISM. The results are shown in Figure 4.7.

A comparison of Figure 4.6 and Figure 4.7 shows that the results of the TBM and

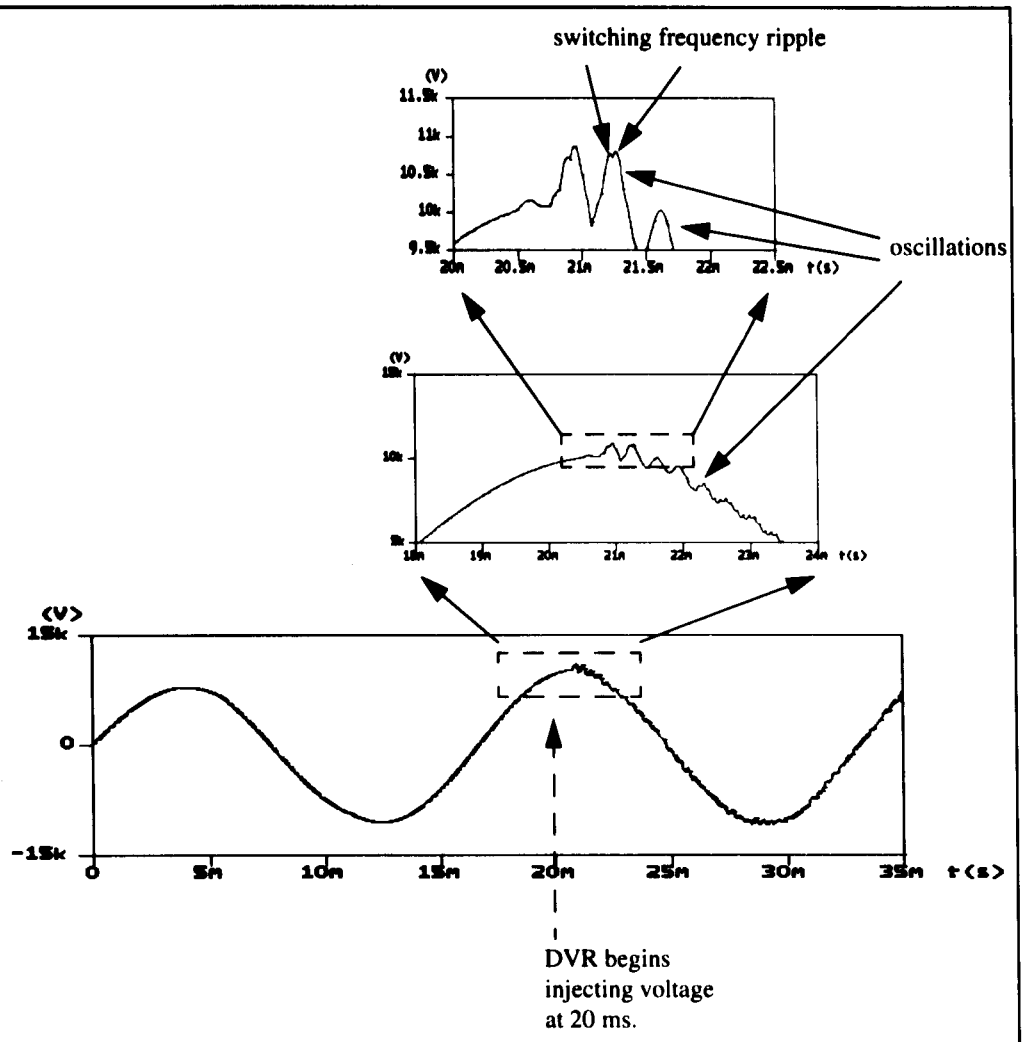

Figure 4.7 Phase A Line to Neutral Voltage on load side (node 3) of DVR - simulation using ISM.

the ISM are not consistent. The ISM shows high frequency oscillations riding on top of the fundamental 60 Hz voltage waveform at node 3. Such oscillations are not observed in the simulation results using the TBM as shown in Figure 4.6. Two explanations are possible - (i) the oscillations are present in the actual system and the TBM has failed to predict these oscillations; (ii) the oscillations are not present in the actual system and the numerical

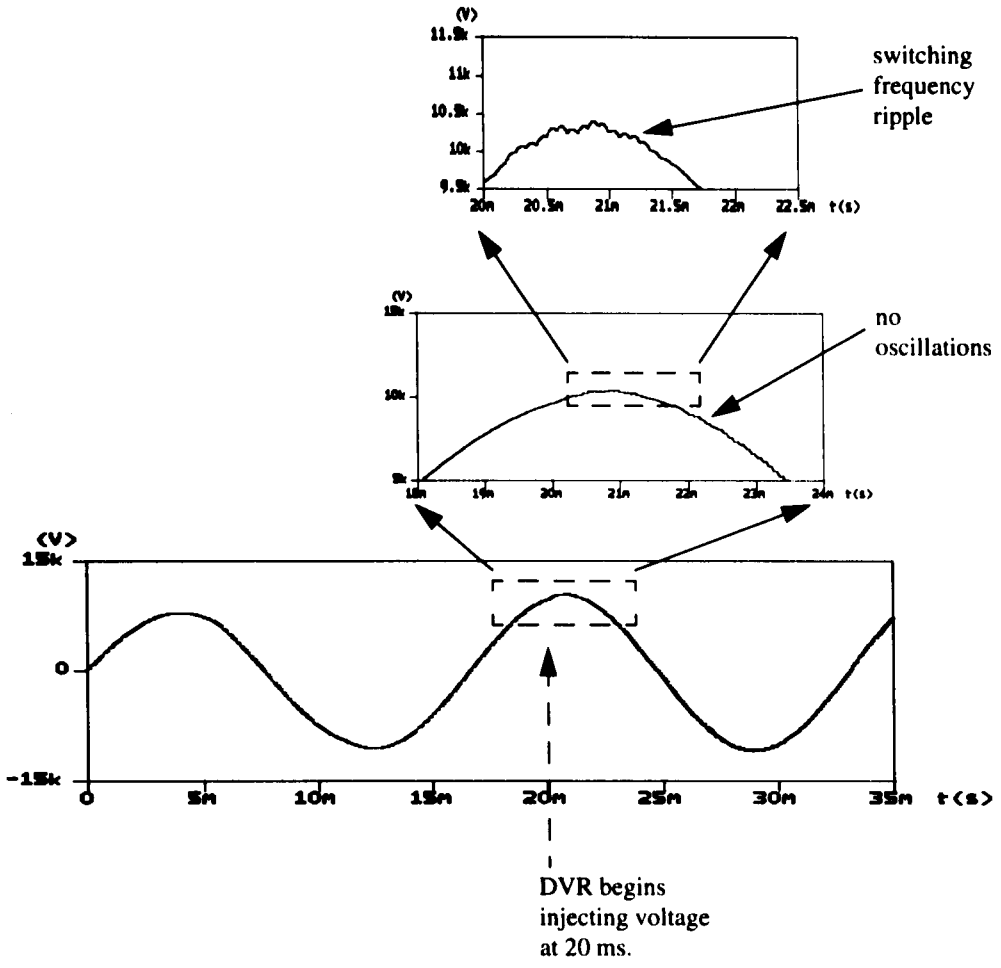

Figure 4.8 Phase A Line to Neutral Voltage on load side (node 3) of DVR - simulation using ISM. The simulator is forced to use a small time step of 0.5 μs.

errors in the ISM has introduced these oscillations. In order to confirm the correct explanation for the observed oscillations, the simulation using the ISM is repeated, but this time with a fixed small time step of 0.5 μs. Note that in the previous simulation using the ISM, the variable time step feature of the simulator is used. In contrast, the next simulation using the ISM is performed by forcing the simulator to take a small time step. The results

are shown in Figure 4.8. The oscillations observed in Figure 4.7 are not observed in Figure 4.8. Hence it can be concluded that the oscillations are introduced due to numerical errors. Table 4.1 shows the CPU time required for the three simulations on an HP Series 700 workstation. It is clearly seen that the numerical errors in the ISM are eliminated only at the expense of computational time. In this simulation study, the TBM is 10 times more computationally efficient than the ISM. It should be pointed out that ideally it is desirable that the simulator automatically selects a time step size necessary to avoid such numerical errors. In the case described here, the SABER simulator failed to automatically avoid the numerical errors and hence a fixed time step size had to be forced upon the simulation algorithm to avoid the errors. However, even if the simulator had succeeded in avoiding the errors, the results would be computationally more expensive than that of the TBM.

Table 4.1. CPU time for simulation of the study of DVR filter parameters.

Model Type	CPU time (s)
TBM	310
ISM (simulator automatically selects time step size)	1570
ISM (time step size forced to 0.5 μs)	2929

4.2.6 Simulation Study - Response to a Three Phase to Ground Fault

The purpose of this simulation is to study the capability of the DVR to regulate the load side (node 2) voltage in the event of a three phase to ground fault on the source side (node 2). Since the time constants involved in the phenomena are much lower than the switching period of the DVR, the TBM with only the dc Fourier term is used for this simulation. Both the dc voltage control loop and the load voltage control loop are kept closed. The system linear load is switched on at 50 ms. The fault is initiated at 100 ms and is cleared at 150 ms. Figure 4.9 shows the simulation results. When the linear load is switched on at 50 ms, the voltage on the source side (node 2) is observed to sag by 0.03 p.u.

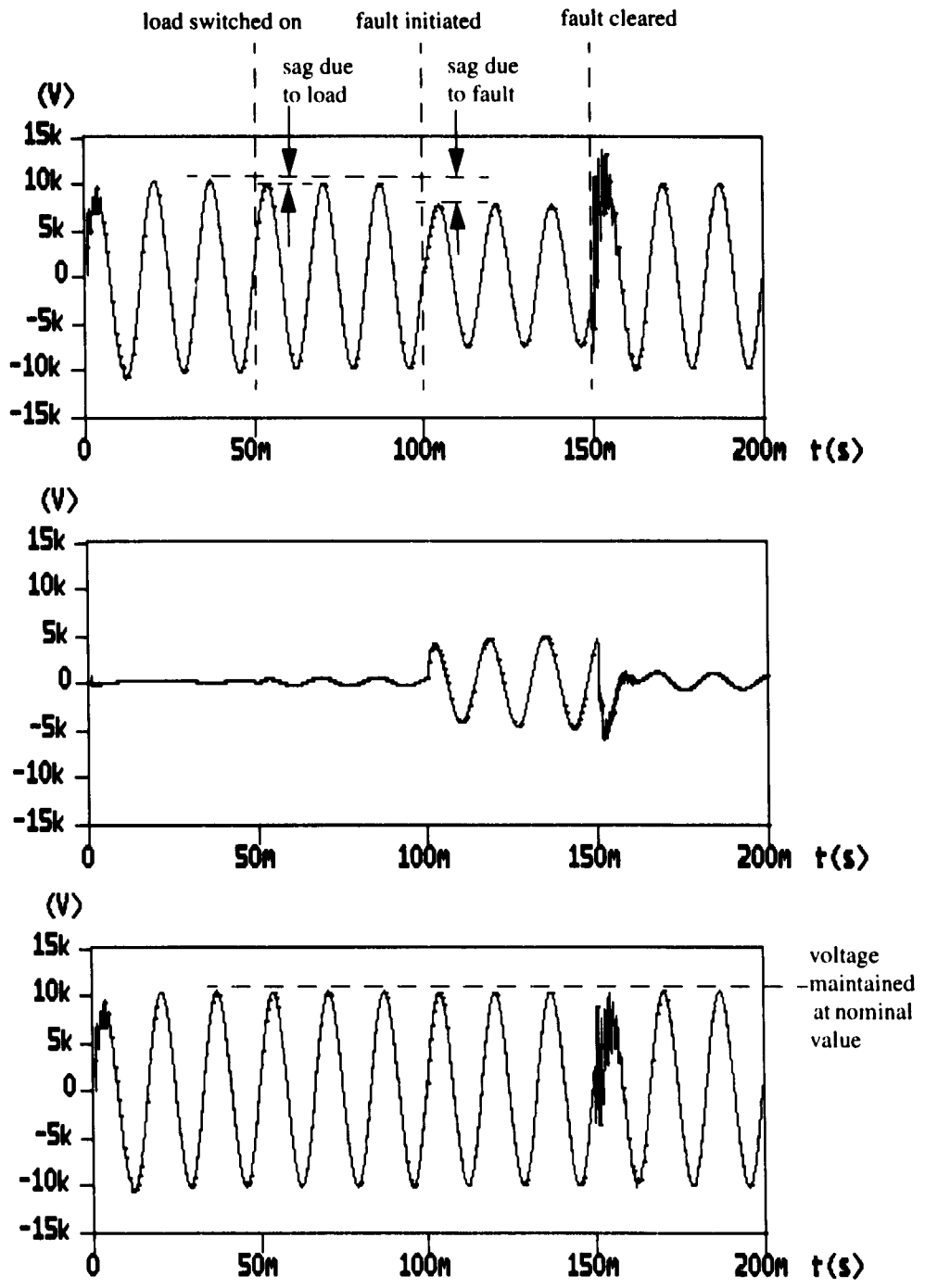

Figure 4.9 Phase A line to neutral voltage - top: source side (node 2) voltage; middle: DVR voltage; bottom: load side (node 3) voltage.

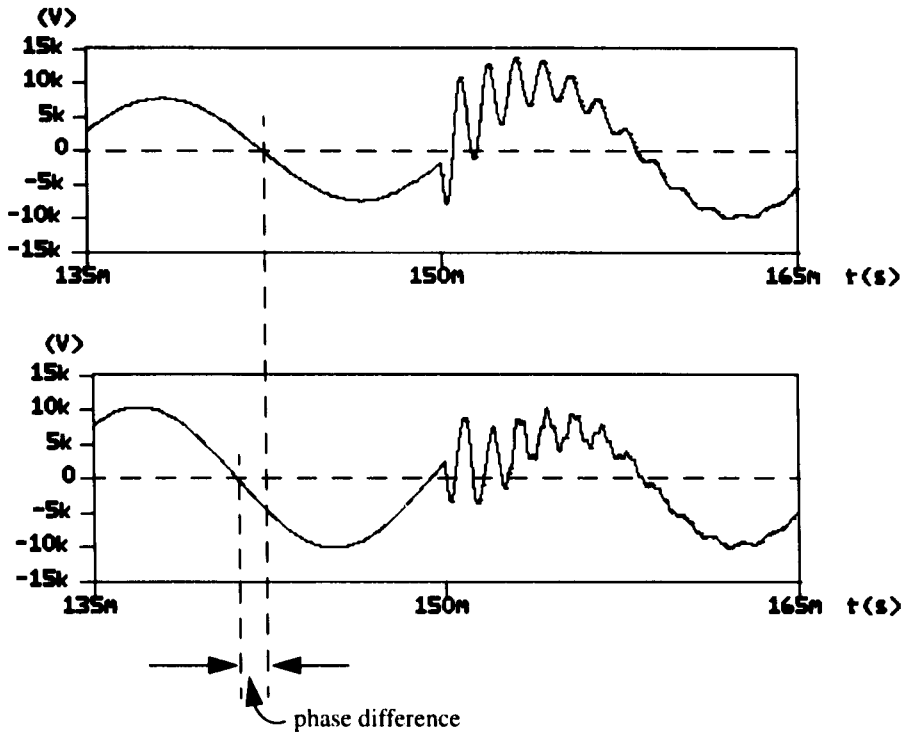

Figure 4.10 Oscillatory transients in the Phase A line to neutral voltage after the fault is cleared - top: source side (node 2) voltage; bottom: load side (node 3) voltage.

During the period of the fault the voltage at node 2 sags by 0.27 p.u. In response to these voltage sags, the DVR injects a voltage into the system such that the load side voltage is maintained at its nominal value. Figure 4.10 shows the results at the instant of fault clearing in more detail. These results show that the oscillatory transients that occur at the time of fault clearing are too fast to be compensated by the DVR. It should also be noted that the node 3 voltage leads the node 2 voltage. This lead is due to the fact that the DVR injects a voltage that is in quadrature with the line currents so that it exchanges only reactive power with the system. If such a phase lag is not desirable for the load, then the DVR controls have to be modified so that it injects a voltage in phase with the source side voltage. The penalty

for such a modification is that the DVR also has to exchange real power with the system.

4.3 Conclusions

As in the case of the STATCOM models, the DVR model is developed by a systematic procedure. The resulting TBM of the DVR is complete with the power converter and its control system. The TBM is extremely effective for simulation studies of the DVR. The observations regarding the efficiency of the TBM are similar to those in the case of the STATCOM (see Section 3.4). In the simulation study for the output filter design, the ISM is observed to introduce oscillations in the voltage waveform. These errors are corrected at the expense of small simulation time steps. In contrast, the TBM does not introduce any such numerical errors and hence it requires a significantly smaller CPU time for simulation. The DVR model is used to study the performance of the DVR in the event of a three phase to ground fault. The simulation results show that the DVR is capable of maintaining the load voltage in the event of the fault. However, the DVR is not capable of compensating the oscillatory transients that occur at the instant when the fault is cleared. Also, due to the control method used, the phase of the load voltage is different from that of the source voltage. Such controls may be undesirable for phase sensitive loads.

5. Conclusions, Contributions and Recommendations for Future Work

The conclusions of this dissertation are presented in this chapter. The contributions of the new switch modeling technique are stated. Recommendations are made for future work.

5.1 Conclusions

The electric power industry is undergoing a revolutionary change. Future power systems may be envisioned as a complex network of classical power system apparatus along with a large number of embedded power electronic converters for power flow control and power quality improvement. For the successful planning and operation of such systems, digital simulations will become essential tools. Even though the speed of computers is increasing rapidly, the demand for faster computational speed is also increasing rapidly. Thus the computational efficiency of simulation models is a critical issue. Due to the wide variety of components that will need to be modeled and simulated, general purpose time domain simulators such as EMTP, SABER and NETOMAC will become standard platforms for performing the simulation studies. This in turn leads to the issue of ease of model implementation in a general purpose time domain simulators. Yet another issue will be the flexibility of the models. Models will find wider applications only if they are flexible as well as easy to maintain. A modular approach to modeling is extremely desirable from flexibility and maintenance point of view. A review of power electronics literature reveals that not all the techniques available in the power electronics literature are useful for the analysis of power converters installed in power systems. A new modeling technique has been presented in this dissertation. The technique yields a Transient Behavioral Model (TBM) of a power converter. The philosophy behind the

development of the TBM has been influenced by the above mentioned issues in the modeling of a future power system. Previously, the Ideal Switch Model (ISM) and the Variable Impedance Model (VIM) have been extensively used for power system transient simulation studies. Due to the discontinuous nature of these models, the simulation time step has to be kept very small during the switching transitions. This reduction in time step results in computational inefficiency. The continuous nature of the TBM overcomes this limitation of the ISM. At the same time, the TBM retains most of the desirable features of the ISM. This makes the TBM more attractive than other techniques available in the power electronics literature, such as the Harmonic Balance Method (HBM) and the Generalized Average Switch Model (GASM), for time domain simulation of large systems using standard circuit simulator. The TBM also allows dynamic variation of accuracy of simulation by simply varying the number of Fourier terms included in the model. For example, a simulation can be started with the TBM using only the dc Fourier term. When the system reaches the desired steady state condition, the simulation can be performed with the TBM using higher order Fourier terms. This feature is extremely useful for power systems simulations where a large amount of computational time is spent in bringing the system to a desired steady state condition.

The most important limitation of the TBM is that it can only be used for circuits which include the PWM configuration shown in Figure 2.1. Secondly, the TBM involves the burden of the computing the describing function. Further, even though the development of the TBM involves only two simple steps, it is still not as easy to implement as the ISM. On the other hand, the use of the ISM may involve additional work on the part of the user to eliminate numerical problems associated with the discontinuous nature of the ISM. Also, since the TBM simulates only up to a predetermined number of harmonics, it requires a the user to exercise judgement over the number of Fourier terms to be included in the model.

Thus, the decision between choosing the TBM or the ISM for a particular modeling application will depend on the trade-offs between computational efficiency, accuracy and ease of implementation.

This dissertation also describes the development of TBMs for three Custom Power Device (CPD) models - (i) a 12-pulse STATCOM, (ii) a Pulse Width Modulated (PWM) STATCOM, (iii) a PWM Dynamic Voltage Restorer (DVR). The 12-pulse STATCOM is capable of compensating the reactive power demand of a load. The PWM STATCOM is capable of regulating the voltage at the coupling point and also compensating the load current harmonics. The PWM DVR is capable of regulating the load side voltage. Presently, only prototypes of such devices have been reported in literature. Further, the design of these devices has to be system specific. A device that may be suitable for one power system, may not be adequate for another system. Hence, for the purpose of model development in this dissertation, a practical 15 kV distribution system with severe power quality problems has been considered. The three devices and their models have been systematically designed using simulation studies of the 15 kV distribution system. The process of model development reveals the sensitivity of these devices to the specifics of the power system in which they are installed. These CPD models are complete with the dc/ac inverter module, sensing module, control module and coupling transformer model. Thus they can be used for detailed analysis of the impact of the devices on a distribution system. The models are modular in nature, hence utility engineers can easily modify the models to investigate different topologies and control techniques.

5.2 Contributions

The following are the contributions made by this dissertation:

Identification of the relative merits and demerits of various power electronics

modeling techniques from the perspective of a power systems engineer: The dissertation provides a systematic review of the various modeling techniques available in power electronics literature. Emphasis has been placed on the usefulness of these techniques to a power systems engineer. The merits and demerits of using different techniques for different types of power system simulation studies have been identified.

Development of the Transient Behavioral Model: A new modeling technique has been introduced. This technique yields a continuous model of a power converter which is superior to previously used discontinuous models due to its computational efficiency. The TBM is superior to the previously used continuous models due to its ease of implementation in standard time domain simulators.

Concept of dynamically varying the accuracy of simulation in a single simulation run: Previously, such changes in accuracy and speed of a model would involve starting simulation using one model, stopping the simulation, transferring the simulation data into another model and then restarting of the simulation. Using the TBM, such changes in accuracy and speed can be conveniently made by simply varying the number of Fourier terms included in the describing function approximation of the switching function generator. This concept is extremely powerful in the case of power systems simulations where a considerable amount of CPU time is spent in bringing the model to the desired initial steady state operating point.

Development of the TBM of a 12-pulse STATCOM and a PWM STATCOM: The TBM technique has been used to develop detailed models for two types of STATCOM's. The performance of the STATCOM's in a practical 15 kV distribution feeder is simulated. The simulations show the critical dependence of the design parameters on those of the system. The performance of the 12-pulse STATCOM for reactive power compensation, and

the performance of the PWM STATCOM for voltage regulation and current harmonic compensation are demonstrated through the simulation studies.

Development of the TBM for a PWM DVR: The TBM technique is used to develop a detailed model of a PWM DVR. As in the case of the STATCOM's, the DVR is simulated in a practical 15 kV distribution feeder. The performance of the DVR in compensating the voltage sag due to a three phase to ground fault is demonstrated.

5.3 Future Work

The TBM technique can be applied to any converter having the switch configuration shown in Figure 2.1. So far, only the continuous conduction mode of the power converters has been demonstrated. Further, only the TBM for force commutated converters has been demonstrated. The technique can be extended to both discontinous as well as naturally commutated converters. However, such an extension requires the inclusion of constraint equations which implicitly determine the on and off periods for the switches. After such an extension, the TBM can also be applied to the modeling of rectifiers and thyristor controlled reactors.

The TBM is a continuous representation of a switched circuit network. Hence it is possible to linearize it around a fixed operating point and perform small signal analysis. Several small signal models are already available in literature. However, the ease of implementing the TBM in a circuit simulator can be exploited even for small signal analysis. Thus the TBM of a power converter can be conceived as a single model that can be used for both small signal frequency domain analysis as well as time domain simulations.

The TBM uses the describing function to approximate the switching function

generator. The direct correspondence between the describing function and the frequency domain behavior of the converter makes the describing function technique attractive for the TBM. However, approximation of the switching function using functions such as Legendre's polynomial, or the Chebychev series can also be investigated from the point of view of computational efficiency.

REFERENCES

[1] Arthur D. Little, Inc., "Power Quality Market Assessment," *EPRI report TR-104372*, RP 3273-09, -10, October 1994.

[2] H. Akagi, "Trends in Active Power Line Conditioners," *IEEE Transactions on Power Electronics*, Vol. 9, No. 3, pp. 263-8, May 1994.

[3] V. H. Tahiliani, H. Mehta, "Custom Power - Utility's Response to Power Quality Issues," *Proceedings of the American Power Conference*, Vol. 2, pp. 1561-5, Chicago, IL, April 1992.

[4] J. Arrillaga, *High Voltage Direct Current Transmission*, Peter Peregrinus Ltd., London, 1983.

[5] S. Lefebvre, A. M. Gole, et. al, "Working Group on Dynamic Performance and Modeling of DC Systems and Power Electronics for Transmission Systems - Report on Test Systems for ac/dc Interaction Studies," *IEEE Transactions on Power Delivery*, Vol. 10, No. 4, pp. 2027-34, October 1995.

[6] L. Gyugyi, "Reactive Power Generation and Control by Thyristor Circuits," *IEEE Transactions on Industrial Applications*, Vol. IA-15, No. 5, September/October 1979.

[7] S. G. Helbing, G. G. Karady, "Investigations of an Advanced Form of Series Compensation," *IEEE Transactions on Power Delivery*, Vol. 9, No. 2, pp. 939-47, April 1994.

[8] K. Clark, B. Fardanesh, R. Adapa, "Thyristor Controlled Series Compensation Application Study - Control Interaction Considerations," *IEEE Transactions on Power Delivery*, Vol. 10, No. 2, pp. 1031-7, April 1995.

[9] N. G. Hingorani, "The Future of Transmission: Switching to Silicon," *EPRI Journal*, pp. 5-13, June 1989.

[10] A. Robert, M. Couvreur, "Arc Furnace Flicker Assessment and Prediction," *12th International Conference on Electricity Distribution*, CIRED, Birmingham, England, Vol. 2, IEE, pp. 17-21, May 1993.

[11] E. Larsen, N. Miller, S. Nelson, S. Lindgren, "Benefits of GTO-based Compensation Systems, for Electric Utility Applications," *IEEE Transactions on Power Delivery*, Vol. 7, No. 4, October 1992, pp. 2056-64.

[12] L. Gyugyi, "A Unified Power Flow Control Concept for Flexible AC Transmission Systems," *Proceedings of the 5th IEE International Conference on AC and DC Power Transmission*, London, September 1991

[13] N. R. Raju, S. S. Venkata, R. A. Kagalwala, V. V. Sastry, "An Active Power Quality Conditioner for Reactive Power and Harmonics Compensation," *IEEE PESC 95 Record*, Vol. 1, pp. 209-14, June 1995.

[14] D. Wuest, H. Stemmler, G. Scheuer, "A Comparison of Different Circuit Configurations for an Advanced Static Var Compensator (ASVC)," *IEEE PESC 93 Record*, Seattle, 1993

[15] C. Schauder, H. Mehta, "Vector Analysis and Control of Advanced Static Var Compensators," *presented at the 5th IEE International Conference on AC and DC Power Transmission*, London, September 1991.

[16] Y. Hayashi, N. Sato, K. Takahashi, "A Novel Control of a Current-Source Active Filter for AC Power System Harmonic Compensation," *IEEE Transactions on Industry Applications*, Vol. 27, No. 2, March/April 1991.

[17] M. R. Iravani, A. K. S. Chandhary, et. al, "Modeling and Analysis Guidelines for Slow Transients - Part II Controller Interactions; Harmonic Interactions," *presented at the PES Winter Meeting*, Baltimore, January, 1996.

[18] N. Mohan, W. P. Williams, T. M. Undeland, R. Nilssen, Olve Mo, "Simulation of Power Electronic and Motion Control Systems - an Overview," *Proceedings of the IEEE, Vol. 82*, No. 8, August 1994.

[19] I. Budihardjo, P. O. Lauritzen, K. Y. Wong, R. B. Darling, H. A. Mantooth, "Defining Standard Performance Levels for Power Semiconductor Devices," *presented at the IEEE IAS Annual Meeting*, Orlando, Florida, October, 1995.

[20] C. L. Ma, P. O. Lauritzen, "A Simple Power Diode Model with Forward and Reverse Recovery," *IEEE PESC 91 Record*, pp. 411-15, June 1991.

[21] C. L. Ma, P. O. Lauritzen, P. Turkes, H. J. Mattausch, "A Physically-Based Lumped-Charge SCR Model," *IEEE PESC 93 Record*, pp. 53-9, June 1993.

[22] *SABER User Manual*, Analogy, Inc., 1995, Beaverton, OR 97075.

[23] *PSPICE User's Manual*, MicroSim Corp., 1987, Irvine, CA.

[24] H. W. Dommel, *EMTP Theory Book*, Microtran Power System Analysis Corporation, May, 1992.

[25] P. Lehn, J. Rittiger, B. Kulicke, "Comparison of the ATP Version of the EMTP and the NETOMAC Program for Simulation of HVDC Systems," *presented at the IEEE/PES Winter Meeting*, New York, January/February 1994.

[26] J. R. Marti, Jiming Lin, "Suppression of Numerical Oscillations in the EMTP," *IEEE Transactions on Power Systems*, Vol. 4, No. 2, pp. 739-747, May 1989.

[27] V. Rajagopalan, K. Debebe, A. Chandrasekaran, S. A. Sudha, "User-friendly Dedicated Power Electronic Converter Simulator," *IEEE Transactions on Industrial Electronics*, Vol. 39, No. 1, February 1992.

[28] V. Rajagopalan, *Computer-Aided Analysis of Power Electronic Systems*, Marcel Dekker, Inc., New York, 1987.

[29] J. G. Kassakian, M. F. Schlecht and G. C. Veghese, *Principles of Power Electronics*, Addison-Wesley Publishing Company, Inc., June 1992.

[30] R. D. Middlebrook, S. Cuk, "A General Unified Approach to Modelling Switching-Converter Power Stages," *IEEE PESC 76 Record*, pp. 18-34, 1976.

[31] S. Cuk, R. D. Middlebrook, "A General Unified Approach to Modeling Switching Dc-to-Dc Converters in Discontinuous Conduction Mode," *IEEE PESC 77 Record*, pp. 36-57, 1977.

[32] R. D. Middlebrook, "A Continuous Model for the Tapped-Inductor Boost Converter," *IEEE PESC 75 Record*, pp. 63-79, 1975.

[33] V. Vorperian, "Simplified Analysis of PWM Converters Using Model of PWM Switch. Part I: Continuous Conduction Mode," *IEEE Transactions on Aerospace and Electronic Systems*, Vol. 26, No. 3, pp. 490-6, May 1990.

[34] V. Vorperian, "Simplified Analysis of PWM Converters Using Model of PWM Switch. Part I: Discontinuous Conduction Mode," *IEEE Transactions on Aerospace and Electronic Systems*, Vol. 26, No. 3, pp. 497-505, May 1990.

[35] A. R. Brown, R. D. Middlebrook, "Sampled-Data Modeling of Switching Regulators," *IEEE PESC 81 Record*, 1981.

[36] S. R. Sanders, J. M. Noworolski, X. Z. Liu, G. C. Verghese, "Generalized Averaging Method for Power Conversion Circuits," *IEEE Transactions on Power Electronics*, Vol. 6, No. 2, pp. 251-9, April 1991.

[37] K. S. Kundert, A. S. Vincentelli, "Simulation of Nonlinear Circuits in the Frequency Domain," *IEEE Transactions on Computer-Aided Design of Integrated Circuits and Systems*, Vol. CAD-5, No. 4, October 1986.

[38] Rowan Gilmore, "Nonlinear Circuit Design Using the Modified Harmonic Balance Algorithm," *IEEE Transactions on Microwave Theory and Techniques*, Vol. MTT-34, No. 12, December 1986.

[39] J. Groves, "Small-Signal Analysis Using Harmonic Balance Methods," *IEEE PESC 91 Record*, pp. 74-79, 1991.

[40] R. Tymerski, "Frequency Analysis of Time-Interval-Modulated Switched Network," *IEEE Transactions on Power Electronics*, Vol. 6, No. 2, pp.297-295, April 1991.

[41] R. Tymerski, "Application of the Time-Varying Transfer Function for Exact Small-Signal Analysis," *IEEE PESC 91 Record*, pp. 80-87, 1991.

[42] R. C. Wong, J. Groves, "An Automated Small-Signal Frequency-Domain Analyzer for General Periodic-Operating Systems as Obtained Via Time-Domain Simulation," *IEEE PESC 95 Record*, pp. 801-808, 1995.

[43] R. C. Wong, H. A. Owen, Jr., T. G. Wilson, "A Fast Algorithm for the Time-Domain Simulation of Switched-Mode Piecewise-Linear Systems," *IEEE PESC 84 Record*, pp. 281-296, 1984.

[44] S. S. Kelkar, F. C. Lee, "A Fast Time Domain Digital Simulation Technique for Power Converters: Application to a Buck Converter with Feedforward Compensation," *IEEE PESC 84 Record*, pp. 397-408, 1984.

[45] C. J. Hsiao, R. B. Ridley, H. Naitoh, F. C. Lee, "Circuit-Oriented Discrete-Time Modeling and Simulation of Switching Converters," *IEEE PESC 87 Record*, pp. 167-176, 1987.

[46] C. C. Liu, Conrad H. K. Chang, Yu-Ti Hsiao, J. M. Bocek, "A Fast-Decoupled Method for Time-Domain Simulation of Power Converters," *IEEE Transactions on Power Electronics*, Vol. 8, No. 1, pp. 37-45, January 1993.

[47] Y. Kang, J. D. Lavers, "Power Electronics Simulation: Current Progress and Future Development," *Proceedings of the IEEE PELS Workshop on Computers in Power Electronics*, August 1994.

[48] I. J Nagrath, M. Gopal, *Control Systems Engineering*, Wiley Eastern Limited, 1982.

[49] E. V. Larsen, M. Sublich, S. C. Kapoor, "Impact of Stray Capacitance on HVDC Harmonics," *IEEE Transactions on Power Delivery*, Vol. 4, No. 1, pp. 637-642, January 1989.

[50] R. Kagalwala, S. S. Venkata, M. A. El-Sharkawi, N. G. Butler, A. Van Leuven, A. P. Rodriguez, I. Kerszenbaum, D. Smith, "Transient Analysis of Distribution Class Adaptive Var Compensators: Simulations and Field Test Results," *IEEE Transactions on Power Delivery*, Vol. 10, no. 2, pp. 1119-25, April 1995.

[51] R. Kagalwala, K. Y. Wong, S. S. Venkata., P. O. Lauritzen, "Modeling and Simulation of Custom Power Devices," *project report submitted to EPRI*, RP 3389-15, June 1995.

[52] J. M. Zavahir, J. Arrillaga, N. R. Watson, "Hybrid Electromagnetic Transient Simulation with the State Variable Representation of HVDC Converter Plant," *IEEE Transactions on Power Delivery*, Vol. 8, No. 3, pp. 1591-1598, July 1993.

[53] G. Morin, L. X. Bui, S. Casoria, J. Reeve, "Modeling of the Hydro-Quebec-New England HVDC System and Digital Controls with EMTP," *IEEE Transactions on Power Delivery*, Vol. 8, No. 2, pp. 559-566, April 1993.

[54] S. Lefebvre, L. Gerin-Lajole, "A Static Compensator Model for the EMTP," *IEEE Transactions on Power Systems*, Vol. 7, No. 2, pp. 477-86, May 1992.

[55] M. Tou, T. Rafesthain, A. Ba-Razzouk, K. Debebe, V. Rajagopalan, "Global Simulation of Multiple Power Electronic Converter System Using a Novel Iterative Method," *Proceedings of the 1992 International Conference on Industrial Electronics, Control, Instrumentation, and Automation*, Vol. 1, pp. 494-9, November, 1992.

[56] J. Vlach, K. Singhal, *Computer Methods for Circuit Analysis and Design*, Van Nostrand Reinhold Company, 1983.

[57] *EMTP Rule Book*, 1992, Electric Power Research Institute, Palo Alto, CA 94304.

[58] F. L. Alvarado, R. H. Lasseter, J. J. Sanchez, "Testing of Trapezoidal Integration with Damping for the Solution of Power Transient Problems," *IEEE Transactions on Power Apparatus and Systems*, Vol. PAS-102, No. 12, pp. 3783-90, December 1983.

[59] T. L. Maguire, A. M. Gole, "Digital Simulation of Flexible Topology Power Electronics Apparatus in Power Systems," *IEEE Transactions on Power Delivery*, Vol. 6, No. 4, pp. 1831-1840, October 1991.

[60] N. Abdel-Rahim, J. E. Quaicoe, "Modelling and Analysis of a Feedback Control Strategy for Three-Phase Voltage Source Utility Interface Systems," *Conference Record of the 1994 Industry Applications Conference*, IEEE IAS Meeting, pp. 895-902, Denver, Colorado, October 1994.

[61] G. T. Heydt, J. Jun, "Rapid Calculation of the Periodic Steady State for Electronically Switched, Time Varying Power System Loads," *presented at the IEEE PES Winter Meeting*, Baltimore, MD, January 1996.

[62] L. J. Bohmann, R. H. Lasseter, "Harmonic Interactions in Thyristor Controlled Reactor Circuits," *IEEE Transactions on Power Delivery*, Vol. 4, No. 3, July 1989.

[63] I. Budihardjo, P. O. Lauritzen, "The Lumped Charge Power MOSFET Model, Including Parameter Extraction," *IEEE Transactions on Power Electronics*, May 1995.

[64] L. Dube, H. W. Dommel, "Simulation of Control Systems in an Electromagnetic Transients Program with TACS," *Proceedings PICA*, 1979.

[65] N. Mohan, T. M. Undeland, W. P. Robbins, *Power Electronics: Converters, Applications and Design*, John Wiley and Sons, 1989.

[66] R. M. Bass, B. S. Heck, R. A. Khan, "Average Modelling of Current-Mode Controlled Converters: Instability Predictions," *International Journal of Electronics*, Vol. 77, No. 5, pp. 613-28, 1994.

[67] L. Gyugyi, N. Hingorani, P. Nannery, N. Tai, "Advanced Static Var Compensator Using Gate Turn-Off Thyristors for Utility Applications," *presented at the CIGRE meeting,* Paris, August 1990.

[68] C. W. Edwards, et. al., "Advanced Static Var Generator Employing GTO Thyristors," *IEEE Transactions on Power Delivery*, Vol. 3, No. 4, October 1988, pp. 1622-1627.

[69] L. Gyugyi, "Dynamic Compensation of AC Transmission Lines by Solid-State Synchronous Voltage Sources," *IEEE Transactions on Power Delivery*, Vol. 9, No. 2, April 1994, pp. 904-11.

[70] Peter Wood, *Switching Power Converters*, Van Nostrand Reinhold Company, New York, 1981.

[71] Fu-Sheng Tsai, V. Joseph Thottuvelil, "Benchmarks for Power Electronics Circuit Simulation," *Proceedings of the IEEE PELS Workshop on Computers in Power Electronics*, 1992.

Appendix A - Abbreviations Used

A.1 Abbreviations Used

AHDL - Analog Hardware Description Language

APLC - Active Power Line Conditioners

APQC - Active Power Quality Conditioner

ASM - Average Switch Model

ASVC - Advanced Static Var Compensator

ASVG - Advanced Static Var Generator

AVC - Adaptive Var Compensator

CPD - Custom Power Device

CSI - Current Source Inverter

DVR - Dynamic Voltage Restorer

EMTP - Electro Magnetic Transients Program

EPRI - Electric Power Research Institute

GASM - Generalized Average Switch Model

HBM - Harmonic Balance Method

HVDC - High Voltage Direct Current

ISM - Ideal Switch Model

PWM - Pulse Width Modulation / Pulse Width Modulated

STATCOM - Static Compensator

STATCON - Static Condenser

SVC - Static Var Compensator

TBM - Transient Behavioral Model / Transient Behavioral Modeling

TCSC - Thyristor Controlled Series Capacitor

TSR - Thyristor Switched Reactor

VIM - Variable Impedance Model

VSI - Voltage Source Inverter

Appendix B - STATCOM Parameters

B.1 12-Pulse STATCOM

The analytical calculations for the following parameters are shown in this section:

- voltage and current rating of dc/ac inverter,
- dc voltage level,
- size of filter components,
- leakage inductance of coupling transformer,
- control system parameters for current control.

For the 12-pulse configuration shown in Figure 3.3, the peak value of the fundamental component of the line to neutral voltage at the output of the inverter is $1.273V_{dc}$. Assuming a 0.1 p.u. drop across the inductance of the adding transformers (L_{xfr1}) and the coupling transformers (L_{xfr2}), the following value for V_{dc} is obtained:

$$V_{dc} = \frac{1.1 \times V_{LN}\sqrt{2}}{1.273} = 8797.2V \qquad \textbf{(B.1)}$$

where V_{LN} = 7.2 kV is the RMS value of the system line to neutral voltage.

For a 2 Mvar capacity STATCOM, the rated current of the inverter is:

$$I_{rated} = \frac{S}{3V_{LN}} = 92A \qquad \textbf{(B.2)}$$

For 0.1 p.u. voltage drop across the L_{xfr1} and L_{xfr2}, the total impedance of L_{xfr1} and L_{xfr2} should be 0.1 p.u. Assuming that L_{xfr1} and L_{xfr2} are each 0.05 p.u.:

$$L_{xfr1} = L_{xfr2} = 0.05 \times \frac{V_{LN}}{I_{rated}} = 5.3mH \qquad \textbf{(B.3)}$$

The output filter consists of tuned series LC elements. Lf1 and Cf1 are tuned to the 10.9 (close to 11th) harmonic frequency. Lf2 and Cf2 are tuned to the 12.9 (close to 13th) harmonic frequency. Selecting the size of the filters to be 100 kvar each, the following values are obtained:

$$\begin{aligned} L_{f1} &= 34.8mH \qquad C_{f1} = 1.7\mu F \\ L_{f2} &= 24.9mH \qquad C_{f2} = 1.7\mu F \end{aligned} \tag{B.4}$$

The design of the dc side capacitor depends upon the expected unbalance in the system voltage and the acceptable ripple in the dc voltage of the inverter. Under normal steady state operation, the STATCOM currents are 90^0 out of phase with the system line to neutral voltages. If the system voltages and the STATCOM currents are given by:

$$\begin{aligned} v_a &= kV\sin(\omega t) \qquad v_b = V\sin\left(\omega t - 120^0\right) \qquad v_c = V\sin\left(\omega t + 120^0\right) \\ i_a &= I\sin\left(\omega t - 90^0\right) \qquad i_b = I\sin\left(\omega t - 210^0\right) \qquad i_c = I\sin\left(\omega t + 30^0\right) \end{aligned} \tag{B.5}$$

where k is the unbalance factor in the phase A voltage. The instantaneous power transferred from the system to the STATCOM is:

$$P_{inst} = v_a i_a + v_b i_b + v_c i_c = (k-1)\frac{VI}{2}\sin(2\omega t) \tag{B.6}$$

Thus, in the event of a voltage unbalance, the instantaneous power transfer from the system to the STATCOM will have a 2nd harmonic ripple. The ripple in the instantaneous power wi'l result in charging and discharging of the dc capacitor. The net energy transferred to the capacitor during the charging is found by integrating equation (B.6) from t = 0 to t = ($\pi/2\omega$):

$$\Delta E = (k-1)\frac{VI}{2\omega} \tag{B.7}$$

If r is the ripple factor in the capacitor voltage, then the charging and discharging of the capacitor will result in a voltage ripple from V_{dc} to $(1+r)V_{dc}$. Equating the energy

transferred (ΔE) to the change in stored energy of the capacitor, the following relation is obtained:

$$C_{dc} = (1-k)\frac{VI}{2\omega r V_{dc}} \tag{B.8}$$

The value of V_{dc} is obtained by equation (B.1). The simulation study described in Section 3.3.5 shows that the value of V_{dc} obtained by equation (B.1) is inadequate. The refined value of V_{dc} determined in Section3.3.5 is used for determining the value of C_{dc}. For $V = V_{LN}\sqrt{2}$, $I = I_{rated}\sqrt{2}$, $\omega = (2*\pi*60)$, $r = 0.001$, $k = 0.95$:

$$C = 1134\mu F \tag{B.9}$$

The gains of the PID block in Figure 3.4 determine the input voltage applied to the VCO's. Assuming that the increase (decrease) in the frequency of the VCO output is limited to +10 Hz (-10 Hz) and that the maximum current error (i_{qe}) is equal to I_{rated}, the gain for the proportional block is selected as:

$$k_p = \frac{10}{\sqrt{2}I_{rated}} = 0.04 \tag{B.10}$$

After repeated simulations in time domain, the gain of the derivative block is selected as:

$$k_d = 0.0003 \tag{B.11}$$

The integral block of the PID block is not used, hence its gain (k_i) is set to 0.

B.2 PWM STATCOM

The analytical calculations for the following parameters are shown in this section:

- voltage, current and switching frequency rating of dc/ac inverter,
- dc voltage level,

- size of the filter components,
- leakage inductance of tie transformer,
- control system parameters for the current and voltage loops.

The line to line voltage at the output of the inverter takes values $+V_{dc}$, 0 or $-V_{dc}$ depending on the status of the inverter switches (see Figure 3.11). If V_{LL} is the magnitude of the system line to line voltage, then the maximum voltage that appears across the combination of the filter inductor (L_f) and the leakage impedance (L_{xfr}) is given by (V_{dc} - V_{LL}).

The magnitude (peak) of the line to line voltage at the inverter output is V_{dc}. Assuming a 0.1 p.u. voltage drop across the coupling transformer and the filter inductor, the desired dc voltage level is given by:

$$V_{dc} = 1.1 \times \sqrt{2} V_{LN} \times \sqrt{3} = 19.4kV \qquad \text{(B.12)}$$

where V_{LN} = 7.2 kV is the rms value of the system line to neutral voltage and $\sqrt{3}$ is the turns ratio of the coupling transformer. The current rating of inverter is same as the current rating of the STATCOM:

$$I_{rated} = \frac{S}{3V_{LN}} = 92A \qquad \text{(B.13)}$$

where S = 2 Mvar is the three phase var rating of the STATCOM. V_{dc} and I_{rated} determine the minimum voltage and current ratings of the power electronic switches of the inverter. Using a safety margin of 50%, the switch voltage and current ratings for the 15 kV, 2 Mvar STATCOM are 28.1 kV and 138 A respectively. In practice, the choice of switching frequency (f_s) of the inverter depends on the speed of the power electronic switches available at the desired current and voltage ratings. For the sake of this discussion, it is assumed that Insulated Gate Bipolar Transistors (IGBT's) rated 28.1 kV and 138 A are

available and that these IGBT's are capable of switching at a 6060 Hz frequency.

For 0.1 p.u. voltage drop across the filter inductor (L_{fl}) and the coupling transformer (L_{xfr}), the total impedance of L_{fl} and L_{xfr} should be 0.05 p.u. Assuming that L_{fl} and L_{xfr} are each 0.05 p.u.:

$$L_{f1} = L_{xfr} = 0.05 \times \frac{V_{LN}}{I_{rated}} = 5.3mH \tag{B.14}$$

The selection of C_f depends on the desired cut off frequency of the filter. The cut off frequency (f_c) of the output filter should be sufficiently lower than the switching frequency (f_s). At the same time, f_c should be sufficiently larger than the frequency of the highest harmonic that is to be compensated by the STATCOM. Hence, an f_c of 3060 Hz is selected. The corresponding filter capacitor value is:

$$C_f = \frac{1}{(2\pi f_c)^2 L_f} = 2.1\mu F \tag{B.15}$$

In order to provide a low impedance path to the switching frequency currents, a small inductor (L_{f2}) is added in series with C_f. L_{f2} is selected such that the combination of L_{f2} and C_f resonate at the switching frequency:

$$L_{f2} = \frac{1}{(2\pi f_s)^2 C_f} = 1.4mH \tag{B.16}$$

Equation (B.8) is used to determine the size of the dc capacitor required. The value of V_{dc} is obtained by equation (B.1). The simulation study described in Section 3.3.5 shows that the value of V_{dc} obtained by equation (B.1) is inadequate. The refined value of V_{dc} determined in Section3.3.5 is used for determining the value of C_{dc}. For $V = V_{LN}\sqrt{2}$, $I = I_{rated}\sqrt{2}$, $\omega = (2*\pi*60)$, $r = 0.001$, $k = 0.95$:

$$C = 110\mu F \tag{B.17}$$

The selection of the parameters for the control system has been done by making an

initial estimate of each parameter and then refining the value by observing the time domain response. For gain of the proportional block of the current controller determines the magnitude error in the current controller. Assuming that the duty cycle of the switch should be 1 for a current error approximately 10%, the initial estimate of the gain for the proportional block for the current control loop is selected as $k_p = 0.01$. The initial estimate for the gain for the integral block is selected as $k_i = 50$. After repeated simulations in time domain simulations, the final values selected for kp and k_i are 0.01 and 500 respectively.

Open loop simulation of the systems shows that injecting a reactive current of magnitude 100 A gives a voltage boost of 1 kV at node 3. Hence the initial estimate of the gain for the proportional block in the system voltage control loop is selected as k_p = (0.25*100/1000) = 0.025. The initial estimate of the gain for the integral block is selected as $k_i = 0.25$.

The gain for the proportional block in the dc voltage control loop is selected such that for a 10% drop in the nominal value of V_{dc}, the STATCOM responds by absorbing real current of magnitude $\sqrt{2}\,I_{rated}$. Using this criteria, $k_p = 0.05$ is selected. A small gain of 0.005 is selected for the integral block (k_i).

Appendix C - DVR Parameters

C.1 PWM DVR

The analytical calculations for the following parameters are shown in this section:

- voltage, current and switching frequency rating of dc/ac inverter,
- dc voltage level,
- size of the filter components,
- leakage inductance of tie transformer,
- control system parameters voltage control loop.

The DVR is a series connected device, hence the power electronic switches of the DVR are expected to carry the line currents. Assuming that the system load is of 2 Mvar, the maximum line current is 92 A (rms). Providing a 50% safety margin, the power electronic switches of the DVR must have a current rating (I_{rated}) of 138 A. In the event of a single line to ground fault, the entire line to neutral voltage will appear across the switches of the DVR. Again, providing a 50% safety margin, the switches have to be rated at $1.5\sqrt{2}\,V_{LN}$ = 15.27 kV. In practice, the choice of switching frequency (f_s) of the inverter depends on the speed of the power electronic switches available at the desired current and voltage ratings. For the sake of this discussion, it is assumed that Insulated Gate Bipolar Transistors (IGBT's) rated 15.27 kV and 138 A are available and that these IGBT's are capable of switching at a 6060 Hz frequency. Thus a switching frequency (f_s) of 6060 Hz is selected.

The dc voltage level of the inverter is determined by the maximum voltage that is to be injected into the system. Assuming that the DVR is expected to inject a maximum

voltage of $0.5V_{LN}$, the dc voltage level is given by:

$$V_{dc} = \frac{1.1 \times V_{LN} \times \sqrt{2}}{2} = 5600 \qquad \text{(C.1)}$$

Since the DVR is inserted in series with the system, it is desirable to have as small a series impedance as possible. This places an upper limit on the choice of the filter inductors and the coupling transformers. At the same time, the filter inductor has to be large enough to filter out the switching frequency harmonics. Based on this, the following values are selected for the filter inductor (L_f) and the coupling transformer (L_{xfr}):

$$L_f = L_{xfr} = 0.025pu = 2.65mH \qquad \text{(C.2)}$$

The filter capacitor is selected so that the cut-off frequency of the filter is 3030 Hz. Hence C_f = 1.021 μF is selected. The size of the dc capacitor is selected using equation (B.8). For a worst case unbalance of k = 0.5, and a dc voltage ripple of r = 0.01, the following value of C_{dc} = 1400 μF is obtained.

The selection of the parameters for the control system has been done by making an initial estimate of each parameter and then refining the value by observing the time domain response. In order to avoid excessive voltage drop during the charging of the DVR dc capacitor, the input signal for real voltage injected (inp_d) is limited to 0.1. The gain (k_p) of the proportional block for the control of V_{dc} is selected so as to give inp_d = 0.1 for a 10% error in the dc voltage (V_{dc}). The gain of the proportional block for the control of load side voltage is selected so as to give inp_q = 1.0 for a voltage error of magnitude V_{dc}. As in the case of the 12-pulse STATCOM, a more extensive method of obtaining the initial estimate of the control system parameters is by frequency domain analysis. However, the approach used in this dissertation involves more effort in time domain analysis to obtain the control system parameters.

Vita

Name:	Raxit Avinash Kagalwala
Date of Birth:	April 05, 1969.
Place of Birth:	Surat, India.
Education:	
July 86 - July 90	Indian Institute of Technology, Kharagpur, India. Bachelor of Technology in Electrical Engineering. A Software for Current Rating Calculations of Transistorized Inverters.
Sept. 90 - Dec. 92	University of Washington, Seattle, U.S.A. Master of Science in Electrical Engineering. Transient Analysis of an Adaptive Var Compensator.
Jan. 93 - June 96	University of Washington, Seattle, U.S.A. Ph. D. in Electrical Engineering. Modeling and Simulation of Custom Power Devices.

Publications:

1. R. Kagalwala, S. S. Venkata, M. A. El-Sharkawi, et. al, "Transient Analysis of Distribution Class Adaptive Var Compensators: Simulation and Field Test Results," *IEEE Transactions on Power Delivery*, April, 1995.

2. R. Kagalwala, S. S. Venkata, P. O. Lauritzen, A. Sundaram, R. Adapa, V. V. Sastry, "Models of a Dynamic Voltage Restorer (DVR)," *presented at the North American Power Symposium (NAPS)*, Bozeman, Montana, 1995.

3. R. Kagalwala, S. S. Venkata, P. O. Lauritzen, N. R. Raju, A. Sundaram, R. Adapa, "Detailed Modeling of a Distribution Level Static Condenser (STATCON)," *presented at the International Power System Transients (IPST) Conference*, Lisbon, Portugal, 1995.

4. N. R. Raju, S. S. Venkata, R. Kagalwala, V. V. Sastry, "An Active Power Conditioner for Reactive Power and Harmonic Compensation," *presented at the Power Electronic Specialists Conference (PESC)*, 1995.